



**VNiVERSIDAD D SALAMANCA**

DEPARTAMENTØ DE INGENIERÍA CARTØGRÁFICA Y DEL TERRENØ

**TESIS DOCTORAL**

**Análisis Estructural de Infraestructuras a partir de  
la Hibridación de Sensores Geomáticos**

Alberto Villarino Otero

2015



Universidad de Salamanca  
Escuela Politécnica Superior de Ávila  
Departamento de Ingeniería Cartográfica y del Terreno

AUTOR:

Alberto Villarino Otero

DIRECTORES:

Dr. Diego González Aguilera

Dra. Belén Riveiro Rodríguez

2015

Aviso legal:

Se informa al lector que la presente Tesis Doctoral ha sido efectuada según la normativa, impuesta por la Universidad de Salamanca, en el formato de presentación por compendio de publicaciones. Se advierte a todo aquel que quiera disponer, consultar, citar, reproducir o difundir las publicaciones incluidas en la misma el deber de respetar los derechos reservados a las editoriales de las publicaciones intervinientes.





La presente Tesis Doctoral corresponde a un compendio de tres artículos científicos publicados por revistas de impacto que se especifican a continuación:

### **1. Successful Applications of Geotechnologies for the Evaluation of Road Infrastructures**

Alberto Villarino<sup>1</sup>, Belén Riveiro<sup>2</sup>, Joaquín Martínez-Sánchez<sup>3</sup> and Diego González-Aguilera<sup>1</sup>

<sup>1</sup>Department of Land and Cartographic Engineering, High Polytechnic School of Avila, University of Salamanca, Hornos Caleros, 50, 05003 Ávila, Spain.

<sup>2</sup>Department of Material Engineering, Applied Mechanics and Construction, School of Industrial Engineering, University of Vigo, Rúa Maxwell s/n, 36310 Vigo, Spain.

<sup>3</sup>Department of Natural Resources and Environmental Engineering, School of Mining Engineering, University of Vigo, Rúa Maxwell s/n, 36310 Vigo, Spain.

*Remote Sens.* **2014**, *6*, 7800-7818; DOI:10.3390/rs6087800

### **2. The Integration of Geotechnologies in the Evaluation of a Wine Cellar Structure through the Finite Element Method**

Alberto Villarino<sup>1</sup>, Belén Riveiro<sup>2</sup>, Diego González-Aguilera<sup>1</sup> and Luis Javier Sánchez-Aparicio<sup>1</sup>

<sup>1</sup>Department of Land and Cartographic Engineering, High Polytechnic School of Avila, University of Salamanca, Hornos Caleros, 50, 05003 Ávila, Spain.

<sup>2</sup>Department of Material Engineering, Applied Mechanics and Construction, School of Industrial Engineering, University of Vigo, Rúa Maxwell s/n, 36310 Vigo, Spain.

*Remote Sens.* **2014**, *6*, 11107-11126; DOI:10.3390/rs61111107

### **3. Geometrical Issues on the Structural Analysis of Transmission Electricity Towers Thanks to Laser Scanning Technology and Finite Element Method**

Borja Conde-Carnero<sup>1</sup>, Alberto Villarino<sup>2</sup>, Manuel Cabaleiro<sup>1</sup> and Diego González-Aguilera<sup>2</sup>

<sup>1</sup>Department of Material Engineering, Applied Mechanics and Construction, School of Industrial Engineering, University of Vigo, Rúa Maxwell s/n, 36310 Vigo, Spain.

<sup>2</sup>Department of Land and Cartographic Engineering, High Polytechnic School of Avila, University of Salamanca, Hornos Caleros, 50, 05003 Ávila, Spain.

*Remote Sens.* **2015**, *7*, 11551-11569; DOI:10.3390/rs70911551



# ANÁLISIS ESTRUCTURAL DE INFRAESTRUCTURAS A PARTIR DE LA HIBRIDACIÓN DE SENSORES GEOMÁTICOS

Tesis Doctoral presentada por Alberto Villarino Otero

## INFORME DE LOS DIRECTORES DE TESIS

La Tesis Doctoral “*Análisis Estructural de Infraestructuras a partir de la Hibridación de Sensores Geomáticos*”, presentada por Alberto Villarino Otero, se inserta en la línea de investigación de evaluación de la seguridad estructural de infraestructuras mediante el uso de técnicas no destructivas. Mediante esta Tesis Doctoral se han abordado diferentes ámbitos de aplicación tales como infraestructuras asociadas a carreteras, estructuras de infraestructura eléctrica y edificaciones históricas subterráneas.

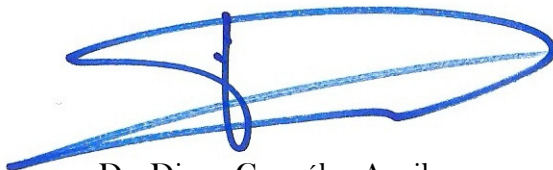
Los resultados obtenidos con todas y cada una de las metodologías presentadas dieron lugar a la publicación de diferentes artículos científicos, todos ellos actualmente publicados en una revista de reconocido prestigio en el ámbito de la geomática, sometidos a la revisión anónima por pares e indexada en las bases de datos del Journal Citation Report (JCR), encontrándose en el primer cuartil (Q1) de la categoría de Remote Sensing (IF 3.180, posición 5/28).

Dadas las condiciones presentadas, se considera que la presente Tesis Doctoral se ajusta, de modo óptimo, a las condiciones requeridas para la presentación de la misma por la modalidad de “compendio de publicaciones”, conforme los requisitos expuestos en el Reglamento de Doctorado de la Universidad de Salamanca.

La calidad de las metodologías desarrolladas propuestas, así como su validación en diferentes sistemas estructurales, queda irrefutablemente reconocida después de su publicación en revistas de reconocido prestigio y alto factor de impacto en el ámbito de la geomática.

Y para los efectos oportunos, los directores informan favorablemente la citada Tesis Doctoral para su presentación y defensa pública.

En Ávila, a 30 de noviembre de 2015



Dr. Diego González Aguilera



Dr. Belén Riveiro Rodríguez



## **AGRADECIMIENTOS**

Llegado este punto, no puedo concluir sin recordar y mostrar mi sentido agradecimiento a las personas que, en mayor o menor medida, contribuyeron para que pudiera terminar la Tesis Doctoral.

En primer lugar tengo que agradecer a mis directores Belén Riveiro Rodríguez y Diego González Aguilera, por su apoyo, paciencia y dedicación. Sus consejos y correcciones me han guiado durante el periodo de investigación, posibilitando la culminación de la Tesis Doctoral.

A mi familia, en especial a mis padres, quienes han sufrido conmigo el esfuerzo del trabajo realizado, su constante ánimo y sacrificio me han proporcionado una completa formación académica. A mi hermano, su asesoramiento y asistencia en momentos difíciles ha sido un importante apoyo.

Agradecer a mis amigos, por escucharme y ser comprensivos por el tiempo que nos le he podido dedicar durante el camino que ha supuesto esta etapa. A compañeros ingenieros, su experiencia profesional y conocimiento me ha servido de importante refuerzo en consultas técnicas durante el periodo de investigación.



## RESUMEN

Resulta incuestionable la función que desempeñan las infraestructuras, desde posibilitar el desarrollo de un país hasta el valor sentimental que representan para las sociedades. Pero en determinadas circunstancias se muestra desconocido el estado estructural actual de una infraestructura, condicionando con ello la vida útil de las construcciones, además de poner en riesgo la calidad de su servicio o su integridad global. Esta tarea de evaluación estructural se dificulta de manera considerable en las ocasiones en las que no se dispone de información geométrica, debido a la inexistencia de la documentación gráfica de su diseño, o causada por modificaciones a lo largo del tiempo.

Motivado por ello, la presente Tesis Doctoral centra su esfuerzos en desarrollar y aplicar métodos y procedimientos de trabajo para obtener modelos geométricos, de manera precisa y eficiente, de diferentes tipos de infraestructuras con los que llevar a cabo análisis que evalúen su comportamiento estructural. El modelado geométrico se consigue a partir de una metodología basada en la hibridación de diferentes técnicas geomáticas de carácter no invasivo, utilizando sensores tales como el láser escáner terrestre 3D (TLS) y el georradar (GPR). Estos modelos obtenidos son implementados en programas de análisis numérico mediante el método de los elementos finitos (MEF) que permiten diagnosticar su estado estructural.

Con el fin de corroborar la aplicabilidad de los procedimientos desarrollados, estos son empleados en diferentes tipos de infraestructuras: por un lado, las asociadas a las infraestructuras viarias, de vital importancia en el desarrollo social y cultural. Por otro, la edificación subterránea contemplada dentro del Patrimonio Histórico y por último, torres metálicas en celosía para el transporte de energía eléctrica, tan necesaria en los tiempos presentes.

A raíz de los resultados obtenidos, se concluye que los sensores geomáticos adquieren un protagonismo esencial en el conocimiento de la geometría de una construcción. Por un lado, la metodología de hibridación del TLS y el GPR suministra abundante y completa información de las características geométricas y físicas. Por otro lado, ambos se establecen como complemento perfecto para suministrar datos al análisis numérico por elementos finitos, con el que evaluar mecánicamente una estructura.



# ÍNDICE

<b>1. INTRODUCCIÓN .....</b>	<b>13</b>
<b>2. HIPÓTESIS DE TRABAJO Y OBJETIVOS .....</b>	<b>21</b>
<b>3. ARTÍCULOS CIENTÍFICOS .....</b>	<b>23</b>
3.1 Successful Applications of Geotechnologies for the Evaluation of Road Infrastructures .....	25
3.2 The Integration of Geotechnologies in the Evaluation of a Wine Cellar Structure through the Finite Element Method .....	47
3.3 Geometrical Issues on the Structural Analysis of Transmission Electricity Towers Thanks to Laser Scanning Technology and Finite Element Method.....	69
<b>4. CONCLUSIONES .....</b>	<b>91</b>
<b>5. LÍNEAS DE INVESTIGACIÓN FUTURAS .....</b>	<b>95</b>
<b>6. REFERENCIAS BIBLIOGRÁFICAS .....</b>	<b>97</b>
<b>7. ANEXO. FACTOR DE IMPACTO DE LAS PUBLICACIONES .....</b>	<b>103</b>



## **1. INTRODUCCIÓN**

Aunque no existe en la literatura una definición generalmente aceptada de infraestructura, se podría definir esta desde un punto de vista ingenieril como: *“El conjunto de estructuras de ingeniería e instalaciones que constituye la base sobre la cual se produce la prestación de servicios, que se consideran necesarios para el desarrollo de fines productivos, personales, políticos y sociales”*.

Es bien conocido que las infraestructuras tienen un papel decisivo en el desarrollo de un país, ya que componen los pilares básicos del sistema productivo, de la distribución de bienes y servicios y de la movilidad de las personas. Desde las civilizaciones más antiguas hasta el mundo presente (Wright, 2004; Herranz, 2004; Pereira, 2005), estas han constituido un elemento de dinamización económica y creación de empleo, además de favorecer a una amplia gama de industrias y servicios vinculados. Son consideradas uno de los factores que hacen posible y condicionan, de una manera global, el proceso de crecimiento económico, social y cultural de un país.

Pero deben tenerse en cuenta dos aspectos importantes de las infraestructuras desde su punto de vista constructivo. Por un lado, estas son diseñadas y construidas con determinados materiales y bajo unas condiciones establecidas, que hacen posible que cumplan su servicio durante su ciclo de vida (Silva, 2001). Por otro lado, no existen habitualmente labores estipuladas de control sobre las infraestructuras, entendiendo que son estructuralmente seguras durante el periodo de vida útil para el que fueron diseñadas.

Sin embargo existen múltiples factores a lo largo del tiempo, como por ejemplo: defectos de montaje, modificación de las cargas de servicio, acciones ambientales o accidentales, el deterioro de los materiales e incluso factores a priori desconocidos, que originan daños en dichos sistemas estructurales.

Esto puede suponer importantes consecuencias como reducir la seguridad estructural, limitar el periodo de vida útil o incluso poner en riesgo la integridad global de la construcción.

Es en este punto donde el conocimiento del estado estructural actual de las infraestructuras toma especial relevancia, sirviendo esta información de mejora y complemento en los planes de conservación, durabilidad y sostenibilidad de las mismas (Libro verde, 2011; Rui-Wamba, 2011). Esto permitirá por un lado preservar el patrimonio de las infraestructuras, con el especial valor y arraigo cultural que estas representan para la sociedad, y por otro optimizar la gestión de recursos, prolongando la vida útil de las mismas y evitando con ello los costes de construcción de otras nuevas.

El otro aspecto a destacar, es que para evaluar estructuralmente una construcción se necesita previamente información métrica, tanto de su geometría exterior como de las características de los materiales que la constituyen. Esta información se obtiene típicamente a partir de los planos originarios de su diseño y posterior ejecución, o en el caso de estructuras tipificadas a través de prontuarios, manuales o normativas (Albermani et al., 2003; Guang-lin et al., 2009). Pero en determinados casos, y especialmente en infraestructuras de cierta antigüedad, estos planos están incompletos y/o apenas acotados, por lo que son completados con mediciones in situ, observaciones y fotografías (Mark, 1982; Hernández et al., 2003) conllevando una importante cantidad de medios y tiempo, además de no generar modelos geométricos precisos. Este hecho es de especial importancia, ya que una información detallada de la geometría externa e interna es necesaria para generar un modelo estructural lo más cercano posible a la realidad.

Los dos importantes aspectos anteriores establecen unas necesidades que motivan la realización de la Tesis Doctoral, cuyo **objetivo general** es desarrollar una metodología que permita generar modelos geométricos precisos 3D de una infraestructura, para su posterior implementación en programas informáticos de cálculo numérico que evalúen su comportamiento estructural, y que posibiliten planes que prolonguen la vida útil de las infraestructuras.

Dicha metodología será empleada en la investigación de tres ámbitos complementarios de estudio, con el fin de desarrollar un método de trabajo aplicable a este tipo de infraestructuras, como son: las estructuras asociadas a las carreteras, la edificación contemplada dentro del Patrimonio Histórico y las torres metálicas en celosía para el transporte de energía eléctrica.

Llegado este punto, es donde entran en escena los sensores y técnicas geomáticas (fotogrametría terrestre, TLS y GPR), que han sido elegidas en esta Tesis Doctoral como tecnologías de aplicación en la obtención de modelos geométricos, debido a su carácter no invasivo (Annan, 2003; Farjas et al., 2008; Lorenzo et al., 2012), lo que representa una gran ventaja en cuanto a la preservación de la construcción. El uso de técnicas invasivas (ej. excavaciones, perforaciones de prueba, etc.) conllevaría un deterioro de los materiales y el consiguiente daño al bien patrimonial.

En particular, el escaneado láser y la fotogrametría terrestre se presentan como técnicas no-destructivas apropiadas en la obtención, de manera rápida, eficiente y con un alto grado de detalle, de información métrica que permita generar un modelo 3D de una construcción (Vosselman et al., 2001; Capra et al., 2005; Arayici et al., 2007; Mañana-Borrazas et al., 2008; Riveiro et al., 2011; Molina et al., 2012).

Por su parte, el GPR es un método geofísico de teledetección que permite identificar las características físicas de los materiales analizados, la homogeneidad del material de relleno o la detección de inclusiones de diferentes materiales (González-Drigo et al., 2008; Orban et al., 2009; Solla et al., 2011; Santos-Assunção et al., 2014; Kanli et al., 2015).

Esta aplicación de los sensores y técnicas geomáticas en la búsqueda de generar un modelo geométrico 3D de una infraestructura, es el punto de partida de la Tesis Doctoral, que se pone de manifiesto con el desarrollo del primer artículo científico titulado “*Successful Applications of Geotechnologies for the Evaluation of Road Infrastructures*”. Este analiza la idoneidad, eficacia y alcance de las técnicas geomáticas en el modelado de las estructuras asociadas a las carreteras. Por un lado, se examina la fotogrametría mediante rectificación de imágenes y orientada hacia la obtención de documentación métrica plana de arcos de puentes históricos; y por otro lado, la fotogrametría múltiple convergente, como método centrado en la generación de modelos tridimensionales de puentes.

En estos casos al tratar con imágenes, no sólo es posible extraer ciertas medidas específicas de las estructuras o sus desgastes (ej. fisuras, fugas, etc.), sino también llevar a cabo una delimitación precisa de los daños o las características del elemento estructural (ej. grietas, elementos desplazados, pérdida de material, desgaste de la superficie, etc.).

Por su parte el estudio con el láser escáner se presenta desde una doble perspectiva. La primera en su versión terrestre (estática) utilizando un láser escáner terrestre, aplicado sobre puentes históricos, con la que se consiguen detalladas nubes de puntos y que tras un preciso tratamiento de estas (Conde et al., 2015) permite visualizar modelos 3D en formato CAD de las superficies de los puentes. La segunda en su versión terrestre (dinámica) utilizando una unidad móvil de escaneo láser, con la muestra de una representación cartográfica de la trayectoria calculada para una carretera, junto con varias nubes de puntos de las infraestructuras asociadas a la misma.

Aunque la aplicación de las técnicas mencionadas se lleva a cabo con éxito, esta se realiza de manera individual sin combinación entre ellas. Esto brinda la idea que da lugar al desarrollo de unidades móviles de inspección de infraestructuras de carretera que integren diferentes sensores geomáticos (láser escáner, cámaras termográficas, perfilómetros, GPR, etc.), posibilitando no solo la monitorización masiva de elementos (ej. aceras, túneles, puentes y taludes) sino mostrar incluso, gracias al GPR, datos de parámetros no visibles, como la estructura interna del pavimento, patologías del firme, etc. Todo ello implica destacables ventajas: automatización y mejora de la productividad en el inventario geométrico e inspección de las carreteras y sus infraestructuras asociadas, así como evitar la subjetividad en el diagnóstico del estado actual de estas. Además, en la era tecnológica actual, se hace prácticamente necesario desarrollar una aplicación de *software* que sirva de sistema de gestión de carreteras, integrando el inventario geométrico en una base de datos que permita acometer tareas de inspección y diagnóstico.

Es esta parte final del primer artículo, en la que se aborda la combinación de sensores geomáticos, la que nos abre la puerta en busca de un nuevo avance de la investigación. Para ciertas aplicaciones estas técnicas geomáticas han sido utilizadas con éxito desde un enfoque multidisciplinar, pero sin aprovechar de forma óptima las sinergias obtenidas de su hibridación, además de ser empleadas en construcciones de ingeniería civil pero de marcado carácter lineal y a nivel de superficie, como es el caso de los puentes históricos (Lubowiecka et al., 2009; Solla et al., 2011).

En este sentido, el segundo artículo científico titulado “*The Integration of Geotechnologies in the Evaluation of a Wine Cellar Structure through the Finite Element Method*” trata de integrar las geotecnologías del TLS y GPR, con el objetivo de desarrollar un completo modelo geométrico de una edificación subterránea. Se desarrolla un método de trabajo que hibride las técnicas geomáticas del TLS y GPR de manera óptima, a fin de obtener un modelo computacional con el que realizar un análisis estructural que determine su estado actual.

Con ello se pretende crear una metodología que no requiera excesiva especialización y conocimiento, y que pueda ser aplicada con éxito a este tipo de construcciones. En este caso la infraestructura en estudio es una edificación de carácter patrimonial, en concreto una bodega perteneciente al Patrimonio Histórico de la ciudad de Toro (Zamora), y que constituye una de las señas de identidad en la vida cultural de las sociedades de esta comarca. En este caso de estudio, los perfiles obtenidos con el GPR sobre la bodega son georreferenciados sobre la base de los datos geométricos recogidos por TLS, con lo que se obtiene un modelo geométrico en 3D, con información detallada de la geometría externa y la composición interna de los elementos constitutivos. Los datos integrados son implementados en programas de análisis numérico por elementos finitos, obteniendo interesantes conclusiones acerca de su estado actual.

Es en este momento de la investigación donde el método de cálculo por elementos finitos toma especial relevancia. De hecho, en el campo de la ingeniería civil y la arquitectura, las estrategias de análisis numérico por elementos finitos (Zienkiewicz y Cheung, 1967) han acaparado gran parte de la atención científica (Lubowiecka et al., 2011; Van de Ven et al., 2004). Estas metodologías numéricas, en contraposición con las estrategias de cálculo más tradicionales como la estática gráfica (Huerta, 2008) o el análisis límite (Heyman, 1997; Riveiro et al., 2011), se han situado como soluciones apropiadas a diferentes necesidades ingenieriles, permitiendo incluso la evaluación estructural de construcciones históricas (López et al., 1998; Roca et al., 2010) y siendo objeto de estudio en diferentes situaciones: análisis dinámico (Martínez et al., 2007), sísmico (Endo et al., 2015) o modelos de daño continuo (Roca et al., 2013).

Cabe destacar, que el análisis estructural en estas edificaciones subterráneas presenta ciertas particularidades respecto a las que actualmente existen sobre estructuras en superficie (Arias et al., 2007; Gonen et al., 2013; Saloustrós et al., 2015), ya que estas edificaciones tienen la singularidad de encontrarse confinadas bajo una masa de tierra. Esto obliga a realizar un estudio diferente de las coacciones a las que se encuentra sometida, así como un análisis diferenciado que modele la masa de terreno que gravita sobre la bóveda de la bodega, con el fin de poder determinar las cargas que se transmiten a esta.

La inevitable y consecuente asociación entre la componente geométrica y el análisis estructural, hace que las metodologías geomáticas citadas anteriormente se sitúen como perfectas compañeras del análisis numérico por elementos finitos. Este hecho y el grado de detalle obtenido con el estudio del TLS en el artículo anterior, sienta la base de una nueva investigación, llevada a cabo en el tercer artículo científico titulado “*Geometrical Issues on the Structural Analysis of Transmission Electricity Towers Thanks to Laser Scanning Technology and Finite Element Method*”. En este artículo se comprueba el potencial del TLS en la generación de modelos geométricos precisos de estructuras complejas que nutran de datos al análisis numérico. Las infraestructuras para esta investigación son las estructuras metálicas en celosía, en este caso las que forman las torres de soporte de cables eléctricos de alta tensión.

Una importante apreciación radica en que investigaciones realizadas en infraestructuras de este tipo centran sus estudios en otros aspectos como: determinar el efecto que distintos desplazamientos de la cimentación tienen sobre las torres, teniendo en cuenta la no linealidad geométrica y del material (Shu et al., 2011; Yang et al., 2013), dar soluciones para las mejoras en el diseño y refuerzo de las cimentaciones (Kuang et al., 2002; Zhang et al., 2006) y averiguar las causas que produjeron el colapso estructural en determinadas torres, bien por cargas excesivas o por un defecto de los materiales que las forman (Klinger et al., 2011; Rao et al., 2012; Komorski et al., 2013). Además, en las situaciones anteriores, se parte de un modelo geométrico obtenido de prontuarios o planos de ejecución existentes, considerando estos como correctos, no verificando por lo tanto la geometría y perfiles metálicos de las mismas, así como la posible existencia de defectos o imperfecciones en el montaje de las torres.



Esto hace necesario dar el salto hacia una estrategia que audite en primer lugar la calidad geométrica de las torres. Además, en este caso concreto de estudio, la antigüedad de las torres impide la existencia de documentación que especifique las características geométricas de las mismas; mientras que la toma de datos con otros medios, como la medición manual o la topografía tradicional, implica un alto nivel de riesgo, además de no permitir el grado de detalle obtenido con tecnologías láser. Por lo que el TLS se presenta como una herramienta rápida y precisa para conocer la geometría en detalle de este tipo de infraestructuras.

Los conjuntos de datos de nubes de puntos obtenidos con el TLS son procesados con precisión (Tang et al., 2010; Laefer et al., 2011; Walsh et al., 2013), resultando modelos compatibles para implementar en programas de análisis numérico por elementos finitos. Los modelos geométricos reales obtenidos, detallan tanto la geometría y dimensiones de los perfiles que constituyen las torres, como todo tipo de particularidades (ej. desvío de la verticalidad y horizontalidad o imperfección en la conexión de los perfiles metálicos).

Esta información establece las bases de un análisis estructural posterior, que compara diferentes modelos estructurales, teniendo en cuenta la geometría real y el diseño original. Los resultados obtenidos corroboran la notable influencia que este tipo de imperfecciones tienen sobre el comportamiento estructural de las torres.



## **2. HIPÓTESIS DE TRABAJO Y OBJETIVOS**

Se establecen **tres hipótesis de trabajo** en la presente Tesis Doctoral:

1. Se puede caracterizar geoméricamente una infraestructura con la aplicación individual o conjunta de técnicas geomáticas como la fotogrametría, el TLS y el GPR.
2. Con los datos obtenidos de la caracterización se pueden generar modelos geoméricos detallados en 3D de una infraestructura.
3. El modelo geomérico obtenido puede ser utilizado para realizar diferentes análisis estructurales que evalúen el grado de seguridad actual.

Los **objetivos** que se pretenden alcanzar durante el desarrollo de la Tesis Doctoral son:

1. Analizar la utilización de manera individual o combinada de técnicas geomáticas como la fotogrametría, el TLS y el GPR, para obtener modelos geoméricos precisos de infraestructuras.

Esto será aplicado a las estructuras asociadas a las carreteras, utilizando los datos obtenidos como plataforma de gestión que mejore las labores de inspección y mantenimiento de estas infraestructuras lineales.

2. Desarrollar un método de trabajo a partir de la hibridación del TLS y el GPR para generar un modelo geomérico 3D de una edificación subterránea, realizando un análisis estructural por el MEF que identifique su estado estructural actual.

Se elige como caso de estudio la Bodega del Ayuntamiento de la localidad de Toro (Zamora). La conservación y mantenimiento de este tipo de construcciones, que forman parte del Patrimonio Histórico de la localidad, es un aspecto fundamental debido a la importancia económica y cultural que la industria vitícola tiene en la región.

3. Crear un modelo *as built* en estructuras metálicas complejas, mediante el uso del TLS, identificando con ello todo tipo de particularidades de su montaje (ej. perfilería, la geometría de unión y defectos) que son consideradas en diferentes modelos estructurales, analizando la influencia que esto tiene en el estado de deformaciones y tensiones de las torres.

Se someterán a estudio las estructuras que forman las torres de soporte de cables eléctricos, constituidas por perfiles metálicos en celosía. Tres torres de diferentes dimensiones y características geométricas son utilizadas en el estudio, con el fin de llevar a cabo un análisis y comparativa de resultados.

### **3. ARTÍCULOS CIENTÍFICOS**

A continuación se muestran los tres artículos científicos publicados en revistas internacionales de impacto. Antes de cada artículo original se describe un breve resumen que recoge el trabajo de investigación de cada uno de ellos.



### **3.1 Successful Applications of Geotechnologies for the Evaluation of Road Infrastructures**

#### **RESUMEN**

Este trabajo presenta los resultados obtenidos, a lo largo de varios años de investigación, sobre la utilización de diferentes técnicas geomáticas en el campo de la ingeniería civil y, en particular, en su aplicación a la gestión de la red de carreteras y estructuras asociadas.

La fotogrametría digital terrestre y el láser escáner son técnicas geomáticas que permiten obtener información métrica de manera rápida y eficaz de una infraestructura, generando modelos geométricos detallados en 2D y 3D. Esa modelización es adaptada para la integración en los diferentes métodos de cálculo estructural de arcos de puentes históricos, realizando evaluaciones estructurales basadas en la teoría del análisis límite y simulaciones numéricas mediante el método de los elementos finitos a partir de modelos discretos de los elementos de los arcos.

La hibridación de diversos sensores geomáticos, sincronizados y perfectamente calibrados, posibilita el desarrollo de una unidad de cartografiado móvil que lleve a cabo la monitorización masiva de elementos en la trayectoria de una carretera y sus infraestructuras asociadas. Este volumen de datos permite reconstruir la geometría 3D del entorno del vehículo gracias al escáner láser móvil, así como la medición de elementos no visibles mediante la tecnología de georradar. La información puede ser implementada en un sistema de gestión, que integre el inventario geométrico en una base de datos que permita acometer tareas de inspección y diagnóstico.

Entre los principales avances obtenidos destacan: la calidad métrica de los resultados adquiridos con técnicas geomáticas en el modelado en 2D y 3D, y la alta productividad en la cuantificación de parámetros de inventario e inspección de las carreteras. El desarrollo de herramientas *hardware* y *software* posibilita la automatización de las tareas de gestión, control y mantenimiento involucradas en las infraestructuras viarias.





Letter

## Successful Applications of Geotechnologies for the Evaluation of Road Infrastructures

Alberto Villarino <sup>1</sup>, Belén Riveiro <sup>2</sup>, Joaquín Martínez-Sánchez <sup>3</sup> and Diego Gonzalez-Aguilera <sup>1,\*</sup>

<sup>1</sup> Department of Land and Cartographic Engineering, High Polytechnic School of Avila, University of Salamanca, Hornos Caleros, 50, 05003 Avila, Spain; E-Mail: avillarino@usal.es

<sup>2</sup> Department of Material Engineering, Applied Mechanics and Construction, University of Vigo, Rúa Maxwell s/n, Campus Lagoas Marcosende, 36310 Vigo, Spain; E-Mail: belenriveiro@uvigo.es

<sup>3</sup> Department on Natural Resources and Environmental Engineering, School of Mining Engineering, University of Vigo, Rúa Maxwell s/n, Campus Lagoas Marcosende, 36310 Vigo, Spain; E-Mail: joaquin.martinez@uvigo.es

\* Author to whom correspondence should be addressed; E-Mail: daguilera@usal.es; Tel.: +34-920-353-500; Fax: +34-920-353-505.

Received: 1 July 2014; in revised form: 4 August 2014 / Accepted: 7 August 2014 /

Published: 21 August 2014

---

**Abstract:** This work reports the results obtained over several years of research into the application of different geomatic techniques in the field of civil engineering and, in particular, in their application to the management of road systems and associated structures. Among the main advances obtained are the quantification of parameters during the inventorying and inspection of infrastructures, the metric quality of the results and the development of hardware and software tools for the automation of road systems management.

**Keywords:** geotechnologies; mobile mapping system; road infrastructures; terrestrial laser scanning; photogrammetric methods; software development

---

### 1. Introduction

The infrastructure of a country plays a crucial role in the national economy. Conservation of such systems is key to improving a country's economic strength. Transport systems are the most intensely demanded infrastructures, and investments in road networks usually represent the highest percentage

of all investments in transport. For example, 5317 million euros were invested in Spain in 2012, which represents 45.2% of the total investment in transport infrastructure [1]. The overall set of communications networks in developed countries is huge, and in Europe, in recent years, Spain has been outstanding, with more than 165,000 km of roads, which represents 3% [1]. Thus, in view of the costs of constructing new transport systems, the maintenance of extant systems should be a strategic objective. In this sense, roads and associated structures require conservation and maintenance, and these must be guaranteed in order to optimize economic resources and to maintain a productive economy for a country. Furthermore, within a scenario such as the present one, scourged by a lack of economic resources, it is crucial to prioritize investments, making use of mechanisms that will help to make decisions based on objective facts about resource allocation. Aspects, such as the exploitation and safety of road networks, are now hot-spots in current Spanish society, where traffic accidents are one of the major problems facing the various administrations. For instance, 89,519 accidents happened in Spain in 2013, 10% being due to a lack of conservation of infrastructure [2]. Current inspection systems are mainly based on reports drafted by technicians, who base their findings on the visual inspection of the infrastructures (experience); although the degree of technical know-how of these individuals is considerable, in most cases, the reports consist merely of the acquisition of digital images and georeferencing of the data gathered during visits. The use of these traditional procedures contrasts with the need to have objective, quantifiable data that will allow the best decisions to be made and the actions proposed to be prioritized. In [3], we can find a highway research program report developed in the USA that is focused on the use of advanced geospatial data, technologies, tools and information in the department of transportation projects. The key objectives were to summarize and document the current state of the practice through detailed online questionnaires and literature reviews. Interesting conclusions have been obtained, such as that nearly 85% of the departments of transportation (DOTs) surveyed seems to regularly use geospatial technologies, with more than 50% indicating that they are proactive in researching new technologies. Almost two-thirds of the DOTs stated that most divisions had integrated advanced geospatial technologies into their daily workflows. The top three barriers to technology adoption are cost, inertia and technical expertise. The technologies most frequently used by DOTs are global positioning systems (GPS), geographical information systems (GIS) and video logging. However, newer technologies, such as cloud computing, machine control, electromagnetic imaging, unmanned airborne vehicles (UAVs) and interferometric synthetic aperture radar (inSAR/ifSAR), are not yet well integrated. On the other hand, the DOTs are experiencing a paradigm shift in their geospatial workflows as the technology moves from two-dimensional (2D) to three-dimensional (3D).

In recent years, geomatic methods have undergone an important series of developments. Currently, some technologies have now reached maturity in other engineering applications (3D laser scanning, thermography, ground penetrating radar, *etc.*), whose adaptation to the 3D cartography of roads has been an important challenge. In this sense, the investigation reported here does not only address the adaptation of geotechnologies to this field, but also pursues the exploitation of the data acquired and their usefulness in tasks involving geometric inventorying, the inspection of wear (fissures, leakages, cracks, *etc.*) and damage assessment, as well as their incorporation into more advanced procedures, such as the structural assessment of infrastructures associated with road networks.

Here, we offer a compendium of the work carried out between 2006 until the present. The analysis focuses on the application of geomatic methods (photogrammetry, laser scanning and the integration of both) in the field of structures. The work summarized here includes the definition of sensors and the acquisition of data, together with the development of informatics applications that, on the one hand, allow the information provided by geometric sensors to be consulted and interpreted and, on the other, input these into the databases stipulated by Spanish legislation for the geometric inventorying of roads and associated infrastructures and as guidelines for damage assessment.

## 2. Materials

The materials used to digitize infrastructures in 3D comprised conventional topographic instrumentation (as a method for validating the results) and the basic instruments to obtain a geometric and radiometric reconstruction of objects: photographic cameras for the case of photogrammetric methods and a laser scanner for the case of laser scanning approaches. Different tools were used as auxiliary supports in the various experiments carried out.

### 2.1. Photographic Cameras

With a view toward facilitating the use of geomatic methods in the work involving the inspection and assessment of infrastructures, one important aspect to be taken into account is the simplicity of the devices to be used, which must, at the same time, ensure the quality of the documents generated. Thus, the photogrammetric methods developed here were based on simple methodologies for data acquisition that would not require advanced knowledge of geomatic methods. In this sense, different single-lens reflex (SLR) cameras with fixed-focus lenses were used, depending on the requirement of the work to be undertaken.

#### Geometric Calibration of the Cameras

To exploit the photographic data correctly, and hence, generate geometric models with precision, it is necessary to reconstruct the mathematical model of the generation of the image in the camera. This process is known as internal orientation of the photogrammetric process and is achieved by a process of camera calibration at the laboratory with fixed acquisition parameters before data are collected in the field. To calibrate the camera, different commercial software packages were employed, among them the calibration module of Photomodeler Pro™ and the AICON 3D system photogrammetric restitution platform. The calibration procedure was accomplished using standards with markers of known position, which enabled the problems (principal distance, position of principal point of the image and distortions of the lens) to be solved simply. The internal orientation parameters obtained for the various cameras used can be consulted in [4].

Considering the distances involved in this work and the pixel size of the sensors, it was possible to attain spatial resolutions at the sub-centimeter level, which makes the technique highly appropriate for acquiring the geometry of linear structures.

## 2.2. Laser Scanning Systems: Terrestrial and Mobile.

### 2.2.1. Static Laser Scanning System (TLS) (Riegl LMS Z390i)

In the cases addressed here, we used a time of flight (ToF) scanning device from Riegl, model LMS-Z390i [5]. The measurement window ranged between 1.5 m and 400 m, with a nominal error in distance measuring of 6 mm at 55 m under normal conditions of lighting and reflectivity. This device used an infra-red laser with a wavelength of 1.54  $\mu\text{m}$ . The spherical field of vision encompassed 80° on the vertical plane and 360° on the horizontal one. The maximum scanning resolution was 0.002°, with a divergence of the laser of 0.3 mrad, and the point acquisition ratio was 11,000 points per second. The radiometric resolution of the intensity attribute was 8 bits.

### 2.2.2. Mobile Scanning System (MLS) (Lynx Mobile Mapper)

The mobile system used was a Lynx Mobile Mapper, manufactured by Optech Inc. [6]. The Lynx system comprises two LiDAR sensor heads with a nominal error of 8 mm that form a 90° angle between their respective rotation axes and 45° with respect to the trajectory of the vehicle, optimizing the avoidance of occlusions. The acquisition range of this system reaches 500,000 points per second, with a field of view on the scanning plane of 360° (each sensor head). The navigation system used was an LV 520 from Applanix that integrates an inertial measurement unit with an azimuth determination system comprising two antennas (GAMS), with an angular resolution of 0.015° and 0.005° in roll and pitch, together with a positioning precision of 0.02 m on *XY* and 0.05 m on *Z*. All of these values were obtained after post-processing differential correction using GPS bases [7]. The Optech LiDAR devices provided up to four echoes per pulse, with their respective attributes of radiometric resolution intensity of 12 bits.

## 3. Methodologies

### 3.1. Photogrammetric Methods: 3D and 2D Geometric Reconstruction

In this work, we used different approaches for the metric documentation of infrastructures associated with roads from photographic images. Two basic methodologies can be defined, one of them oriented towards obtaining flat metric documents (that is, in two dimensions) and the other focused on the generation of three-dimensional models of objects.

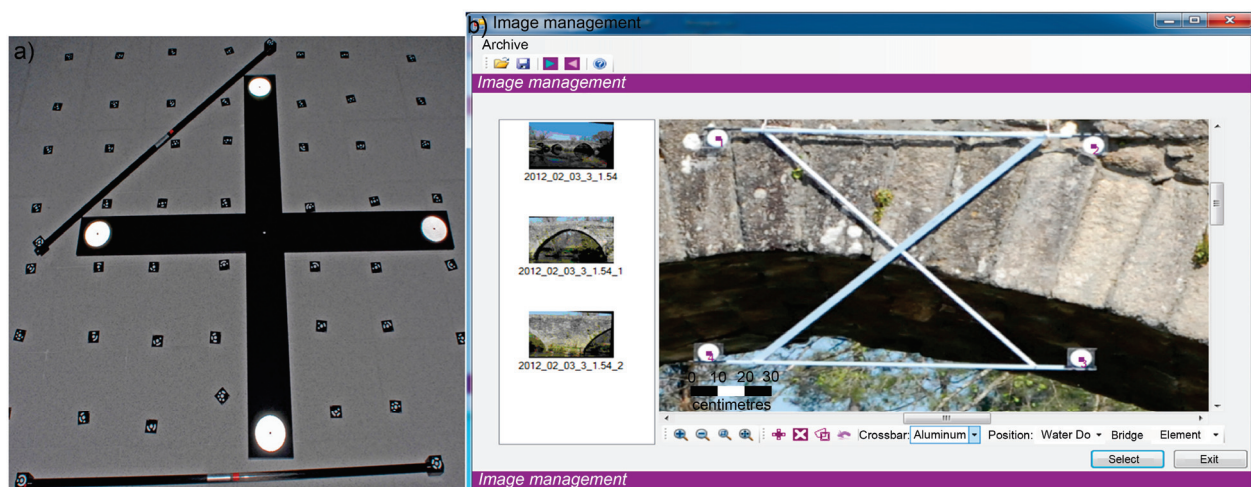
#### 3.1.1. 2D Photogrammetric Modeling

The method chosen to acquire 2D metrics was governed by the need to have a low-cost method that would guarantee reliable metric results when using simple documentation operations. To accomplish this, we used a method based on photogrammetric rectification, by means of which the geometry of the center of perspective of the images captured is transformed into a Euclidean projection, allowing metric measurements to be performed on a plane [8].

To achieve this transformation, it is necessary to know the coordinates of at least four unaligned control points located on the same plane (which defines the projection plane). To apply this method to

the documentation of infrastructures, such as the spandrel walls and abutments of bridges, surfaces and pavements, *etc.*, auxiliary support tools were developed for control points, whose relative position was known after calibration at the laboratory. The next figure (Figure 1a) shows an example of a crossbar developed during the calibration in the laboratory and during data acquisition in the field on a stone-block bridge arch (Figure 1b).

**Figure 1.** Image of auxiliary tools for the rectification of images at the time of (a) calibration at the laboratory and (b) *in situ* measurements. The 2D position of the center of the round white targets is measured with great precision, thereby guaranteeing the correct transformation of the images.



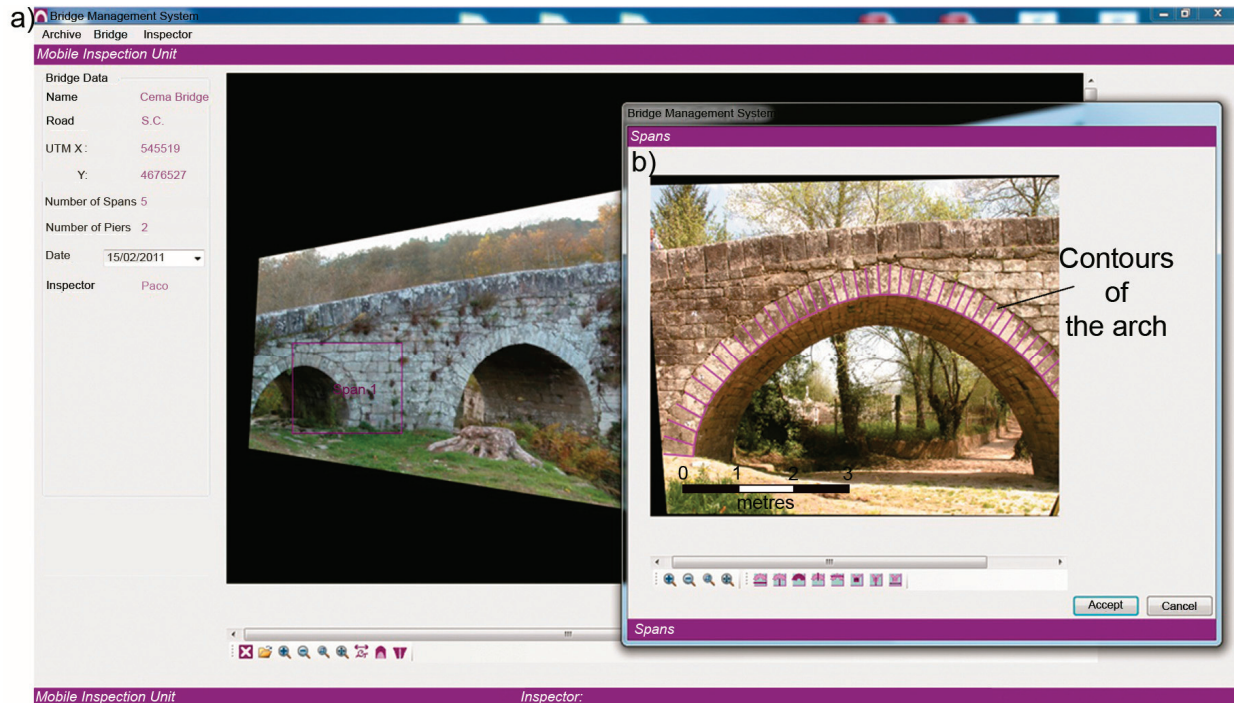
### 3.1.2. Acquisition of Images

The methodology used for data acquisition consisted simply of taking photographs with calibrated cameras or even with conventional cameras without needing to calibrate the camera beforehand. Once the control points in the images had been identified and the photogrammetric algorithms had been implemented, it was possible to obtain the metric properties on the principal rectification plane. Since we were dealing with images, it was not only possible to extract certain specific measurements of the structures or their wear (fissures, leaks, *etc.*), but also to perform a precise demarcation of the damage or characteristics of the structural element (cracks, displaced elements, loss of material, surface wear, *etc.*). The next figure (Figure 2) shows the demarcation of a rectified image corresponding to the stone arch after this methodology had been implemented using software designed for the *in situ* inspection and structural assessment of stone arches. This software incorporates a database for geometric inventorying according to the guidelines of geometric inventorying [9] and basic inspection of passage works [10].

Finally, knowledge of the geometry of the arch, at the barrel ends, of these structures allows the information to be exploited during the process of structural assessment according to the theory of limit analysis, as reported in the Results section.



**Figure 2.** (a) Visualization of the application of image rectification, allowing geometric parameters stored in the database to be acquired. (b) In the rectified image of the arch, note the contours of the arch to be input in the software for the analysis of structural stability.



### 3.1.3. 3D Photogrammetric Modeling

The second strategy of photogrammetric reconstruction was based on the principles of convergent multi-station photogrammetry. This strategy allows the reconstruction of 3D objects with great precision, using bundle block adjustment. During the process, the calculation of the coordinates of all of the points is done simultaneously, using an iterative process based on least-squares fitting, so that the errors in the calculation of the 3D position of the points of interest can be minimized.

When using convergent photogrammetry, it is crucial to ensure the correct design of the station network. In this sense, it is necessary to seek optimum convergence angles of  $90^\circ$  between cameras. This angle is defined as the smallest angle formed by the straight lines defined by the principal distance of the camera at each station. It is also necessary to maintain overlaps above 60% between photographs in order to guarantee the generation of a precise model. The following figure (Figure 3) shows an optimum configuration for cameras during the inspection of vertical clearance of bridges on a highway.

It is also necessary to count reference points on the object in order to endow the 3D model generated with scale. To accomplish this, it is usual to take control points using topographic instruments, such as total stations when accurate models and quality control of the measurements are required, or more portable instruments, such as scale bars, when the priority is freedom of movement and portability during data acquisition, as happens in inventory or damage assessment campaigns.

**Figure 3.** Optimum configuration of the cameras of a convergent multi-station network for data acquisition during the inspection of clearance heights below overhead roads. This camera configuration is optimal, since it provides good intersection angles, as well as a validation based on the third right camera.



The 3D coordinates of the points identified in the images are usually computed simultaneously to the relative orientation of the cameras, and this is done by identifying a minimum of six points on overlapping images and using least-squares fitting [11]. To obtain a dense point cloud that will allow the contours of interest to be delimited, massive restitution is performed (manually or automatically). This merely consists of finding the intersection of the laser beams (spatial intersection).

### 3.2. Laser Scanning of Roads and Associated Infrastructures

As detailed in the Introduction, the process of generating 3D point clouds differs between static and mobile systems. This makes it necessary to perform a pre-processing of the different types of information, and hence, very different methodologies are used during data acquisition in the field.

#### 3.2.1. Terrestrial Laser Scanning

Laser scanning is appropriate when the aim is to document objects or specific structures in detail. This is the case of bridges, walls, deterioration on certain stretches of roads, *etc.*

When the objective is to carry out an investigation using this technique, the planning and optimization of the station network with the instrument become paramount, since it is necessary to



acquire the important details of the structure, and at the same time, to ensure that all of the point clouds acquired from the different points of view can be recorded later in the same coordinate system.

The data acquisition phase, or scanning of the study object, is usually divided into two steps: a preliminary low-resolution scan (low point cloud density) is performed to determine the geometry of all of the surroundings of the scanner and to locate the linking points between the different stations (or control points when their absolute position is known). Following this, a detailed scan is performed on the area of interest, allowing the object or damage to be modeled in detail.

Finally, to obtain radiometric information about the surfaces of objects, as well as intensity data, it is customary to take photographic images, which, after the inner and exterior orientation parameters have been determined, can be used to texturize the point clouds collected by the scanner.

Once the field work has been completed, it is necessary to define the coordinate reference system (CRS) and then record it, either by linking points when common points have been taken between stations or by making use of the geometry itself of the object to achieve the assembly of the global point cloud.

Once the point cloud that defines the 3D reality has been created, different filters are used to homogenize its density, remove undesired points in the modeling and delete redundant information that would only distort the final model. This process is performed using the software Riscan Pro<sup>®</sup>, from the laser company, Riegl. The next figure (Figure 4) shows a view of the point cloud of the Segura Roman Bridge, on the international highway from Castelo Branco (Portugal) to Cáceres (Spain), using two different visualizations: the first using only the intensity data recorded for each point (Figure 4a) and the second incorporating RGB information after orienting the photographic images (Figure 4b).

**Figure 4.** Visualization of a 3D point cloud as a function of (a) the intensity of the reflected laser beam or (b) the photorealistic texture of the object.

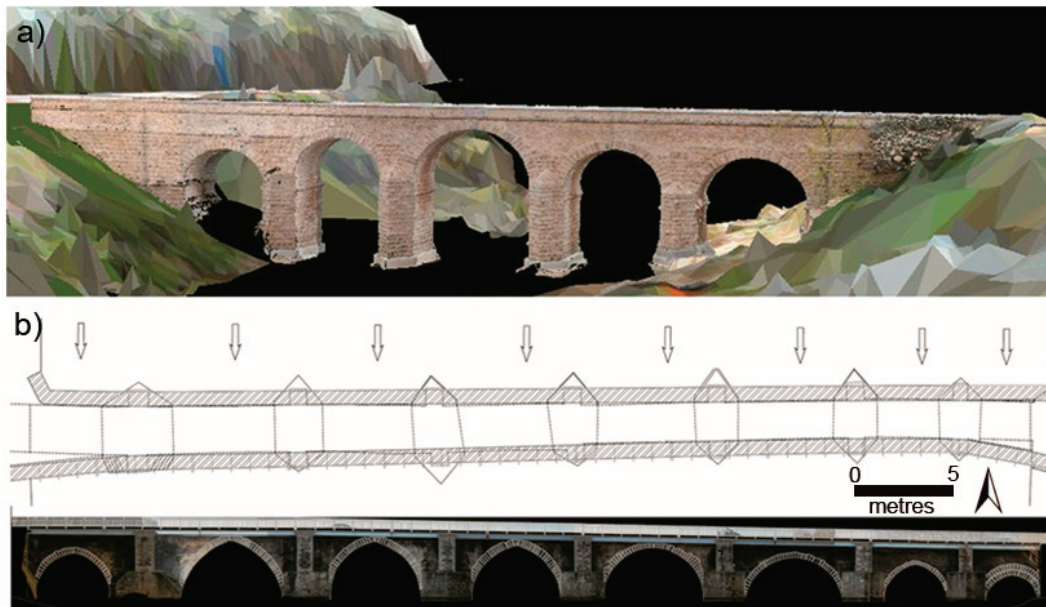


When it is desired to exploit the 3D model of the object, for example for structural assessment, it is common to triangulate the point cloud in such a way that it generates a 3D model of the surfaces of the bridge, similar to digital terrain models (DTM), and then export this to an exchange file of a CAD model. When detailed plans of the structure or orthoimages are required, a texturing process is employed, consisting of the projection of texture onto each of the triangles. The next figure (Figure 5)



shows a photorealistic model of the Segura Roman Bridge and the detailed maps generated at the Roman Bridge in Lugo before its restoration.

**Figure 5.** (a) Photorealistic model of the Segura Roman Bridge; (b) Detailed plans of the Lugo Roman Bridge (Spain).



### 3.2.2. Mobile Laser Scanning

As explained in Section 2.2, the construction of the point cloud in a mobile scanning system depends on two subsystems: the navigation system and the LiDAR sensor. These sensors are synchronized through the time stamp and GPS information from the navigation system. The Applanix POS 520 navigation system uses the LV-POSView software. This system is the first one that must be initiated, since it is responsible for ensuring the synchronicity of the other devices. It also allows the frequency of data acquisition to be selected, typically 200 Hz for the inertial system and 1 Hz for the GPS.

The software that controls the LiDAR systems is called LYNX Survey, and for it to function properly, (a) it needs to have the Applanix system connected previously and (b) it must be sending data. It allows the frequency of LiDAR data acquisition to be set between 75 kHz and 500 kHz for each of the scanners. In this software, there is a library that also permits the acquisition of photos obtained from cameras.

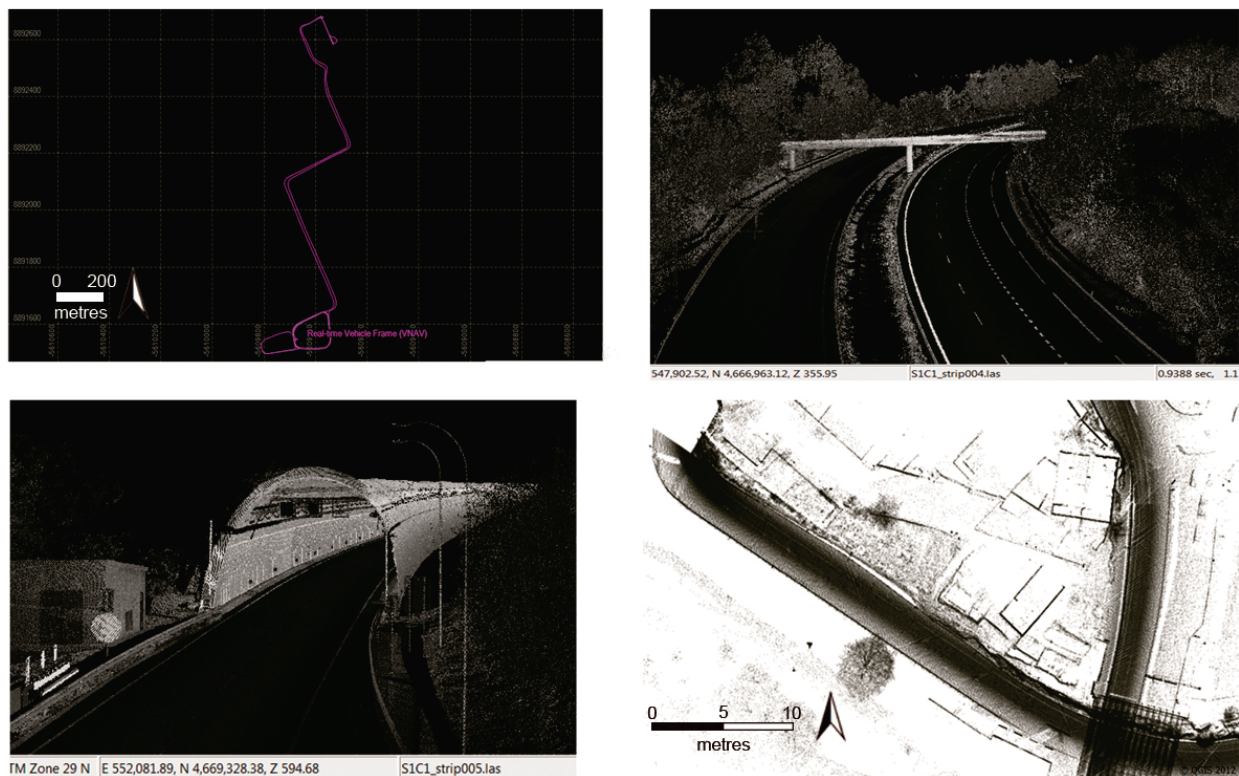
Regarding data processing, the first step consists of generating a precise trajectory on which the data from the others sensors are synchronized, in this case, the LiDAR data and cameras, if they are oriented inside the vehicle. To do so, the software that allows the import of the RINEX files corresponding to the base stations close to the survey site is used to correct the GPS data. Additionally, by applying algorithms based on the Kalman filter [12], it is possible to integrate the different navigation sensors (GPS system, inertial system and encoder), in which there is precise information about the trajectory and the measurement of the GPS time corresponding to each point.

Once the trajectory has been generated, the next step is to fuse the navigation data with the LiDAR data. The LiDAR system of a mobile unit is a 2D measuring system that requires the navigation file for the generation of 3D point clouds. Furthermore, since the origin of both systems of coordinates is different, the use of a calibration file that implements the translation and rotation matrix between both coordinate systems (external orientation of the sensors in the vehicle) is essential.

Once the point cloud has been reconstructed, the operations coincide with those explained in the previous section. One particularity of the data acquired from mobile systems is related to the huge computational volume they occupy, which may also correspond to large extensions of terrain. Thus, the incorporation of the data in geographical information systems (GIS), and, in particular, with the road network, now means that the technique is a very useful tool for management, as detailed in the Results section. Moreover, not only do the files allow one to work based on 2D GIS, but also, the technique becomes ideal for the input of information into 3D GIS.

The next figure (Figure 6) shows a cartographic representation of the trajectory calculated for a road survey together with several point clouds of infrastructures associated with roads in the Regional Community of Galicia, together with LiDAR data converted to SHP (ESRI Shapefile) and loaded in Quantum GIS.

**Figure 6.** Trajectory and examples of point clouds obtained with the mobile scanning system.



### 3.3. Structural Evaluation of Road Infrastructure

The methodologies for geometric reconstruction presented above were applied for structural purposes. The aim was to build geometric models that could be imported into the tasks of structural assessment. In this sense, for the particular case of stone or concrete structures, it is particularly useful

to build the detailed 3D model of the construction in order to be able to carry out more realistic structural calculations. Successful examples of application follow.

### 3.3.1. Structural Assessment of Arch Bridges Based on Limit Analysis Theory: The 2D Approach

The first set of experiments performed consisted of the use of flat metric documents, such as rectified images and the delineation on the elevation plane of the bridge arches to carry out structural assessment work. To do so, within the framework of limit analysis theory, we considered methods for the analysis of the structural stability of masonry arches.

Masonry arches are hyperstatic structures, which imply the possibility of infinite numbers of pressure lines [13]. For a structure subjected to pure compression to remain at equilibrium, the pressure lines must be kept inside the arch ring defined by the intrados and extrados. Accordingly, equilibrium in a stone arch can be visualized via a pressure line. Thus, on the basis of the geometric information extracted from the structure, as well as the mechanical properties of the material, it is possible to evaluate different collapse mechanisms of bridges by varying the position and value of the load. In this sense, according to the different hypotheses concerning the formation of hinges in the arch, it is possible to determine the lowest load value that would cause the arch, and hence the bridge, to collapse. The results of the present work can be consulted in detail in the work by [14]. Likewise, since the arch thickness of the inner parts of the vaults may not necessarily coincide with the thickness measured at the vault ends, an integral methodology was developed by integrating ground penetrating radar, aimed at determining the values of arch thickness across the entire vault. Details of this work can be found in [15].

**Figure 7.** (a) Geometric inventory software inspection; (b) *in situ* structural assessment from image rectification.



Similarly, the above methodology was implemented in the metric inspection tool of arches based on image rectification. This application, therefore, has photogrammetric rectification tools that allow metric documents to be obtained for use in the calculation of structural stability, as well as to perform both geometric inventories and routine inspections of the bridges. Within the framework of a bridge management system, this approach allows access to the real geometry of the structure in a simple way for the operator (improving safety and access), together with data digitalization and *in situ* structural



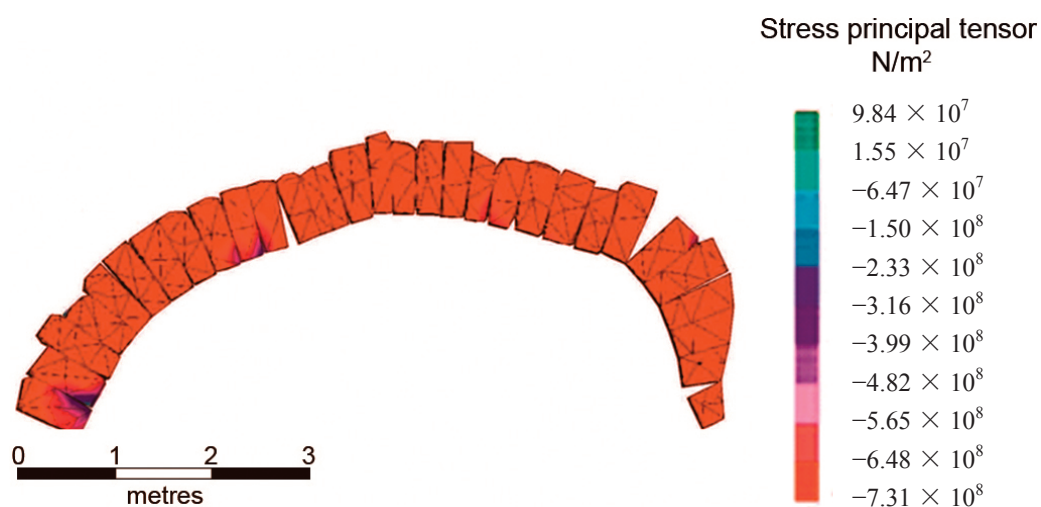
assessment. The next figure (Figure 7) shows a photo of the geometric inventory module over an image interactively, together with the results of the stability analysis of one of the arches studied.

### 3.3.2. 3D Structural Assessment Using Micromodeling Technique and Finite Element Modelling

In order to build more realistic structural models, the detailed 3D geometry of the structures was exported to platforms involving more sophisticated methods for the structural analysis, such as the case of the finite elements method (FEM). One of the methods consisted of modeling an arch bridge as a discontinuous model of voussoirs. This model was chosen according to the formulation of the plastic analysis that allows masonry arches to be analyzed through the line of pressure that transforms the arch into a mechanism, when the truss line reaches the limit of the arch ring at a sufficient number of points (joints).

The discontinuous model was created by photogrammetric restitution of the points that delimit each of the granite voussoirs of the arch. Joints between voussoirs do not transmit tensile stresses, so contacts were modeled, allowing only the transmission of compression stresses, with no displacements between the blocks and no resistance to traction. The stone was assumed to deform elastically, and the behavior of the arch was evaluated under monotonic variation of loading. In the model built, it was possible to estimate the collapse loads from the diagram that related load and displacement between blocks, obtained by varying the loads in an iterative process, determining load peaks. For each voussoir and load level analyzed, a finite-element model was built, determining the distribution of stresses inside each block and at the interfaces. The FEM model of the voussoirs was built using tetrahedral elements with second-order interpolation, with three degrees of freedom per node (translation). The contact defined between voussoirs allows the connection between nodes and faces of contiguous elements [16]. The next figure (Figure 8) shows the distribution of stresses in the 3D model, in which it is easy to note the formation of the collapse mechanism. The details of the methodology used for this case can be consulted in [16].

**Figure 8.** Distribution of stresses and the appearance of plastic hinges during the formation of a mechanism in the geometric model built from the photogrammetric survey.



### 3.3.3. Determination of the Structural Failure of Arches on the Basis of Information from the First Hinge: FEM in 2D

As in the previous case, starting out with detailed information about the geometric reality of masonry arches, it was possible to validate methodologies for the determination of critical loads using elastic frame analysis. To accomplish this, accurate elevation plans of bridges were imported into software for planar structural analysis using the finite elements method. The methodology consisted of defining the arch ring in detail from the photogrammetric restitution. Following this, the analysis consisted of assessing the internal forces for the loads applied assuming elastic behavior for the material, since the deformations caused by the loads are minimum. Based on the information about the first hinge, a plastic analysis was performed until the mechanism appeared. It was thus possible to compare the critical load values for both situations. A detailed description of this can be seen in [17].

## 4. Preliminary Findings in the Automation of Road Monitoring: Results and General Discussion

### 4.1. New Tools for Road Inventory

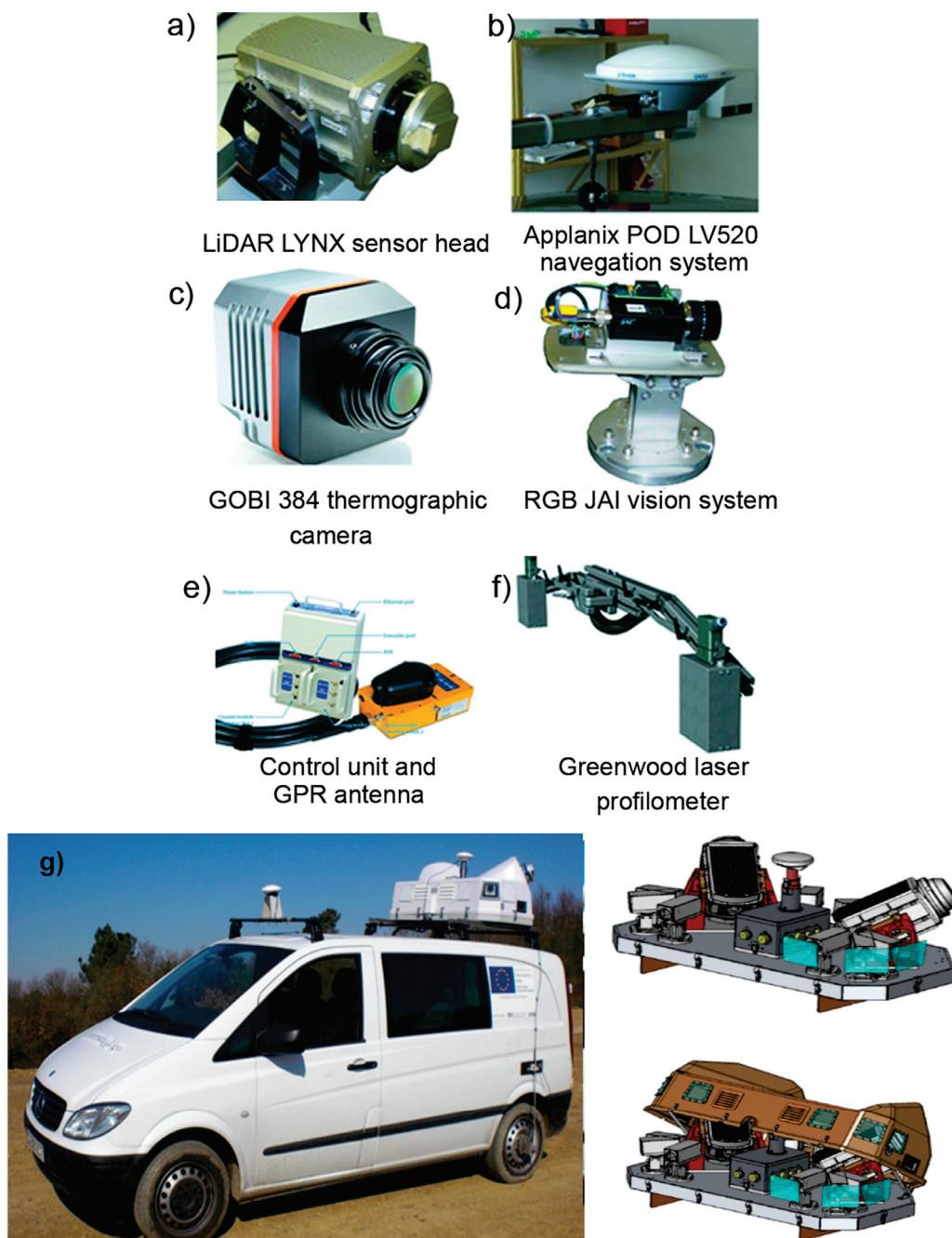
From the experience obtained in the above investigations, in 2010, a project was started up based on the same technologies, but was much more ambitious: the development of a mobile mapping unit with the final aim of automating the geometric inventorying and inspection of both roads and their associated infrastructures. The core idea was to obtain high productivity in performing the inspection works and avoiding subjectivity in the diagnosis of the current state of the infrastructures.

The need therefore arose to have a vehicle-laboratory that would allow the acquisition and management of all of the field data, with the best degree of automation possible. This led to the creation of a mobile inspection unit, composed of different geomatic elements or sensors necessary for the collection of data of the infrastructures, together with software applications and processes for the synchronization of sensors and georeferencing of the information gathered. The mobile mapping system allows the massive monitoring of elements (pavements, tunnels and slopes) and functions synchronously with the motion of the vehicle, as explained in Section 3.2, so that measurements can be georeferenced automatically. The inspection unit is integrated by:

- A laser scanning system composed of two LiDAR sensor heads; the system is the Lynx Mobile Mapping from Optech (Section 2.2) (Figure 9a).
- A navigation system for georeferencing information and synchronizing the data acquired. The unit installed in the vehicle was the LV 520 from Applanix (Section 2.2) (Figure 9b).
- A thermographic camera. This sensor allows the capturing of thermographic images in motion with the purpose of detecting thermal differences on the surfaces measured. The thermographic camera selected for the vehicle was a GOBI 384 camera from Xenics (Figure 9c).
- A multi-camera computer viewing system. A set of four JAI RGB cameras was installed for the capture of images in motion (Figure 9d).
- A ground penetrating radar, integrating an antenna with several frequencies, which allows the inspection of the subsoil between 0 and 1 m. A Ground Couple system from MALA Geosciences was used (Figure 9e).

- A laser profilometer from the Danish company, Greenwood, which allows the measurement of the International Regularity Index (IRI) [18] of roads by means of the use of two laser rangefinders (Figure 9f).
- The vehicle offers a step forwards in the state-of-the-art of road inspection in which the various sensors used have been integrated for the first time (Figure 9g).

**Figure 9.** (a) LiDAR LYNX sensor head; (b) Applanix POD LV520 navigation system; (c) GOBI 384 thermographic camera; (d) RGB JAI vision system; (e) control unit and GPR antenna; (f) Greenwood laser profilometer; (g) vehicle for the inspection of roads and associated infrastructures; (right) detail of the disposition of LiDAR heads, cameras and GNSS antenna.

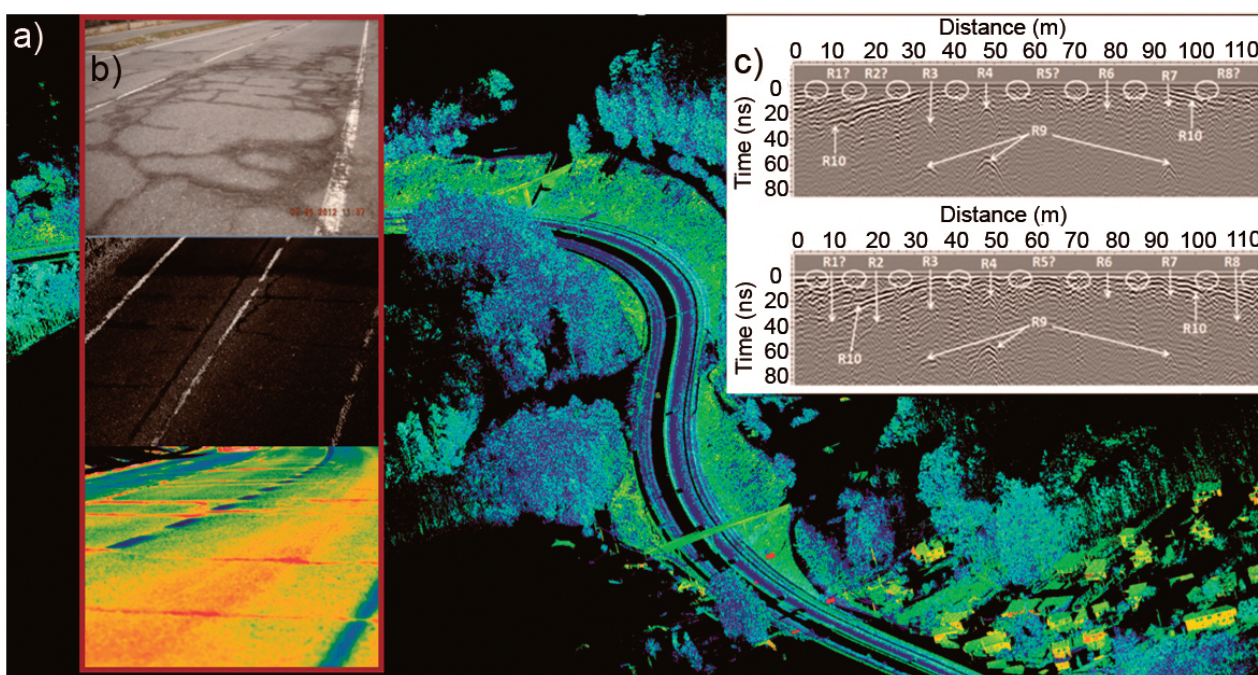




Each time the vehicle sets off on a measuring excursion, it is able to reconstruct the 3D geometry of the surroundings (up to 200 m) of the route followed by it, with centimeter precision.

At the same time, the vehicle records visible and thermographic images of elements of interest (pavement, structures, *etc.*). Figure 10 shows some of the data recorded by the different sensors integrated in the vehicle. The data provided by each sensor are used for inspections and individual analyses of each element and, at the same time, feed the geometric inventory parameters of the road and associated elements

**Figure 10.** (a) View of a point cloud of a highway; (b) visualization of cracks on the pavement through a visible image, point cloud and thermogram; (c) 2D radargrams acquired on a bridge that show the characteristics of the internal structure of the work.



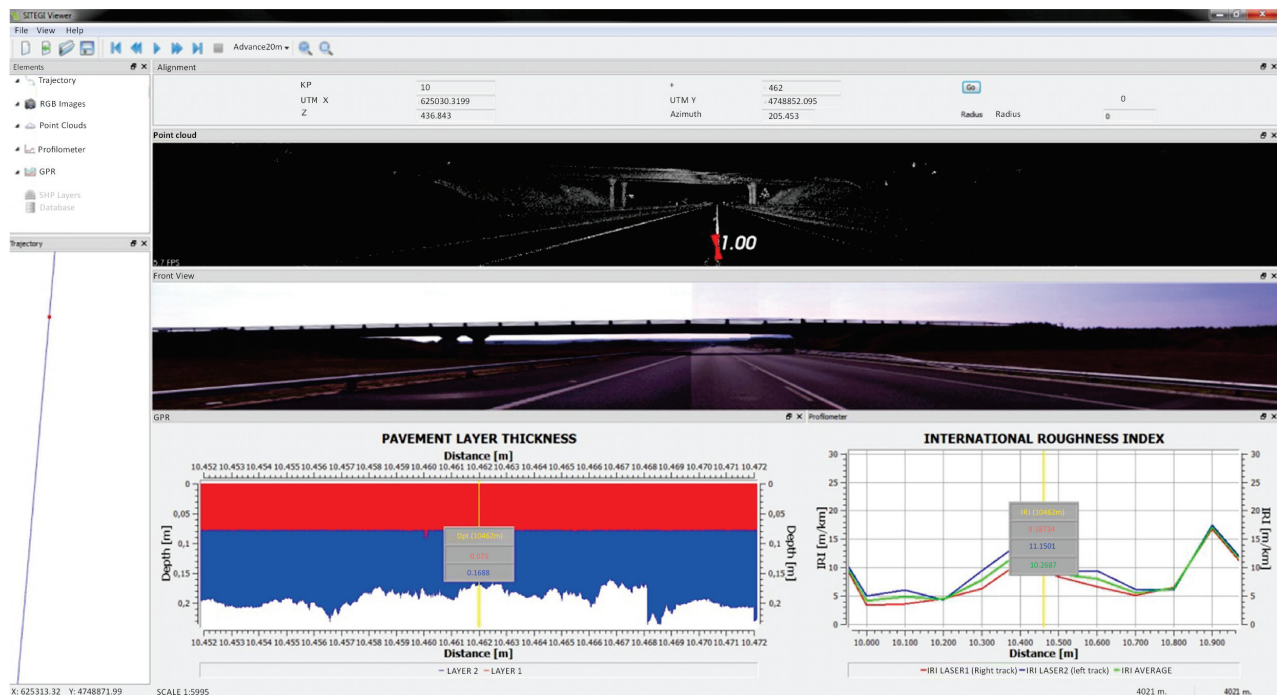
#### 4.2. Management Software

For the handling of all of the information gathered by the inspection unit, a software application was developed that allows the visualization and editing of the database that constitutes a management system of road infrastructures. The software application consists of a tree view, which encloses those elements imported from the different sensors. By means of this tree view, it is possible to achieve the configuration, pre-visualization and access to certain properties of the elements.

The right-hand side of the screen is a visualization area. As mentioned, since all of the elements are linked to the trajectory data, it is possible to navigate through the elements synchronically with the trajectory. The application allows the advance in the trajectory to be configured at 1, 5 and 20 m, and it is also possible to increase or decrease the duration of this interval. Furthermore, it is possible to move the visualizing point to a particular milestone of the road to provide the inventory or inspection data required by the database of the management system.

The next figure (Figure 11) shows the application interface in which (from left to right and from top to bottom) the following can be seen: the window with the trajectory of the vehicle, a colored point cloud with intensity data concerning the return of the laser beam, a RGB panoramic image, a window to evaluate pavement thickness derived from GPR data and a window with the IRI of the pavement in that stretch.

**Figure 11.** Road management software interface with windows showing the data acquired from different sensors.



#### 4.3. Geometric Road Inventory and Trends toward Automation

One of the original aims of the project was to develop a management system that integrates the geometric inventory and routine inspection database, whose data is directly extracted from massive inspection campaigns with the mobile inspection unit. The database developed is able to store all of the information established in the codes of the Spanish Transport Administration. These tables are fed with the geometric and radiometric data recorded by the different geomatic sensors once they have been processed. It should be noted that the description of the inventory parameters is established not only on the basis of visible measurements, but also on the basis of the measurement of non-visible elements (pavement thicknesses and the presence of anomalies on the road surface).

In recent years, the scanning technique has proven to be highly suitable for different applications that require data processing adapted to specific individual problems. Accordingly, existing methodologies must be improved to guarantee the quality of the results sought in each case. This has meant that research into geomatic technologies has advanced towards the development of automatic data-processing algorithms. The issue is further exacerbated by the fact that the management of the information acquired with geotechnologies is no trivial task and normally demands advanced



knowledge of geomatics. Along these lines, another important limitation is the need to use highly specific software packages, which are usually expensive to purchase and maintain.

The use of platforms, such as MATLAB, is a highly suitable option, because they operate with a high-level technical computing language and offer an interactive environment for numerical calculus, visualization and the programming of algorithms for the automatic processing of point clouds. Several algorithms oriented towards the automation of the processes required for the inspection of road infrastructures, and structural assessment, can be found in the works of [19–22].

## 5. Conclusions

This work offers a review of the circumstances in which geomatic technologies were successfully applied to the structural assessment of infrastructures associated with roads. Initially, the photogrammetric and scanning laser techniques were successfully exploited to construct structural models that allowed an assessment of the structural safety of bridges. In these works, the detailed geometric models generated with the geomatic technologies were adapted for integration in different methods and calculation theories of these structures, from both 2D and 3D perspectives. Following this, thanks to the development of the scanning technique for mobile technology, vehicles integrating several synchronized geomatic sensors were built up for the documentation and assessment of road infrastructures.

Within a strategy aimed at automation during the management and maintenance tasks involved in road infrastructures, the development of new instruments for advanced inventorying/inspection that will allow the necessary information to be gathered from the efficient management of road infrastructures is considered to be crucial. The challenge addressed here consisted in the use of new vehicles with automated sensor systems for the acquisition of large volumes of geolocalized data that were later digitalized *in situ* (laser scanner, georadar, thermography, RGB cameras, profilometry, *etc.*). The development of an integrated management platform that offers a further step forwards as regards the objectivity and quality of the results of the inspection provides a noteworthy improvement in the productivity of all of the associated tasks and an improvement in the safety conditions of operators.

To exploit the whole volume of data, an integrated management platform was developed. Supported by a 3D GIS, this permitted the management of the geometric inventorying and inspection tasks of linear structures according to State norms concerning roads. This management platform allows operators to get into a virtual reality environment to complete all of the inspection tasks.

The present work shows that geomatic methods can not only contribute to documenting structures, but also that they are steadily becoming the basic sensors for the exploration, management and efficient maintenance of roads and their associated infrastructures.

## Acknowledgments

This work has been partially supported by the Spanish Ministry of Economy and Competitiveness through the project “HERMES-S3D: Healthy and Efficient Routes in Massive Open-Data based Smart Cities (Ref. TIN2013-46801-C4-4-R) and by Xunta de Galicia (Grant No. CN2012/269).

## Author Contributions

All authors contributed extensively to the work presented in this paper.

## Conflicts of Interest

The authors declare no conflict of interest.

## References

1. Dirección General de Tráfico. *Principales Cifras de la Siniestralidad Vial España 2013*; Dirección General de Tráfico: Madrid, Spain, 2013.
2. Ministerio de Fomento. *Los Transportes, y Las Infraestructuras Informe Anual 2012*; Centro de Publicaciones Secretaría General Técnica: Madrid, Spain, 2013.
3. Transportation Research Board 2013. *National Cooperative Highway Research Program 2013*; National Academy of Sciences USA: Washington, DC, USA, 2013.
4. González, H.; Riveiro, B.; Armesto, J.; Arias, P. Verification artifact for photogrammetric measurement systems. *Opt. Eng.* **2011**, *50*, doi:10.1117/1.3598868.
5. Riegl Laser Measurement Systems. Available online: <http://www.riegl.com/nc/products/terrestrial-scanning/> (accessed on 5 June 2013).
6. OPTECH. Homepage of the Company OPTECH. Available online: <http://www.optech.ca> (accessed on 5 June 2011).
7. Puente, I.; González, H.; Martínez, J.; Arias, P. Review of mobile mapping and surveying technologies. *Measurement* **2013**, *46*, 2127–2145.
8. Luhmann, T.; Robson, S.; Stephen, K.; Harley, I. *Close Range Photogrammetry: Principles, Methods and Applications*; Whittles Publishing of Caithness: Caithness, UK, 2006.
9. D.G. de Carreteras Ministerio de Fomento. *Guía para la Realización de Inventario de Obras de Paso*; Centro de Publicaciones Secretaría General Técnica: Madrid, Spain, 2009.
10. D.G. de Carreteras Ministerio de Fomento. *Guía para la Realización de Inspecciones Básicas de Obras de Paso*; Centro de Publicaciones Secretaría General Técnica: Madrid, Spain, 2009.
11. Ghilani, C.D.; Wolf, P.R. *Adjustment Computations: Spatial Data Analysis*, 4th ed.; John Wiley and Sons: New Jersey, NJ, USA, 2006.
12. Kalman, R.E. A new approach to linear filtering and prediction problems. *J. Basic Eng.* **1960**, *82*, 35–45.
13. Lourenço, P.B. *Computational Strategies for Masonry Structures*; Delft University: Delft, The Netherlands, 1996.
14. Riveiro, B.; Morer, P.; Arias, P.; de Arteaga, I. Terrestrial laser scanning and limit analysis of masonry arch bridges. *Constr. Build. Mater.* **2011**, *25*, 1726–1735.
15. Riveiro, B.; Solla, M.; de Arteaga, I.; Arias, P.; Morer, P. A novel approach to evaluate masonry arch stability on the basis of limit analysis theory and non-destructive geometric characterization. *Autom. Constr.* **2013**, *31*, 140–148.

16. Riveiro, B.; Caamaño, J.C.; Arias, P.; Sanz, E. Photogrammetric 3D modelling and mechanical analysis of masonry arches: An approach based on a discontinuous model of voussoirs. *Autom. Constr.* **2011**, *20*, 380–388.
17. Carr, A.J.; Jáuregui, D.; Riveiro, B.; Arias, P.; Armesto, J. Structural evaluation of historic masonry arch bridges based on first hinge formation. *Constr. Build. Mater.* **2013**, *47*, 569–578.
18. Sayers, M.W.; Gillespie, T.D.; Paterson, W.D. Guidelines for the conduct and calibration of road roughness measurements. *World Bank Tech.* **1986**, *46*.
19. Milani, G.; Esquivel, Y.W.; Lourenço, P.; Riveiro, P.; Oliveira, D.V. Characterization of the response of quasi-periodic masonry: Geometrical investigation, homogenization and application to the Guimarães Castle, Portugal. *Eng. Struct.* **2013**, *56*, 621–641.
20. Gonzalez, H.; Puente, I.; Martínez, J.; Arias, P. Automatic segmentation of road overpasses and detection of mortar efflorescence using mobile LiDAR data. *Opt. Laser Technol.* **2013**, *54*, 353–361.
21. Riveiro, B.; González, H.; Varela, M.; Jauregui, D.V. Validation of terrestrial laser scanning and photogrammetry techniques for the measurement of vertical underclearance and beam geometry in structural inspection of bridges. *Measurement* **2013**, *46*, 784–794.
22. Holgado, A.; Gonzalez-Aguilera, D.; Arias, P.; Martinez, J. Semiautomatic extraction of road horizontal alignment from a mobile LiDAR system. *Comput.-Aided Civil Infrastruct. Eng.* **2014**, doi:10.1111/mice.12087.

© 2014 by the authors; licensee MDPI, Basel, Switzerland. This article is an open access article distributed under the terms and conditions of the Creative Commons Attribution license (<http://creativecommons.org/licenses/by/3.0/>).



### **3.2 The Integration of Geotechnologies in the Evaluation of a Wine Cellar Structure through the Finite Element Method**

#### **RESUMEN**

Esta publicación desarrolla una metodología basada en la integración de técnicas geomáticas no invasivas, como el TLS y el GPR, con el análisis numérico mediante el método de elementos finitos. El objetivo final es generar modelos precisos de simulación numérica que permitan evaluar estructuralmente una edificación subterránea. Para validar esta metodología se ha empleado como caso de estudio la Bodega del Ayuntamiento de Toro (España), donde este tipo de construcciones juegan un papel importante, económica y culturalmente, en la industria vitícola de la región.

La falta de información histórica, el desconocimiento de la geometría inicial y de las características físicas de los materiales, motivan el desarrollo de un método de trabajo que aproveche las sinergias obtenidas de la hibridación del TLS y el GPR. Así los datos obtenidos del estudio con el TLS proporcionan información detallada, en forma de una nube de puntos, que contiene la geometría externa de la bodega. Tras un procesamiento de la información se concibe un modelo geométrico en 3D y en formato CAD.

Por su parte los perfiles obtenidos de la prospección geofísica con el GPR identifican las características físicas de los elementos constituyentes. Esta información es georreferenciada con el modelo geométrico obtenido con el TLS, consiguiendo una caracterización detallada de la geometría externa e interna de la bodega.

El modelo geométrico CAD, resultante del procesamiento de las nubes de puntos provenientes del TLS, es implementado de manera semiautomática para su simulación estructural mediante un modelo continuo por elementos finitos. A partir de la teoría de los estados límites se analizan las tensiones y deformaciones a las que está sometida la bodega, identificando zonas críticas de la estructura como esfuerzos de tracción excesiva y patrones de agrietamiento.

Como resultado de la actividad investigadora desarrollada, es posible concluir, que la hibridación de técnicas geomáticas no invasivas, TLS y GPR, junto con la simulación por elementos finitos, permite disponer de manera rápida y eficaz de modelos numéricos capaces de evaluar estructuralmente el estado actual de una construcción subterránea. Esto posibilita determinar los valores límite de carga, y servir de herramienta de decisión en la planificación de acciones de rehabilitación y mantenimiento de la arquitectura patrimonial.

Case Report

## The Integration of Geotechnologies in the Evaluation of a Wine Cellar Structure through the Finite Element Method

Alberto Villarino <sup>1</sup>, Belén Riveiro <sup>2,\*</sup>, Diego Gonzalez-Aguilera <sup>1</sup> and Luis Javier Sánchez-Aparicio <sup>1</sup>

<sup>1</sup> Department of Land and Cartographic Engineering, High Polytechnic School of Avila, University of Salamanca, Hornos Caleros, 50, 05003 Avila, Spain; E-Mails: avillarino@usal.es (A.V.); daguilera@usal.es (D.G.-A.); luisj@usal.es (L.J.S.-A.)

<sup>2</sup> Department of Material Engineering, Applied Mechanics and Construction, School of Industrial Engineering, University of Vigo, Rúa Maxwell s/n, Campus Lagoas Marcosende, 36310 Vigo, Spain

\* Author to whom correspondence should be addressed; E-Mail: belenriveiro@uvigo.es; Tel.: +34-986-813-661; Fax: +34-986-811-924.

External Editors: Henrique Lorenzo, Nicolas Baghdadi and Prasad S. Thenkabail

Received: 23 June 2014; in revised form: 29 October 2014 / Accepted: 30 October 2014 /

Published: 11 November 2014

---

**Abstract:** This paper presents a multidisciplinary methodology to evaluate an underground wine cellar structure using non-invasive techniques. In particular, a historical subterranean wine cellar that presents a complex structure and whose physical properties are unknown is recorded and analyzed using geomatics and geophysics synergies. To this end, an approach that integrates terrestrial laser scanning and ground penetrating radar is used to properly define a finite element-based structural model, which is then used as a decision tool to plan architectural restoration actions. The combination of both techniques implies the registration of external and internal information that eases the construction of structural models. Structural simulation for both stresses and deformations through FEM allowed identifying critical structural elements under great stress or excessive deformations. In this investigation, the ultimate limit state of cracking was considered to determine allowable loads due to the brittle nature of the material. This allowed us to set limit values of loading on the cellar structure in order to minimize possible damage.

**Keywords:** masonry structure; terrestrial laser scanning; ground penetrating radar; sensor registration; finite element method

---

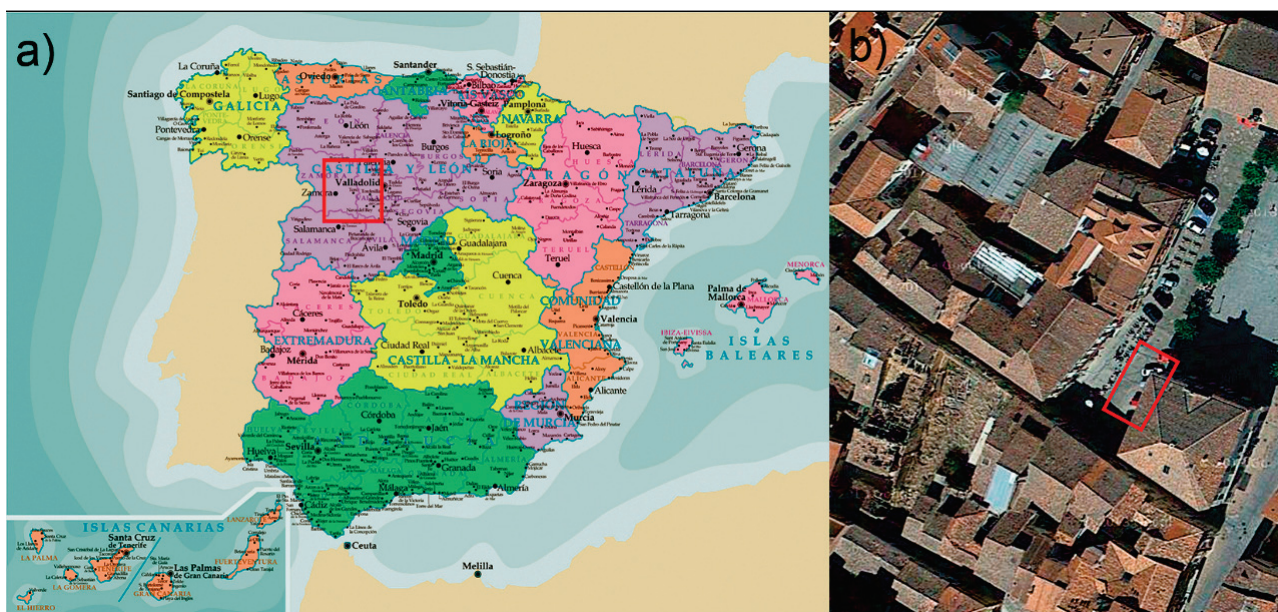


## 1. Introduction

In Castilla-Leon region, wine cellars constitute a patrimonial legacy of singular value. The types of materials and forms of construction are very diverse. In addition, the wine industry plays an important role in the agricultural economy in this region. It is a sophisticated industry, which provides a high added value, but deeply rooted in socio-cultural customs and traditions. This strong combination between modern and traditional systems has made the wine industry the main key for economic development in these areas. Through regulatory policies, the traditional production and marketing systems related to wine have been improved, providing also added value on all heritage elements related to wine.

In this paper, we focus on the study case of “Toro’s Council” wine cellar due to its complex geometry, unknown materials, internal structure analysis and, last, but not least, its heritage restoration. The underground structure is located in the municipality of Toro (Zamora) in the west of Spain (Figure 1a). This wine cellar was built centuries ago as a part of a noble building of great historical and architectural value; today, it forms part of the underground of the Town Hall of Toro (Figure 1b). Over the years, this historic building has suffered decay, invasion of vegetation in walls, paths and even major changes as a result of urban development. At present, policies to promote the wine regions are clearly committed to architectural restoration and rehabilitation of this wine cellar. Thereby, they recover their importance by fitting to more modern uses, becoming elements that reinforce the cultural identity. However, given the underground features of this wine cellar, it has been necessary to integrate different sensors, such as terrestrial laser scanner (TLS) and non-invasive ground penetrating radar (GPR), in order to perform thorough research.

**Figure 1.** (a) Location of the wine cellar: Toro, Zamora, Spain; (b) top view and location of the “Toro’s Council” wine cellar.





The conjunctions of TLS and GPR provide us a whole metric 3D structure of the external and internal areas inside the wine cellars. In particular, GPR geophysical methods enable the identification of the size, shape and direction of inaccessible areas, such as walled, hidden areas or areas where there have been landslides. Multidisciplinary approaches have been applied for the documentation of historic structures, as is the case of: [1], who applied GPR and photogrammetric techniques to document megalithic tombs; and [2,3], who applied digital photogrammetry and GPR, to evaluate structural damages and possible failures of a mediaeval bridge. Recently a combination of GPR and electrical resistivity tomography (ERT) techniques has been applied to reveal hidden archaeological structures in a mausoleum [4] and in the Acropolis to reveal a bronze foundry complex [5]. On the other hand, in the context of geology and not for archaeological and heritage documentation, [6] used a combination of geomatics and geophysical methodologies for geomorphology characterization of a small mountainous catchment in Scotland. Specifically, they used a TLS (Riegl LPM-i800HA) to create a detailed digital terrain model (DTM) and the Differential Global Positioning System (DGPS) to complement the other geophysical techniques. In a similar way, [7] used TLS data in combination with GPR and ERT to evaluate the stability of cliff sites; more recently, [8] employed a multidisciplinary approach based on GPR, ERT and TLS to investigate the responses of slope stability due to climatic changes in high alpine rock walls.

In this paper, we perform a detailed characterization of the geometry and internal material for the structural evaluation of an underground wine cellar. The approach developed copes with the external geometry applying TLS equipment and with the internal structure using GPR data. Finally, a structural evaluation of the wine cellar based on the previous data and supported by the finite element method (FEM) is applied. The paper is structured as follows: after this introduction, Section 2 describes the sensors used, as well as the methodology developed, putting special emphasis on the pass from the laser point cloud to the computer-aided design (CAD) model, as well as its structural analysis. Section 3 outlines the experimental results, including a technical discussion. A final section is devoted to put across the main concluding remarks.

## **2. Materials and Methods**

When performing a structural modelling of any structure, several models must be considered. First, a conceptual model that represents the physical reality of the structure has to be defined by means of its geometrical description and boundary conditions. Then, a mathematical model that describes the behavior of the structure has to be established. The mathematical or structural model basically refers to the relationships between the variables and parameters that describe the physical model, the constitutive law of materials and the basic theories that model the structural behavior. In this article, the reconstruction of the physical model is assisted by geomatic methods, such as TLS and GPR. Then, the structural modelling was performed following the basis of the classical plate theory by using FEM.

### *2.1. Geometric Reconstruction*

A geomatic survey was conducted in order to generate a 3D model accurately describing the structure of the wine cellar. For that purpose, TLS and GPR techniques were integrated.

### 2.1.1. Terrestrial Laser Scanner for External Geometry

A time-of-flight (ToF) TLS, Trimble GX, was used for recording external geometry (Figure 2a). This scanner covers a field of view of 360° in the horizontal direction and 60° in the vertical direction, enabling the collection of full panoramic views. The distance measurement is obtained with a nominal accuracy of 2 mm at a 10-m range using a wave length of 532 nm. The vertical angular step-width is 0.0014°, and the horizontal one 0.0012°. The diameter of the laser spot is 1 mm at 10 m. The system is able to measure 5000 points per second. The scanner incorporates a dual axis compensator, so the vertical Z-direction is perfectly defined during data acquisition.

Because of the vertical direction limitation, four scanner stations with a resolution of 1 cm at 10 m were required to enclose the whole area. The resulting point cloud (about 4 million) not only generated three-dimensional coordinates (XYZ) of points, but also their intensity values (I) processed using 8-bit electronics. Likewise, all of the profiles defined in the geophysical prospection were identified with artificial targets and georeferenced with the TLS in order to reach valid conclusions. In particular, as we seek to integrate the underground geometry (GPR) of the wine cellar with the results of TLS survey, it was necessary to define a network of control points defined by planar targets performing as a local reference coordinate system. The definition of the reference system is a key factor enabling the results of different methodologies (TLS and GPR) to be merged and compared.

This operation requires the location of these targets along the profiles defined for the GPR measurements, as well as several targets placed in other vertical walls and their own floor for aligning the four scanner stations that enclose the whole external geometry.

### 2.1.2. Ground Penetrating Radar for Internal Structure

A GPR equipment, RIS MF HI-MOD 200–600 MHz (Figure 2b), was used in order to provide information about the internal structure and materials of the cellar, achieving greater efficiency in occluded areas. This equipment was chosen due to its favorable compromise between spatial resolution and depth of detection. This antenna provides 6 m in-depth penetration (under optimum conditions) and a vertical resolution of 5 cm, which indicates the differentiation of two adjacent signals, like different events [9].

Data were acquired with trace intervals of 2 cm and time windows of 100 ns. A total of 4 parallel profiles were surveyed with a distance between profiles of 1 m. Since there was not too much information available about the modification works done in the wine cellar over time, the walls selected were those that at first sight appeared to be built later than the original wine cellar construction, a feature that could indicate the continuity of the wine cellar behind the wall. The workflow followed in the definition of the profiles tries to solve two main problems: (i) tracing profiles with enough length to distinguish the reflections correctly, so that vertical profiles were surveyed; (ii) providing the best interpretation of the profiles based on the TLS georeferencing.

On the other hand, two additional profiles were surveyed and considered as a reference. These reference profiles consist of registering data (TLS and GPR) at locations in which the composition of what exists underground was previously known. The *in situ* procedure consisted of using the walls whose faces are visible following the procedure presented in [10]. The external geometric model was

achieved using the TLS, whereas the morphologic composition of the wall was deduced from the visible walls. Then, a georeferenced grid (at both of the wall faces), using flat reflective targets, marked the path of the antennas during the calibration, and so, this combined information assisted the calibration model and, thus, the registration of TLS and GPR under the same coordinate system. In this way, a first reference profile was surveyed in a wall with a known hole behind; a second reference profile was surveyed in a wall where the composition of material behind was known (conglomerate in a reddish brown clay matrix, corresponding to “Toro’s Red Facies”).

**Figure 2.** (a) Terrestrial laser scanner used for the recording of the external geometry, Trimble GX; (b) ground penetrating radar equipment, RIS MF HI-MOD 200–600 MHz.



### 2.1.3. Data Processing

Geometric data processing was performed following four steps:

- Cleaning and segmentation of point clouds. Data preprocessing may also include manual or automated filtering to remove undesired data, such as reflections, noise or sensor artifacts.
- Alignment. The point clouds from each scan are initially represented in the scanner's local coordinate frame. All of the data need to be aligned in a common coordinate system through a process known as alignment. An automated registration method, iterative closest point (ICP) [11], was applied, supported by the identification of matching points.
- Generating a CAD model. Since the FEM model does not cope with dense laser 3D models, an important step that allows us to pass from 3D point clouds to a solid model was performed. In this case, once the point cloud was converted into a triangulated mesh, cross-sections were extracted, and surface extrusions were performed as follows: first, horizontal and vertical cross-sections were obtained from the mesh in order to represent the basic geometry of the wine cellar. Then, the 3D solid of the wine cellar was modelled by extruding the horizontal cross-section vertically, based on the constraints of the vertical cross-sections.
- Before interpretation of the internal structure, GPR processing filters (low-pass and high-pass filters) were employed in order to reduce any unwanted noise in the raw data. This allowed enhancing

the differences in the information composed of the signals received, and an image of the subsurface (radargram) was produced, including all of the features and/or targets of interest. Consequently, GPR data interpretation could be performed easier. Each radargram was processed by Spiview software by applying the following processing workflow: deconvolution (to improve resolution and avoid multiple reflections); Hilbert's transformation (to obtain some properties of the traversed matter); migration (to provide the true geological position), spectral transformation (to improve resolution and amplify certain signals) and spatial filtering (fast Fourier transform was applied to decrease the effects of noise).

As a result of this process, a final cartographic map in 3D space containing both surface evidence provided by TLS and the GPR interpretation was obtained. In particular, the metric information obtained allowed calibrating radar wave velocities accurately in different zones of the structure, as shown in Section 2.1.2. Knowledge of the most appropriate radar wave velocity allowed for a more exhaustive interpretation of the GPR data. All of the TLS and GPR data processed were used to build a 3D finite element model of the wine cellar.

## 2.2. Structural Modeling

As stated above, the geometric model was built to support the structural analysis. Having a detailed geometric reconstruction of the cellar may allow one to perform a realistic structural evaluation of the built up construction. The simulation of the structural behavior was done following the mathematical principles of classical plates theories.

The Mindlin-Reissner theory of plates [12,13] is an extension of the Kirchhoff-Love plate theory that takes into account shear deformations through the thickness of a plate. These theories are intended for thick plates in which the normal to mid-surface remains straight, but not necessarily perpendicular to the mid-surface. The Mindlin-Reissner theory is used to calculate the deformations and stresses in a plate whose thickness is of the order of a tenth the planar dimensions, while the Kirchhoff-Love theory is applicable to thinner plates.

### 2.2.1. Materials

Modelling the material properties of a historical masonry structure is quite challenging, particularly in the absence of field and laboratory tests. The construction material of the winery is limestone, and according to [2,14,15], a linear and isotropic elastic behavior is assumed. The main mechanical properties of limestone are defined according to [11], the specific weight ( $\gamma$ ) being 27 kN/m<sup>3</sup>, the compressive strength established as  $4 \times 10^4$  kN/m<sup>2</sup>, the tensile strength taken as a tenth of the compressive strength, the Young's modulus of elasticity (E) with a value of  $3.2 \times 10^6$  kN/m<sup>2</sup> and a value of 0.2 for the Poisson's coefficient ( $\nu$ ) taken according to [16].

### 2.2.2. Boundary Conditions

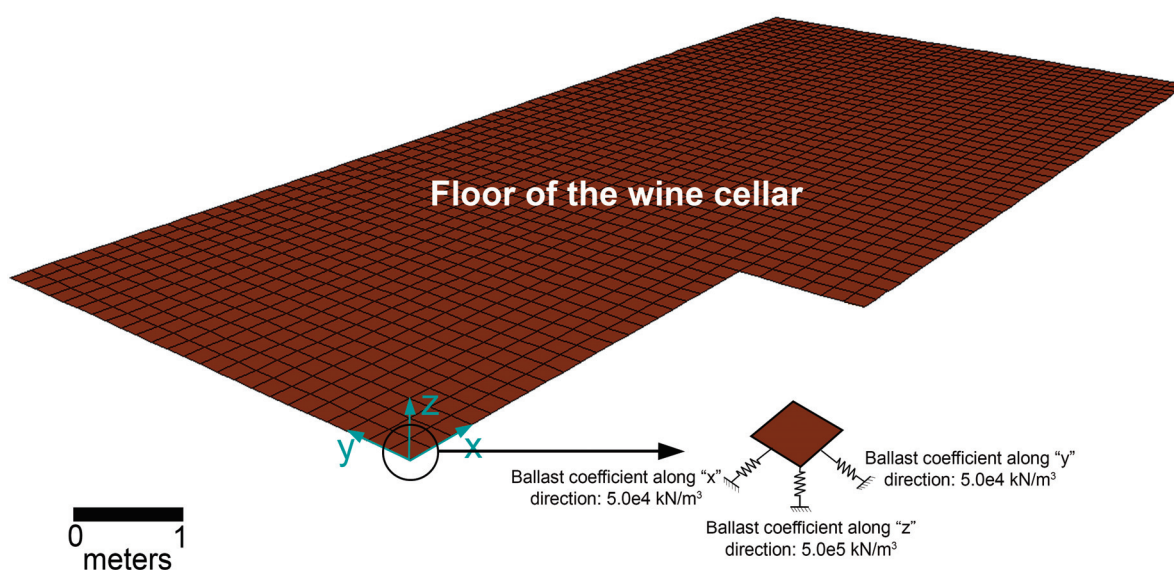
Due to the peculiarity of the construction (*i.e.*, a wine cellar), only constraints on the soil are defined, which restrict the movements in the two horizontal directions and in the vertical. These



constraints are modeled by linear elastic supports, with an elastic coefficient, calculated on the basis of a ballast coefficient that represents the interaction soil-winery.

More specifically, these supports are modeled through the area elements of the ground of the winery with a ballast coefficient estimated as  $5 \times 10^5$  kN/m<sup>3</sup> in the vertical direction according to [17,18]. This is a high value because of being a consolidated soil for years. A ballast coefficient in both horizontal directions was used to compensate for the asymmetry of loads. The ballast coefficient for horizontal loads was equivalent to a tenth of the vertical one. Figure 3 shows the floor model of the wine cellar with the boundary conditions imposed at one of the shell elements; the same boundary conditions are applied to the rest of shell elements.

**Figure 3.** Boundary conditions at the floor of the wine cellar.



### 2.2.3. The Computational Model

Once the conceptual model was created, it was exported to the Drawing Exchange Format (DXF), which allowed the importation of the 3D model into the software for structural analysis. The software SAP 2000 was used to perform the structural computations [19].

For the structure under study, the FEM was defined using a planar shell model whose elements are defined by 4 nodes with 6 degrees of freedom each (shell-thick type), which take into account the contribution of the shear stiffness of the plate, according to the theory of plates in [12,13]. As a result, a model consisted of 8087 nodes and 8122 elements.

Planar elements instead of volumetric ones were selected due to the constant thickness of cellar walls. This simplification allowed carrying out calculations with a better computational performance, preserving the accuracy of the structural model. The averaged thickness of walls was found to be 0.4 m in the elevation walls of the cellar and 0.4 m for the upper walls, corresponding to the barrels.

It is important to note that two large categories of computational models exist: discontinuum models and continuum models. In a discrete or discontinuum model formulation, the structure is divided into large discrete deformable parts connected with interfaces [20]. A unilateral law, possibly

with friction, describes the behavior of the contact surface in each interface, while the discrete elements are assumed to behave elastically. When modelling a masonry structure, building discrete models seems to be a more realistic approach for the representation of the mechanical behavior of the structure. Nevertheless, this approach is computationally very costly, first, due to the geometric description of all of their masonry blocks and also interfaces, and second, due to the requirement of difficult numerical methods [21].

In continuum model approaches, the walls are assumed to be composed of a single material whose mechanical behavior is described by a non-linear constitutive law [22] or the different mechanical behavior between stone and mortar and the anisotropy induced by them are taken into account on the basis of a homogenization theory [23]. For the computational modelling of the wine cellar presented here, a continuum model was used. In particular, a 3D FEM based on the overall geometry taken from TLS was considered, whereas the GPR survey gave important general information about the internal composition of the wine cellar walls. As a result, on site measurements could be applied to make the computer simulation more reliable.

The purpose of the structural modelling was to detect critical zones in the structure and compare these zones with both geomatic results and visual inspection. Cracking is one of the main failure problems of masonry structures. It is assumed that cracking happens when stress reaches a critical failure surface.

#### 2.2.4. Loading Conditions

Different actions were taken into account for the structural simulation:

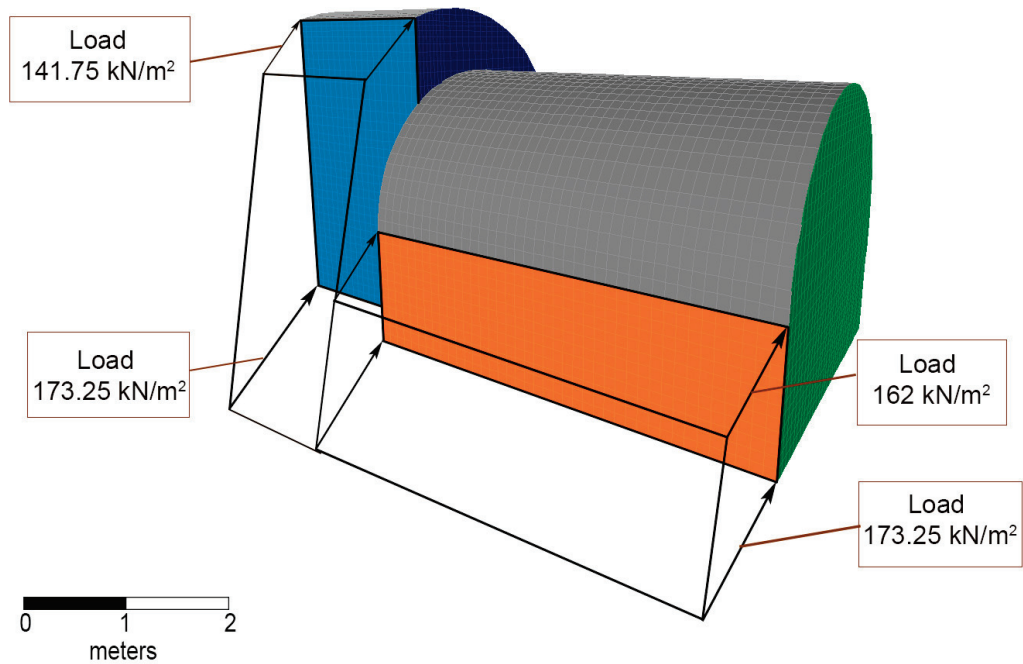
- Dead load (*DL*): defined by the specific weight and the volume of the structural elements of the wine cellar according to the geomatic results.

- The permanent load of the ground (*PLg* ground) is one of the most important loads over the wine cellar and represents the thrust caused by soil on the walls and vaults. The maximum thrust on walls has been calculated using the Rankine theory [24], considering active thrust, since it is assumed that the displacement of walls is subtle. The soil thrust on the walls defining the envelope of the building is considered to be a trapezoidal load. The wine cellar comprises 8 walls with different geometry and upper bounds, so that there are different values of thrust on each wall. As an example, Figure 4 shows the value of soil thrust on two walls of the wine cellar.

The soil thrust on the vault required a different calculation: due to the curved shape of the vault, the soil thrust would result in a hardly-measurable inclined load. This was therefore modelled through finite elements; the vault and the soil above were independently modelled in order to obtain an estimation of the soil loading over the vault as realistic as possible.

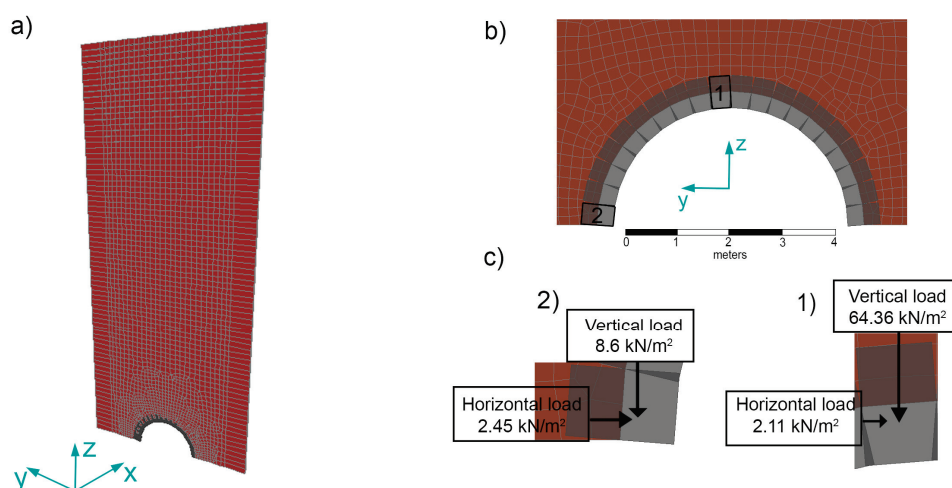
- The data considered for the soil were: specific weight of  $18 \text{ kN/m}^3$ , modulus of elasticity (*E*) of  $8 \times 10^4 \text{ kN/m}^2$  and an internal angle of friction of  $30^\circ$ , according to [18]. Historic documents relate that the height of soil over the vault is 19 m. The model of the vault and the soil consists of a 1 m-thick flat model (Figure 5a). The vault was modeled through 30 discrete bar-type elements, with a length of 25 cm each and a cross-section defined by a thickness of 40 cm and a width of 10 cm.

**Figure 4.** Values of soil thrust on two walls of the wine cellar.



This model provided a value for the thrust caused by soil and the permanent load of the building (*PLb* building) at each element of  $5 \text{ kN/m}^2$  [25]. Figure 5 shows forces acting for two of the elements; the others were obtained analogously.

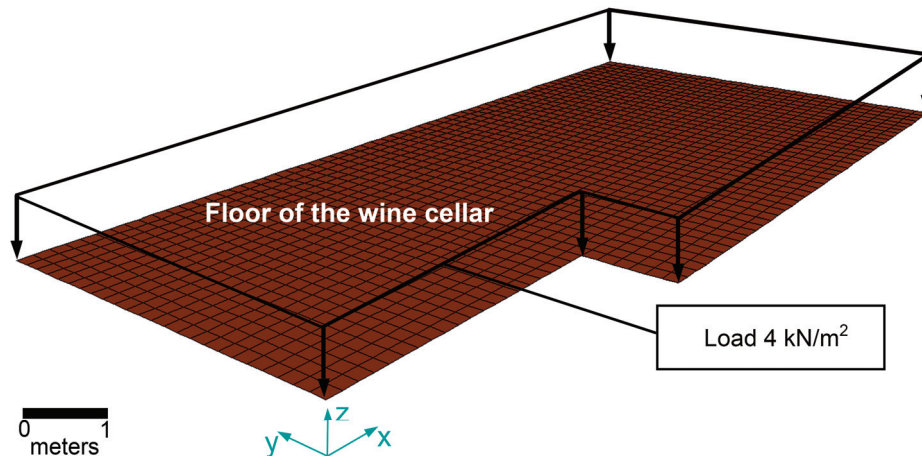
**Figure 5.** (a) Ground-vault model; (b) ground-vault mesh detail; (c) vertical and horizontal thrust (due to weight soil and the permanent load of the building above the wine cellar) over two vault elements.



- Live loads (*LL*) are those loads due to the presence of people inside the cellar and the building; values were taken from [25]. This load includes a service overload of  $3 \text{ kN/m}^2$  in the upper building (*Sb* Building use) and a service overload of  $4 \text{ kN/m}^2$  in the cellar (*Sc* Cellar use). Following the same

procedure explained above, the new live loads on the vault of the cellar were estimated. The service load of  $4 \text{ kN/m}^2$  was introduced as a uniformly distributed load (Figure 6)

**Figure 6.** Service load of  $4 \text{ kN/m}^2$  on the floor of the wine cellar.



The limit states are states beyond which the structure no longer satisfies the design performance requirements; these are classified as ultimate limit state and serviceability limit state. The ultimate limit state (*ULS*) [26] concerns the safety of people and/or the safety of the structure and is the state associated with structural collapse or other similar structural failures, such as excessive deformation, transformation of the structure or any part of it into a mechanism, rupture (cracking) and loss of stability of the structure or any part of it, including supports and foundations. The serviceability limit state (*SLS*) [26] concerns the functioning of the structure or structural members under normal use and the comfort of people. Both limit states will be analyzed for the wine cellar. There are two live loads applied to different areas; therefore, two loading combinations will be calculated for each of these states with different safety coefficients. The combinations of loads and coefficients were estimated according to [26]. Table 1 details the load combinations and the applied coefficients for each limit state and the type of load.

**Table 1.** Load combinations and applied coefficients according to the limit state and the type of load. *SLS*, serviceability limit state; *ULS*, ultimate limit state.

Limit State	Load-Coefficient Type				
	<i>DL</i>	<i>Sb</i>	<i>Sc</i>	<i>PLb</i>	<i>PLg</i>
<i>SLS1</i>	1	0.7	1	1	1
<i>SLS2</i>	1	1	0.7	1	1
<i>ULS1</i>	1.35	1.5	1.05	1.5	1.35
<i>ULS2</i>	1.35	1.05	1.5	1.5	1.35

### 3. Experimental Results and Discussion

The described method has been tested for one of the most representative cellars of the region of Toro, Zamora (Spain): The Town-Hall Cellar. The construction of the cellar of the Town-Hall of Toro took place in 1778 according to the headstones that lie next to the main entrance door. The famous



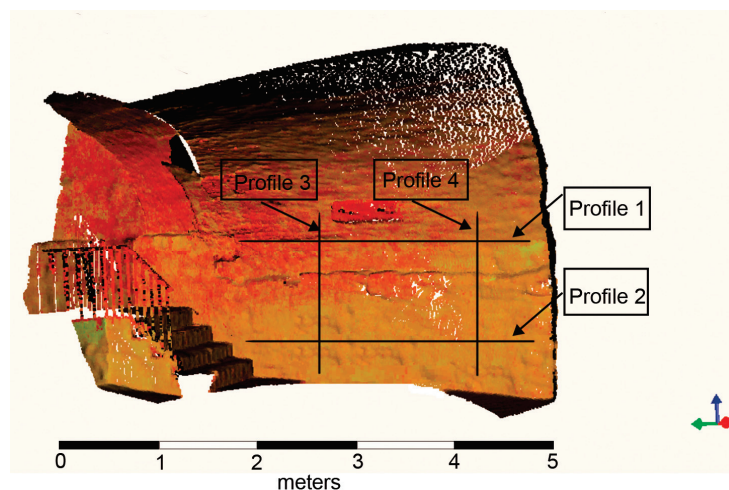
royal architect Ventura Rodriguez signed the project, and the construction was carried out by the notorious local architect, Mr. Francisco Díez Pinilla. The cellar is buried 19 m deep compared to the entrance level of the town hall. The cellar is divided in two areas; the first one has a rectangular shape 5-m long and 3-m wide, surrounded by 2.5 m-high walls and covered by a vault with a 3-m span. The second area has a 3 m-wide squared plan covered by a barrel vault whose walls are located at different heights: 5 m and 2.5 m respectively. The materials used for the construction were rectangular limestone blocks (40-cm wide and 25-cm high), all joined with mortar.

The different results obtained in each phase of the present methodology are described in the following paragraphs.

### 3.1. Geometric Model

The external and internal geometry of the wine cellar was acquired from a combination of TLS and GPR [27], respectively. More precisely, it was necessary to scan at four laser stations. Each scan provides a horizontal coverage of 360° acquiring a point cloud with an average of 1-cm resolution at 10 m and using two single shots per point. The data collection settings ensured more than 50% overlap between clouds of points, guarantying the best alignment. In this way, we obtained a total of approximately eight million raw points in XYZ coordinates for the geometric definition of the interior of the wine cellars. Regarding the internal geometry, four profiles were defined with enough length to distinguish the reflections correctly. The standard procedure is performing horizontal profiles (in a plane orthogonal to the plumb line). However, with walls of reduced width, it was necessary to acquire vertical profiles. In addition, radar profiles were geo-referenced based on geometric data collected by TLS, which constituted a significant advantage towards the success of profile interpretation (Figure 7).

**Figure 7.** 3D laser model with the GPR profiles georeferenced.



As a result of the processing and registration of TLS and GPR, a final geometric 3D model with internal (GPR) and external (TLS) properties was obtained. This 3D geometric model is a CAD product, which will be considered in the structural analysis.

### 3.2. Structural Analysis

#### 3.2.1. Finite Element Model

The format and volume of the geometric data acquired by a laser scanner present important limitations in order to be converted to a finite element model of the construction. For this reason, a semi-automatic process has been carried out with the commercial software, Geomagic, which allowed the laser point cloud to be converted into a solid CAD model. Once the solid geometric model was defined, the structure of the wine cellar could be evaluated through finite element modeling (FEM). SAP2000 software [19] was used to perform the structural evaluation.

The structural analysis was focused in the zone of the wine cellar shown in Figure 8a, which presents the 3D model of the whole cellar. The reason for choosing this part of the winery was motivated by the results found in the GPR campaign, which showed important information about the internal composition of the walls. In this zone, the interpretation showed the existence of materials of low compactness and high porosity, as well as the presence of air voids (red color) behind some of the wine cellar walls (Figure 8b). Figure 9 shows the FEM model of the cellar from laser data.

**Figure 8.** (a) 3D surface model of the wine cellar and the area of study selected for performing the structural evaluation (top view); (b) radargrams that show the presence of air voids and porous materials.

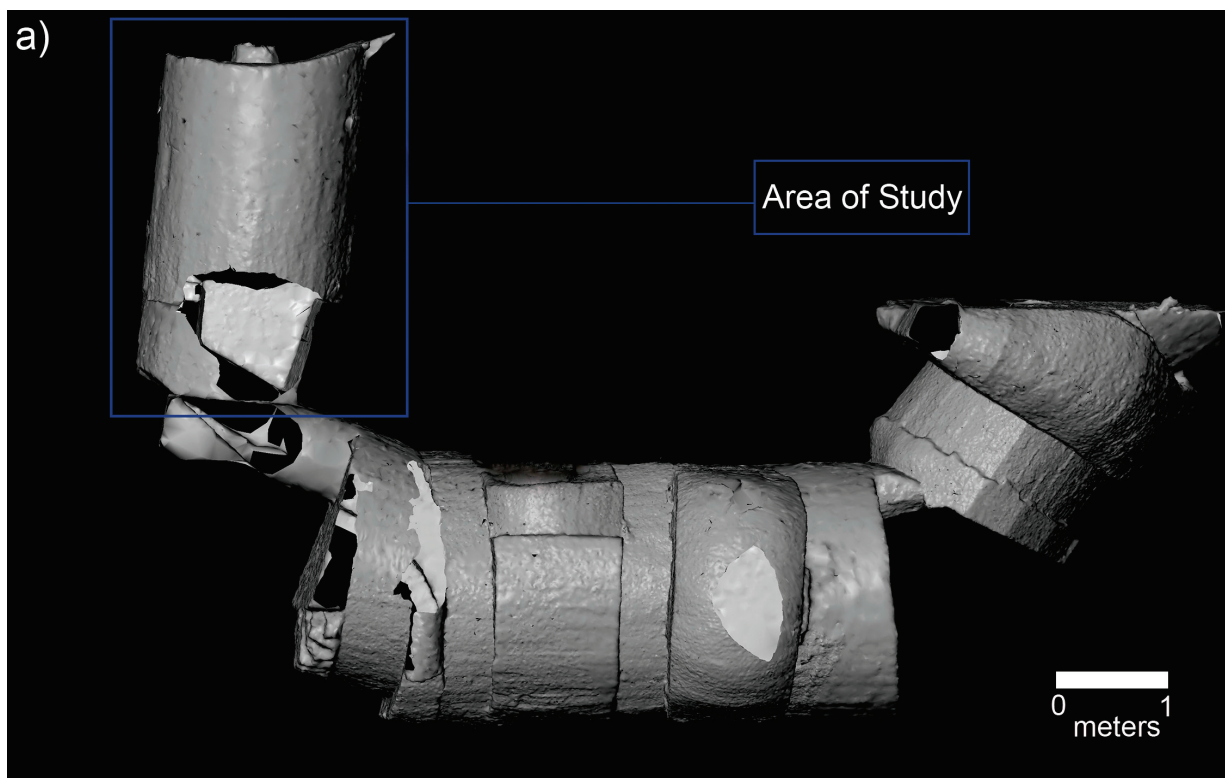


Figure 8.Cont.

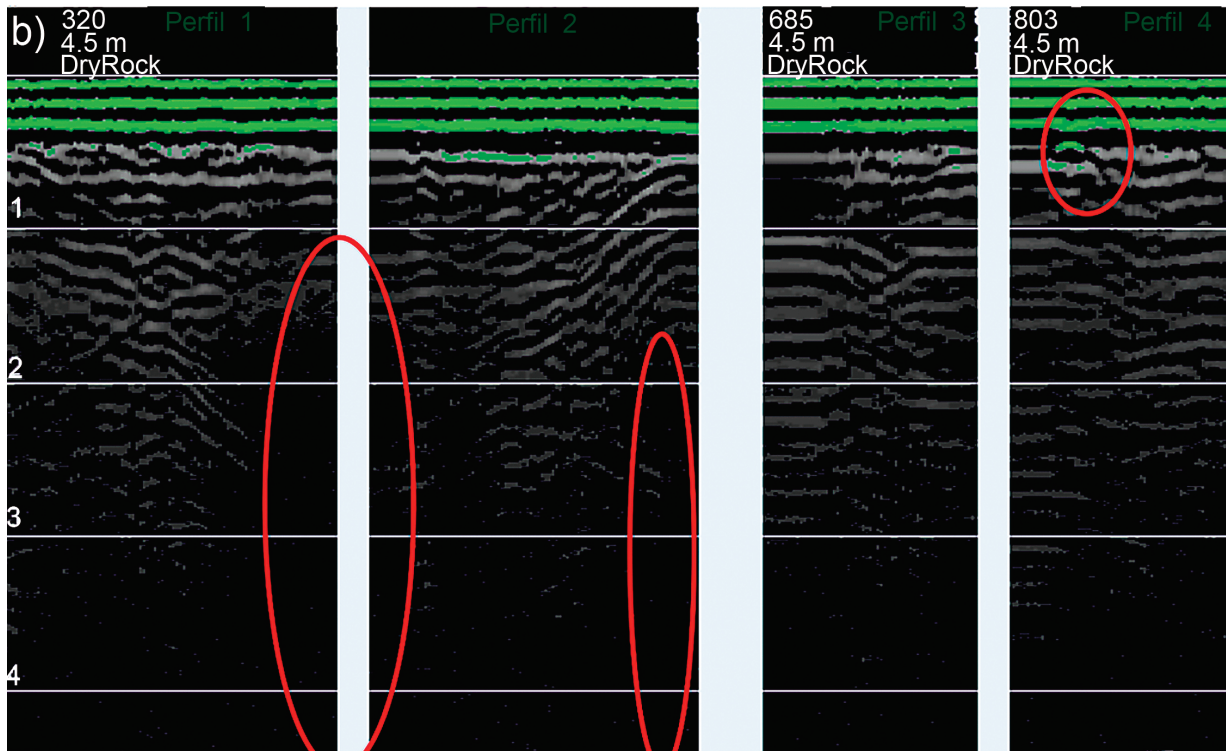
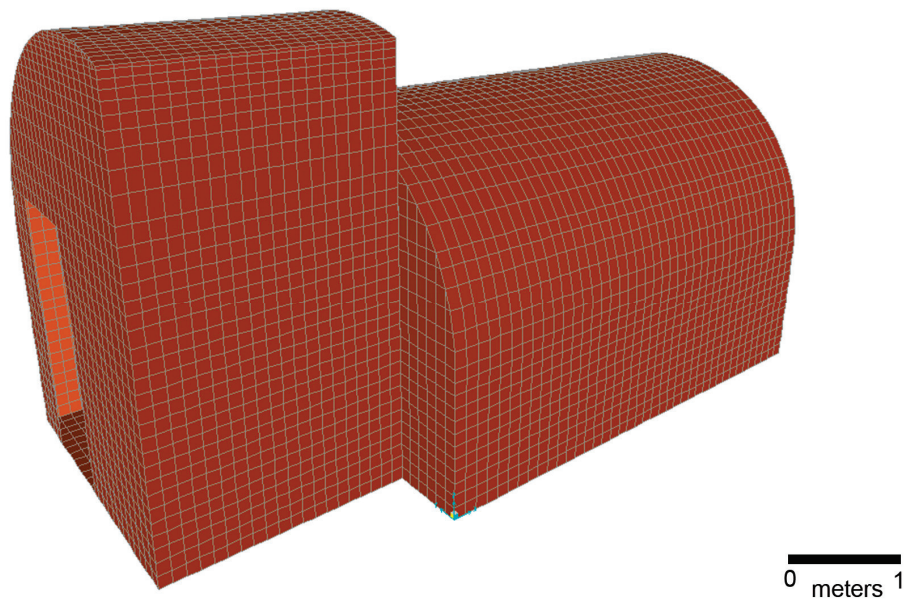


Figure 9. Generation of the FEM model of the cellar from laser data.



### 3.2.2. Results and Discussion of the Structural Analysis

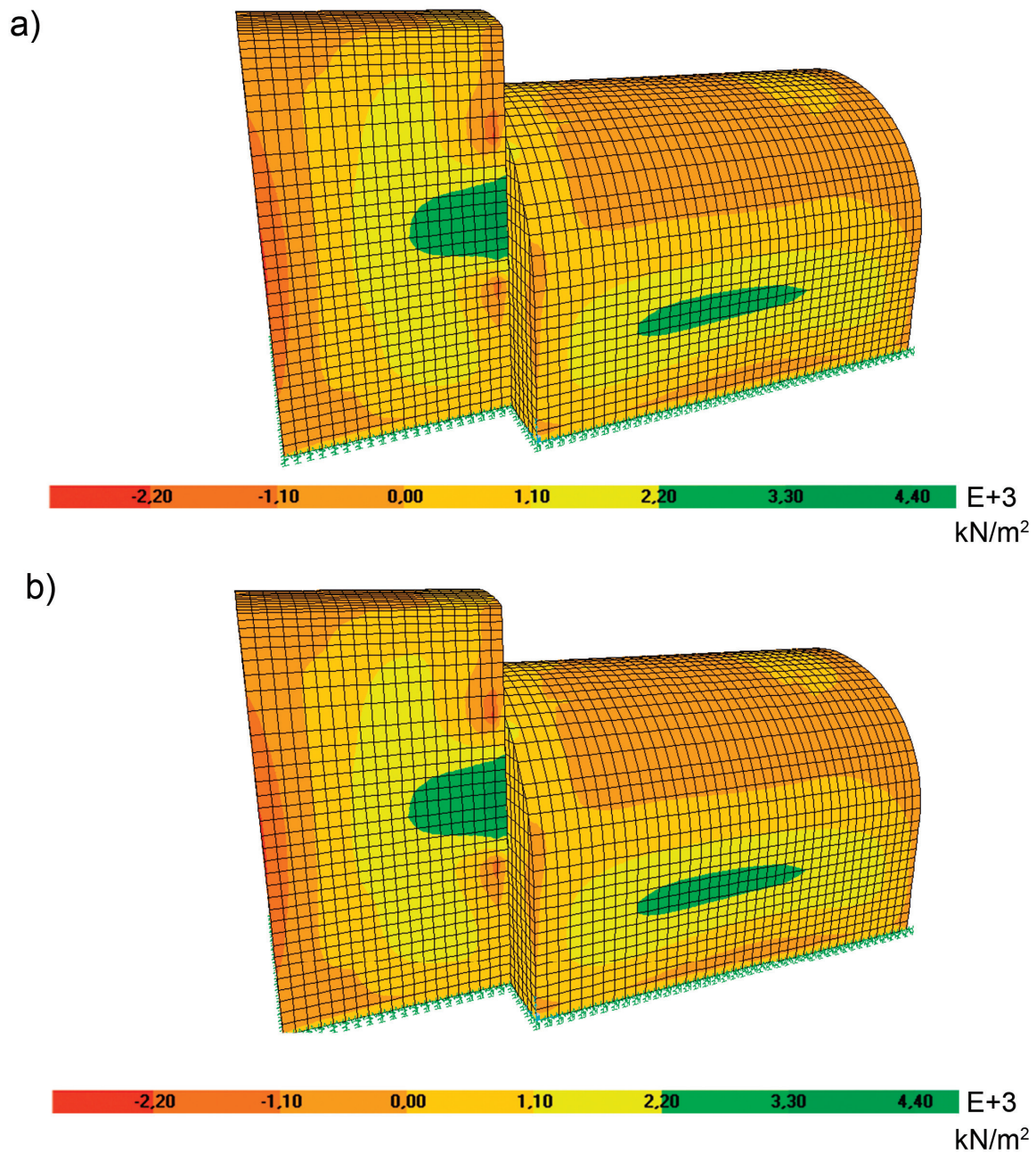
The first part of the analysis examines the principal compressive and tensile stresses in the model as [2,15,28,29] for the purpose of comparing them with the tensile and compression fracture stress of limestone. Even though other authors have developed methodologies for the analysis of masonry



vaults based on the collapse mechanism [30], the work performed in the wine cellar does not evaluate such procedures.

Due to the existence of two ultimate limit states, the following shows the principal stresses of the inner-face of the cellar of both states, taking the thickness of elevation and upper walls as the averaged value (0.4 m) provided by the GPR (Figure 10).

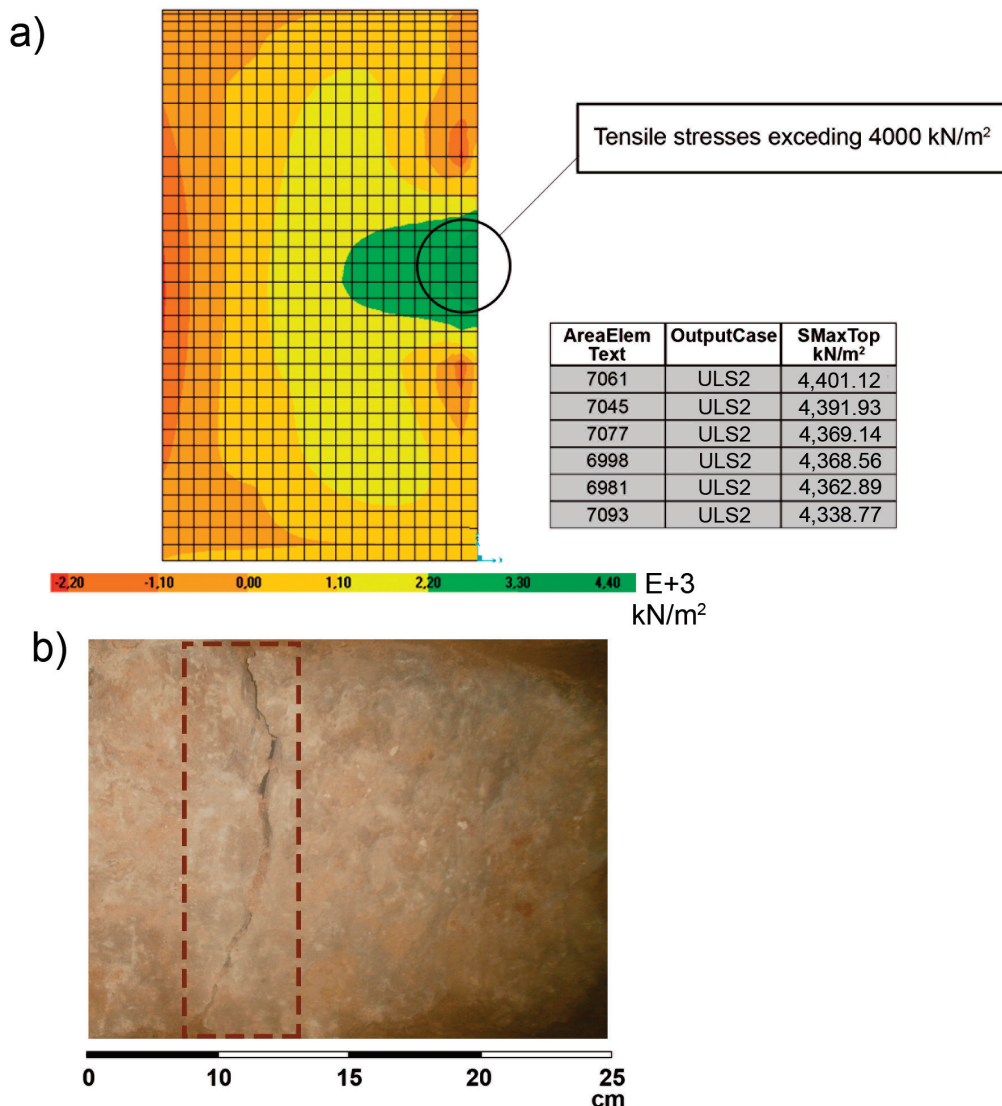
**Figure 10.** (a) Maximum principal stresses (kN/m<sup>2</sup>) in *ULS1* (with averaged thickness values); (b) maximum principal stresses (kN/m<sup>2</sup>) in *ULS2* (with averaged thickness values).



It can be appreciated that the principal tensile and compressive stresses are slightly higher in the *ULS1* (Figure 10a) than in the *ULS2* (Figure 10b). In the *ULS1*, higher compressive stresses occur in

the vault with values of  $2 \times 10^3 \text{ kN/m}^2$ , which do not exceed the compressive strength of limestone, which is  $4 \times 10^4 \text{ kN/m}^2$  (obtained in Section 2.2.1). Consequently, it can be assumed that cracking in the vault will not occur. On the other hand, the highest values of tensile stresses would be found at the walls of the wine cellar due to the tensile stresses that the bending moments would cause on the walls of the cellar, provoked by soil pressure. Figure 11a shows a small area where values near  $4000 \text{ kN/m}^2$  can be found. These values would mean that the tensile fracture point of the limestone has been exceeded. It is expected that the masonry might crack in that area, so a visual inspection of the site was conducted checking for the cracking of masonry in that area. The region of maximum tensile stresses is confined in a very specific area in the cellar, but after the visual inspection, a pattern of fissures in the walls could not be observed. Only an isolated masonry block presented a vertical fissure (Figure 11b).

**Figure 11.** (a) Area of the wall with tensile stresses ( $\text{kN/m}^2$ ) exceeding the tensile breaking point of limestone and the output table of calculation results; (b) photograph of the cracked masonry inside the cellar.

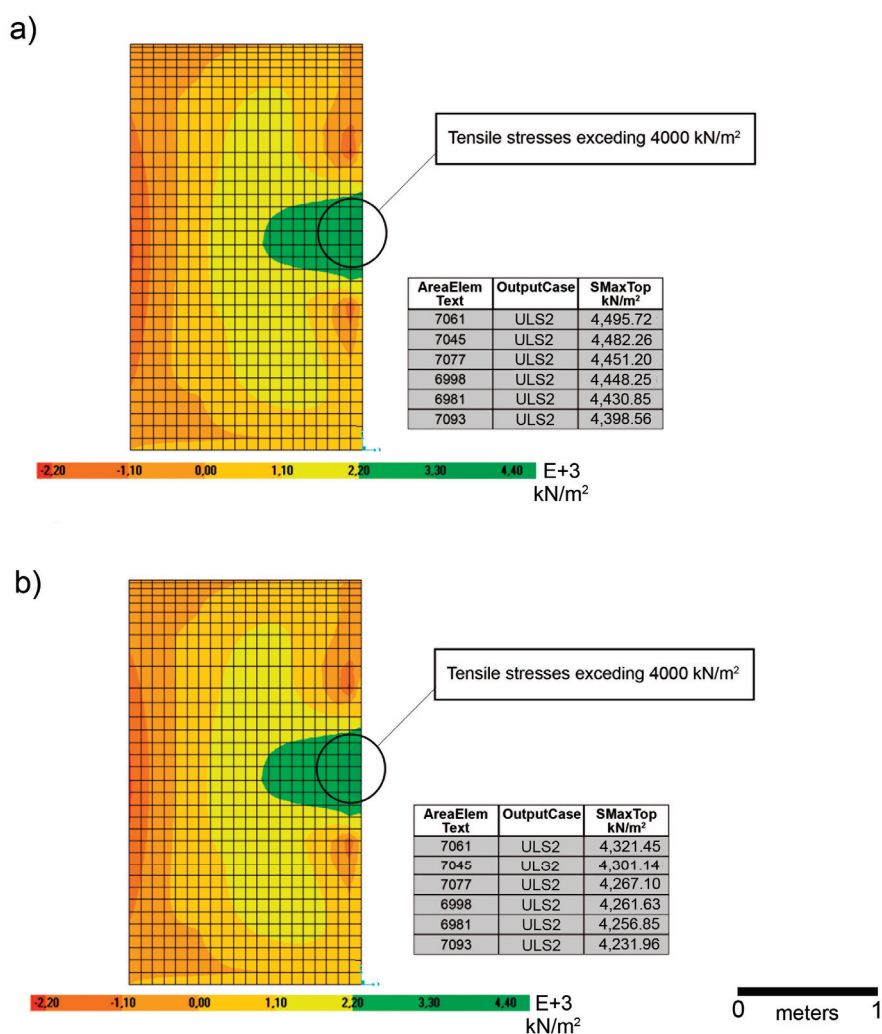


Since the tensile breaking point of limestone in both *ULSs* is only exceeded in a very small area, it is not necessary to limit its loads; the fissuration of a single piece of masonry does not endanger the stability and structural safety of the entire cellar. Although the initial load hypotheses are assumed to be correct, these loads should be established as the maximum allowed, since the increase of loading could produce the breaking of the wall and, thus, affect the stability and structural safety of the wine cellar. In this case, a new structural analysis would be required, taking into account the new loading conditions.

### 3.3. Validation of Results

Considering the averaged thickness values (0.4 m) provided by the GPR and its standard deviation ( $\pm 2$  cm), a sensibility analysis has been performed with the aim of assessing the variation of principal tensile according with the thickness. To this end, the maximum principal tensile for the elevation wall subjected to the major stresses, taking a thickness of 0.38 m and 0.42 m, were obtained. Figure 12 outlines the principal tensile for the different wall thickness according to *ULS2*.

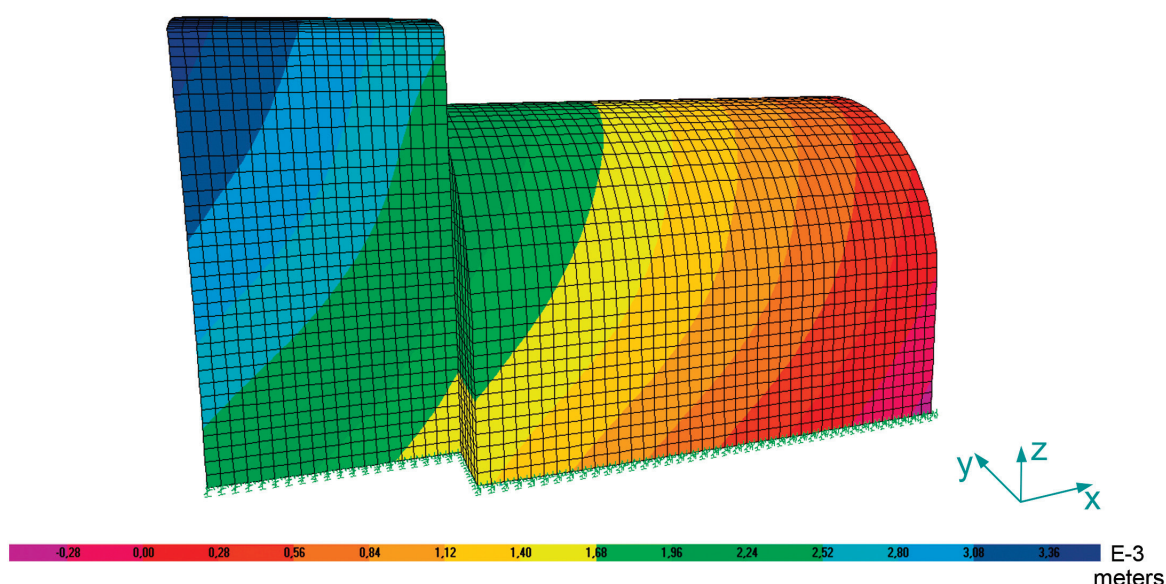
**Figure 12.** (a) Maximum principal tensile ( $\text{kN/m}^2$ ) for the elevation wall with a thickness of 0.38 m; (b) maximum principal tensile ( $\text{kN/m}^2$ ) for the elevation wall with a thickness of 0.42 m.



The results obtained show that the maximum principal tensile for the 0.38-m elevation wall is slightly higher (1%) than that obtained for the averaged thickness (0.40 m). Analogously, a slight decrease is observed when the thickness of the elevation wall is 0.42 m. Anyway, the variations of tensile strength are insignificant due to the reduced standard deviations of the GPR, which confirms that the averaged thickness values considered for the walls are suitable for the structural analysis performed.

The second part of the analysis is a study of the deformations [15,29] in order to identify areas of excessive deformations that could jeopardize the functionality of the building. Figure 13 shows the greatest deformations along the Y-axis of the *SLSI* model. The deformations are in the order of millimeters, the highest value being 3.36 mm. It is observed that these are small values, and this is largely due to the underground confinement of the cellar, which prevents large deformations and does not put at risk its functionality.

**Figure 13.** The deformation of the cellar ( $\times 200$ ) along the Y-axis of the global model and in the *SLSI* model.



#### 4. Conclusions

In recent years, the perception of the role of multidisciplinary science and technology by the stakeholders of the conservation and restoration of historical buildings has changed. In all major fields, geomatic methods and techniques are now seen as central for the study and diagnosis of this type of historical construction.

This paper presents a methodology to evaluate the structural condition of traditional constructions using non-destructive technologies to collect both the external geometry and inner characteristics of the structure. While the terrestrial laser scanner provided only the visible surroundings of the structure with a precision of  $\pm 1$  cm, the ground penetration radar provided a more complete geometry for the construction, focusing on the inner structure. GPR provided information about the internal composition of constructive elements, providing the thickness of walls with averaged errors of  $\pm 2$  cm. Furthermore,



it helped to discard the bulging of the structural walls, collapses and material shortages. The geometric model built using this integral approach allowed for building a more realistic finite element model of the cellar.

Structural simulation for both stresses and deformations through FEM allowed for identifying critical structural elements subjected to excessive tensile stress (4496 kN/m<sup>2</sup>). The tensile state allows us to discover a small area of the wall where the tensile stresses of limestone are overpassed (without endangering the stability and structural safety of the entire cellar. Nevertheless, this situation requires establishing the maximum loading state allowed, so that an increase in loading conditions would require a new structural analysis. The deformations obtained are in the order of millimeters (with a maximum value of 3.36 mm in the Y transversal direction of the main structure), so the functionality of the wine cellar is not under suspicion.

A sensibility analysis was performed in order to quantify the validity of GPR precision to carry out structural analysis. The differences in wall thickness caused by the precision of GPR ( $\pm 2\%$ ) reflected that the tensile stress varies less than  $\pm 1\%$ . As a result, GPR can be accepted as accurate enough for the subsequent structural analysis of the wine cellar.

Among its limitations, the lack of further mechanical information about the properties of the materials, both soil and masonry, is remarkable. Furthermore, the methodology presented here does not account for the soil-structure interaction, so these effects must be evaluated in the future, in order to increase the accuracy of the structural simulation of the wine cellar.

Finally, through this multidisciplinary study, an accurate, reliable and non-destructive diagnosis of the current state of the cellar could be obtained: from its apparent health based on the external geometry to the stress and possible failure based on its internal structure. Therefore, a complete compilation of all of the useful information about the wine cellar is presented through this study.

## Acknowledgments

This study was funded in part by the Universities of Salamanca and Vigo. Authors would like to thank Remote Sensing and the anonymous reviewers which provided numerous comments and suggestions that contributed to improve significantly an earlier version of the manuscript.

## Author Contributions

All authors contributed extensively to the work presented in this paper.

## Conflicts of Interest

The authors declare no conflict of interest.

## References

1. Lorenzo, H.; Arias, P. A methodology for rapid archaeological site documentation using ground-penetrating radar and terrestrial photogrammetry. *Geoarchaeology* **2005**, *20*, 521–535.



2. Arias, P.; Armesto, J.; Di-Capua, D.; González-Drigo, R.; Lorenzo, H.; Pérez-Gracia, V. Digital photogrammetry, GPR and computational analysis of structural damages in a mediaeval bridge. *Eng. Fail. Anal.* **2007**, *14*, 1444–1457.
3. Villarino, A.; Riveiro, B.; Martínez-Sánchez, J.; Gonzalez-Aguilera, D. Successful applications of geotechnologies for the evaluation of road infrastructures. *Remote Sens.* **2014**, *6*, 7800–7818.
4. Nuzzo, L.; Leucci, G.; Negri, S. GPR, ERT and magnetic investigations inside the Martyrium of St Philip, Hierapolis, Turkey. *Archaeol. Prospect.* **2009**, *16*, 177–192.
5. Leopold, M.; Gannaway E.; Völkel, J.; Haas, F.; Becht, M.; Heckmann, T.; Westphal, M.; Zimmer, G. Geophysical prospection of a bronze foundry on the southern slope of the acropolis at athens, Greece. *Archaeol. Prospect.* **2011**, *18*, 27–41.
6. Scheib, A.; Arkley, S.; Auton, C.; Boon, D.; Everest, J.; Kuras, O.; Pearson, S.G.; Raines, M.; Williams, J. Multidisciplinary characterisation and modelling of a small upland catchment in Scotland. *Quest. Geogr.* **2008**, *27*, 45–62.
7. Deparis, J.; Fricout, B.; Jongmans, D.; Villemin, T.; Effendiantz, L.; Mathy, A. Combined use of geophysical methods and remote techniques for characterizing the fracture network of a potentially unstable cliff site (The ‘Roche du Midi’, Vercors massif, France). *J. Geophys. Eng.* **2008**, *5*, 147–157.
8. Keuschnig, M.; Hartmeyer, I.; Jan-Christoph, O.; Schrott, L. MOREXPRT—Monitoring expert systems for hazardous rock walls. In Proceedings of 2010 Annual Meeting of Geomorphology Working Group, Schmittgen, Germany, 26 February 2010; p. 70.
9. Rial, F.I.; Pereira, M.; Lorenzo, H.; Arias, P.; Novo, A. Resolution of GPR bowtie antennas: An experimental approach. *J. Appl. Geophys.* **2009**, *67*, 367–373.
10. Solla, M.; Caamaño, J.C.; Riveiro, B.; Arias, P. A novel methodology for the structural assessment of stone arches based on geometric data by the integration of photogrammetry and ground-penetration radar. *Eng. Struct.* **2012**, *35*, 296–306.
11. Besl, P.J.; McKay, N.D. Method for registration of 3-D shapes. *IEEE Trans. Patt. Anal. Mach. Int.* **1992**, *14*, 239–256.
12. Mindlin, R.D. Influence of rotatory inertia and shear on flexural motions of isotropic, elastic plates. *ASME J. Appl. Mech.* **1951**, *18*, 31–38.
13. Reissner, E. The effect of transverse shear deformation on the bending of elastic plates. *ASME J. Appl. Mech.* **1945**, *12*, 68–77.
14. Baker, I. *A Treatise on Masonry Construction*, 10th ed.; John Wiley & Sons: New York, NY, USA, 1909.
15. Lubowiecka, I.; Arias, P.; Riveiro, B.; Solla, M. Multidisciplinary approach to the assessment of historic structures based on the case of a masonry bridge in Galicia (Spain). *Comput. Struct.* **2011**, *89*, 1615–1627.
16. European Comite International du Beton. *CEB-FIP Model Code 1990*, 1st ed.; Thomas Telford Service Ltd.: London, UK, 1993.
17. Jiménez Salas, J.A. *Geotecnia y Cimientos III. Cimentaciones, Excavaciones y Aplicaciones de la Geotecnia*, 4th ed.; Rueda: Madrid, Spain, 1980.
18. Ministerio de Fomento. Código técnico de la edificación. In *Documento Básico Seguridad Estructural Cimientos*, 1st ed.; Boletín Oficial del Estado: Madrid, Spain, 2007; p. 164.

19. Computers and Structures Inc. *SAP2000, Integrated Finite Element Analysis and Design of Structures*, 7th ed.; Computers and Structures Inc.: Berkeley, CA, USA, 1998.
20. Riveiro, B.; Caamaño, J.C.; Arias, P.; Sanz, E. Photogrammetric 3D modelling and mechanical analysis of masonry arches: An approach based on a discontinuous model of voussoirs. *Autom. Constr.* **2011**, *20*, 380–388.
21. Campo, M.; Drosopoulos, G.A.; Stavroulakis, G.E. Unilateral contact and damage analysis in masonry arches. In Proceedings of 2006 the IUTAM Symposium, Hannover, Germany, 5–8 November 2006; pp. 357–363.
22. Cervera, M.; Pelá, L.; Clemente, R.; Roca, P. A crack-tracking technique for localized damage in quasi-brittle materials. *Eng. Fract. Mech.* **2010**, *24*, 31–50.
23. Anthoine, A. Derivation of the in-plane elastic characteristics of masonry through homogenization theory. *Int. Sol. Struct.* **1995**, *32*, 137–163.
24. Rankine, W. On the stability of loose earth. *Philos. Trans. R. Soc. London* **1857**, *147*, 9–27.
25. Comité Técnico Aen/Ctn 140—Eurocódigos Estructurales. *Eurocode 1: Actions on Structures Part 1-1: General Actions—Densities, Self-Weight, Imposed Loads for Buildings. UNE-EN 1991-1-1:2003*, 1st ed.; Aenor: Madrid, España, 2003.
26. Comité Técnico Aen/Ctn 140—Eurocódigos Estructurales. *Eurocode 0: Basis of structural design UNE-EN 1990:2003*, 1st ed.; Aenor: Madrid, España, 2003.
27. Solla, M.; Lorenzo, H.; Riveiro, B.; Rial, F.I. Non-destructive methodologies in the assessment of the masonry arch bridge of Traba, Spain. *Eng. Fail. Anal.* **2011**, *18*, 828–835.
28. Romera, L.E.; Hernández, S.; Reinosa, J.M. Numerical Characterization of The Structural Behaviour of The Basilica of Pilar in Zaragoza (Spain). Part 1: Global and Local Models. *Adv. Eng. Softw.* **2008**, *39*, 301–314.
29. Romera, L.E.; Hernández, S.; Gutierrez, R. Numerical characterization of the structural behaviour of the Basilica of Pilar in Zaragoza (Spain). Part 2: Constructive process effects. *Adv. Eng. Softw.* **2008**, *39*, 315–326.
30. De Arteaga, I.; Morer, P. The effect of geometry on the structural capacity of masonry arch bridges. *Constr. Build. Mater.* **2012**, *34*, 97–106.

© 2014 by the authors; licensee MDPI, Basel, Switzerland. This article is an open access article distributed under the terms and conditions of the Creative Commons Attribution license (<http://creativecommons.org/licenses/by/4.0/>).

### **3.3 Geometrical Issues on the Structural Analysis of Transmission Electricity Towers Thanks to Laser Scanning Technology and Finite Element Method**

#### **RESUMEN**

Este artículo presenta un enfoque multidisciplinar para la ingeniería inversa y el análisis estructural en complejas estructuras metálicas de las que no existen planos de detalle de su construcción. El método se ha aplicado en tres tipos diferentes de torres en celosía, ubicadas en la provincia de Guadalajara (España) y diseñadas para soportar los cables de transmisión de electricidad de líneas de alta tensión.

La tecnología geomática basada en el TLS es aplicada en las torres para obtener modelos geométricos tridimensionales de alta precisión, que reproducen de forma fiable la realidad geométrica de las torres. Con ello, se determinan las dimensiones de los elementos constituyentes y se detectan imperfecciones geométricas, defectos de montaje y particularidades en el ensamblaje de los perfiles metálicos. Esta realidad se materializa en diferentes modelizaciones que consideren la geométrica real actual (*as built*) y el diseño original.

Tras un procesamiento de la información obtenida con el TLS, los modelos geométricos son exportados en formato CAD y tratados de manera semiautomática para un análisis numérico por elementos finitos. Se realizan diversas simulaciones de las torres, en régimen elástico y lineal, teniendo en cuenta sus singularidades geométricas, así como la rigidez de los nodos de unión de los perfiles y las hipótesis de carga establecidas según la normativa vigente. El propósito final cuantificará el grado de afección de la geometría sobre el comportamiento estructural de las torres.

Los resultados obtenidos en la investigación corroboran al TLS como la técnica geomática idónea para la modelización geométrica de este tipo de estructuras, debido al alto grado de detalle geométrico obtenido y a la seguridad en la toma de datos, dado su carácter remoto. Esta técnica sienta la base del análisis numérico por elementos finitos, que arroja conclusiones significativas sobre la incidencia que la geometría tiene en el estado tensional y de deformaciones de las torres.



Article

## Geometrical Issues on the Structural Analysis of Transmission Electricity Towers Thanks to Laser Scanning Technology and Finite Element Method

Borja Conde <sup>1,†</sup>, Alberto Villarino <sup>2,\*</sup>, Manuel Cabaleiro <sup>1</sup> and Diego Gonzalez-Aguilera <sup>2,†</sup>

<sup>1</sup> Department of Material Engineering, Applied Mechanics and Construction, School of Industrial Engineering, University of Vigo, 36208 Vigo, Spain; E-Mails: bconde@uvigo.es (B.C.); mcabaleiro@uvigo.es (M.C.)

<sup>2</sup> Department of Land and Cartographic Engineering, High Polytechnic School of Avila, University of Salamanca, Hornos Caleros, 50, 05003 Avila, Spain; E-Mail: daguilera@usal.es

† These authors contributed equally to this work.

\* Author to whom correspondence should be addressed; E-Mail: avillarino@usal.es; Tel.: +34-920-353-500; Fax: +34-920-353-501.

Academic Editors: Fabio Remondino, Nicolas Baghdadi, Henrique Lorenzo and Prasad S. Thenkabail

Received: 4 July 2015 / Accepted: 1 September 2015 / Published: 10 September 2015

---

**Abstract:** This paper presents a multidisciplinary approach to reverse engineering and structural analysis of electricity transmission tower structures through the combination of laser scanning systems and finite element methodology. The use of laser scanning technology allows the development of both drawings and highly accurate three-dimensional geometric models that reliably reproduce geometric reality of towers structures, detecting imperfections, and particularities of their assembly. Due to this, it is possible to analyze and quantify the effect of these imperfections in their structural behavior, taking into account the actual geometry obtained, different structural models, and load hypotheses proposed. The method has been applied in three different types of metal electricity transmission towers with high voltage lines located in Guadalajara (Spain) in order to analyze its structural viability to accommodate future increased loads with respect that which are currently subjected.

**Keywords:** non-destructive techniques; structural analysis; Laser Scanning; Finite Element Method; transmission towers; reverse engineering

---

## 1. Introduction

Traditionally, building high-voltage power lines has had few obstacles during their construction phase. Currently, this type of infrastructure is facing a number of setbacks: it has a considerable impact on the environment, on economic activities, and on the expansion of cities, besides its economic cost, including inspections and maintenance. All of these problems have led the companies that use and maintain this infrastructure to consider making the best use possible of the existing lines before placing new lines. Old lines were designed according to the standards of the time in which they were built and they were designed to bear a certain load. In many cases, these towers were designed over forty years ago, so the increased loads that will be placed on them will be far greater than the one for which they were designed. In addition to this fact, the design and execution data of the towers has, in most cases, disappeared, and in other cases, building regulations did not even exist at the time. Due to this, addressing the re-use of existing power lines requires a geometric and structural analysis of the towers to assess their current state.

Formerly, the towers' dimensional analysis was performed through expeditious and manual methods (through the use of a gauge and a measuring tape) that required direct contact with the structure and, therefore, meant high risks and high costs. Afterwards, in search of a remote non-invasive measuring method, classic topographic measuring allowed thorough, notably intense, field work taking angular measurements and determining singular points indirectly through angular intersections. More recently, the existence of reflectorless electromagnetic surveying equipment has allowed direct measurement of distances and angles from a single point, making field work easier and more efficient, although it solely focuses on extracting unique and specific measurements determined by the topographer [1]. This has meant great uncertainty upon the elements of the tower, since the data was only taken at the point where the measurement is performed. In order to have the full representation of the geometry of the structure, in the last years laser scanning has presented as an interesting solution [2,3,4,5], due to the fact that they generate dense real-time point-clouds of the tower's geometry from a distance [6]. However, one of the major limitations of these terrestrial geotechnologies is the overall height of the tower, impossible to cover completely from the ground, which has led to the use of robotic unmanned aerial systems that take aerial images and, through photogrammetric procedures, obtain dense three-dimensional models of this type of infrastructure [7].

As for structural assessment, this kind of structure has been analyzed from different points of view as presented in the literature: the effects of loading in the stability of the tower [8–11]; the effects of the stiffness of connections [12–14]; and causes of failure [15–17]. No previous work was performed in order to evaluate the effect of geometric imperfections such as misalignments of structural members at joints or assembly imperfections.

Therefore, in view of what is mentioned above, this paper presents a non-destructive multidisciplinary approach that is articulated in two stages and that analyzes geometrically and structurally electricity transmission tower structures:

1. The first stage will address a detailed geometric description of the structure (reverse engineering) using a terrestrial laser scanner system, performing an “as built” model that provides information on the structure’s most relevant data, such as geometry, type, and dimensions of the metallic profiles and their assembly drawings.
2. Secondly, and taking the geometric model obtained by the laser system as a starting point, three different structural finite element models will be developed: one model will have an ideal geometry considering the nodes of the transmission tower to be pinned, supposing that this model was the one that was used in the original design of the towers. A second model will be developed with the ideal geometry of the previous model, but considering certain continuous elements of the transmission tower to be rigidly connected at both ends. The third model will use the real geometry obtained from the laser scanner (taking into account all possible initial imperfections as, for example, misaligned structural members at joints) and will also consider the stiffness behavior of the continuous elements of the tower. For its analysis the current Spanish standard for the design of such towers will be taken into account [18]. The analysis will be carried out in a linear elastic regime with the software SAP2000 [19] to obtain data of the displacements and stresses in transmission tower members for each load case established by the current codes. It is expected to obtain conclusions about the performance of these different structural approaches and, therefore, conclude which is the most appropriate modeling strategy in structural assessment procedures when an increase in loads to accommodate new services is demanded.

The paper is outlined as follows: after the introduction, in Section 2, the characteristics of the towers’ considered structural models are described. Section 3 details: the equipment used, the production of the geometric models through computer aided design (CAD) software, and the data used in structural analysis. In section 4 the results are analyzed and end with the reached conclusions.

## 2. Structural Modeling of Truss Structures

A transmission tower could be considered as a three dimensional truss structure [20], which is comprised of a reticular structure formed by discrete elements (bar or rods), joined together at their ends by means of connections without friction and designed to withstand the external forces by means of axial internal forces in their members. The idealized structural model used for the study of this kind of structure is usually based on the following assumptions [21,22]:

1. Individual elements or rods are joined together at their ends by means of connections with no friction, which means the nodes transmit forces but do not transmit moments.
2. The centroidal axis of each member is straight and matches the line that joins each end of the member. The axis of all of the members that end in the same node is cut at a single point; otherwise moments will appear in these members so that the node could be at static equilibrium.



3. Whenever external loads are applied in the nodes, all the elements that comprise the structure are subjected to tensile and compressive forces, since there is no friction at the connections. This means that the self-weight of the elements is replaced with loads applied at their ends. According to [23] bending caused by direct wind loads on the structural elements can be omitted.
4. The cross section of each member has a negligible area compared to its length.
5. The self-weight of the elements is negligible, since the loads supported by the structural elements are usually large in comparison to their weights.

Under the fulfillment of these assumptions, the structural elements are exclusively subjected to axial forces. For the case studies later reported in this paper, given the age of the towers and the virtual inexistence of structural calculation software at that time, it is logical to assume that they were either calculated manually, using the so-called Ritter method [21,22] or graphically, using the Cremona method [21,22].

However when looking at the analyzed tower's "as built" model we found out that assumption 1 and 2 are not true in the case studies herein presented:

1. In the case of members of the towers, their connections are bolted and thus they are not actually frictionless nodes. Additionally, some members, such as the truss chords, are continuous elements, which can evidently transmit moments from one side of a node to another [24]. Thus, these nodes are assumed to be rigidly connected behaving as elastic embedment (or simply rigid joints), which cause local bending moments due to rotations that take place as a consequence of the global deformation of the structure. Such effect causes the so-called secondary bending moments and consequently a secondary stress state, which are juxtaposed to the primary stresses derived from axial forces.
2. Furthermore, truss members that end in the same node do not always cut it at the same point, leading again to an apparition of secondary bending moments. Such bending moments depend upon both proportion of the misaligned or eccentricity and stiffness of the elements.

Both circumstances are observed in all towers herein analyzed. Figure 1 corresponds to an example of the aforementioned issues upon one of the case studies later described (Tower 1). Furthermore, as it can be appreciated, the ideal situation of perfectly-aligned elements assumed in the initial stage of structure design and calculation can suffer variations during its construction on site. This is shown in the "as built" model, obtained with the laser scanner, where small deviations in the horizontality of several truss members and even a small deviation in the vertical alignment of the main body of the tower can be appreciated (Figure 1).

All of these issues question the use of a model with ideal pinned connections, which was possibly the used method at the time of the structure's design and calculation, and whether it is a valid model to perform further calculations at the present time. Therefore, in view of the constraints and considerations discussed above, three different structural models of the towers are tested in order to compare the results with each other and draw conclusions about the deformations and the actual stress state of the tower's elements, all under different load hypotheses established by current standards [18].

- 1 Model with pinned joints and ideal geometry (Model 1). This model is supposed to be the one that was used for the design of the towers. A three-dimensional model with all members



pin-jointed at nodes was developed that took into account all the previously-mentioned assumptions. Accordingly, the adoption of certain assumptions about the geometry provided by the laser scanner was needed in order to adapt the model to an ideal geometry. More specifically, it was assumed that all members concurring in one node were overlapping in a single common point since, in reality, these members were assembled more erratically. For this, the criterion used was to assume that the main vertical members of the tower and the horizontal members were fixed in their position, and the corrections changed the length and exact location of the diagonal braces that connect at each joint. Additionally, the geometry was simplified in certain areas of the horizontal sections of the towers, ignoring the bend and the inclination. Accordingly, vertical deviation of the main bodies of the towers was not taken into account. Finally, the obtained “as built” model measurements of certain modules that form the main body of the towers are simplified to theoretical values. For example, when certain lengths result in 1.99 m or 2.01 m, the value is simplified and considered to be 2 m. For clarity, Figure 2 presents a scheme with the principal structural parts of a transmission tower.

- 2 Model with rigid joints and ideal geometry (Model 2). According to the data proportioned from the “as built” model, assumption 1 is not valid because certain elements, such as truss chords, are continuous elements. Therefore, a second model was elaborated which considers an ideal geometry but where truss chords and horizontal members of the towers are considered rigidly connected at both ends and all other structural components (truss elements) are treated as pin jointed. In this way, the originated secondary bending moments and, consequently, secondary stresses can be taken into account and their impact in comparison to modeling the tower with all ideal pinned joints quantified.
- 3 Model with rigid joints and real geometry (Model 3). In contrast with the two previous models, this approach considers all of the real geometric singularities of the structure and includes them into the simulations; for example, it includes horizontal deviations of truss chords, the vertical deviation of the tower’s main body, as well as assumptions 1–3 obsolescence. To create such a structural model, first a 3D wire-model was produced using the “as-built” model as a dimensional foundation. Secondly, it was imported as a “dxf” file into the structure calculation software SAP2000 [19].

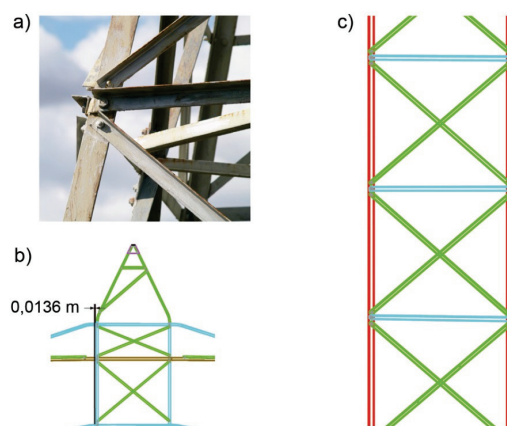


**Figure 1.** (a) Detail of the bolted connections with the inclusion of the eccentricity present at the linkage between profiles; (b) vertical deviation of the main body of tower; (c) horizontal deviation in the members of the main body of tower.

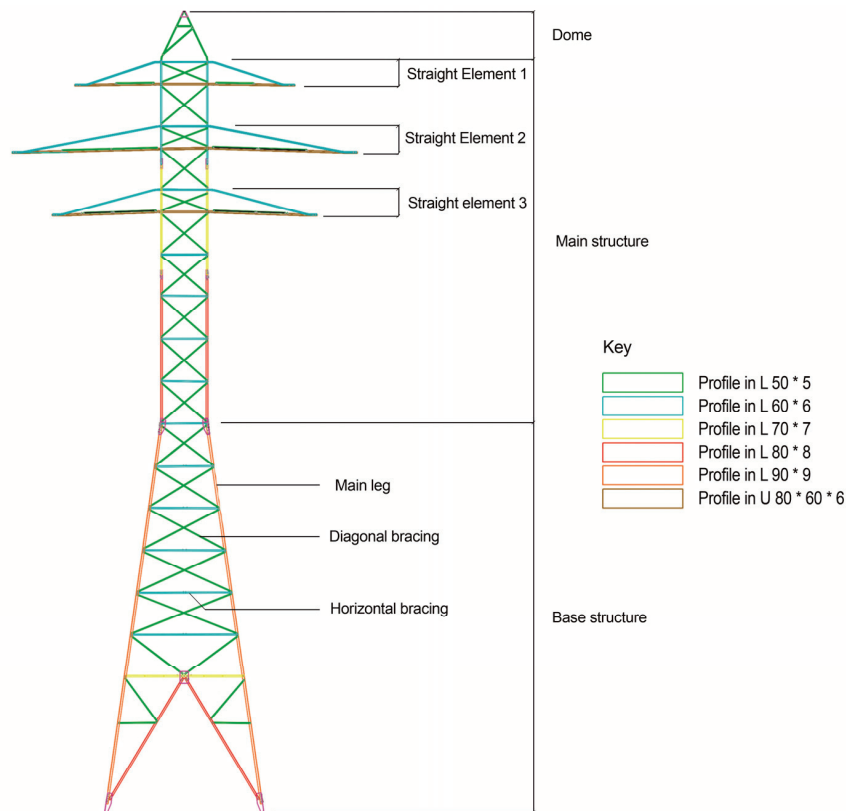


**Figure 2.** Scheme of main structural parts of transmission tower upon draws of one of the cases studies herein analyzed (Tower 1). Data was obtained from laser scanning technology according to the methodology presented in Section 3.

### 3. Methodology

#### 3.1. Geometric Digitalization

A laser scanning survey was conducted in order to generate a 3D model accurately describing the structure of the transmission towers. A time-of-flight (ToF) terrestrial laser scanner (TLS), Leica ScanStation2, was used for recording external geometry. This scanner covers a field of view of  $360^\circ$  in the horizontal direction and  $270^\circ$  in the vertical direction, enabling the collection of full panoramic views. The distance measurement is obtained with a nominal accuracy of 4 mm at 25 m range. The horizontal and vertical angular accuracy is of  $60 \mu\text{rad}$  ( $3.8 \text{ mgon}$ ). The diameter of the laser spot is 4 mm at 50 m. According to the technical specification of the instrument, it has a maximum acquisition rate of 50,000 points per second. The scanner incorporates a dual axis compensator, so the vertical Z-direction is perfectly defined during data acquisition. Due to the complexity of transmission towers and their heights, four scanner stations with a resolution of 5 mm at 25 m were required to enclose the whole structure. The resulting 3D point cloud (about 6 million points per tower) contains geometric data, normally given in Cartesian coordinates (XYZ), as well as the intensity values ( $I$ ). This intensity measurement is referred to as the amount of reflected radiation with respect to the emitted radiation. Typically, this value is normalized in the range of 0–1 or 0–255, 8-bit format in our case. According to the principles of interaction between electromagnetic radiation and matter, the intensity values directly

depend on the physical characteristics of the object surface, the wavelength of the incident radiation, and the distance between the laser and the object.

### 3.2. Geometric Modeling

The geometric modeling of the transmission towers was performed following four steps:

1. Cleaning and segmentation of point clouds in order to remove undesired data, such as reflections, noise or sensor artifacts. This step was performed manually.
2. Alignment of the point clouds from each scan under a common coordinate system. An automated registration method, iterative closest point (ICP) [25], was applied, supported by the identification of matching points and minimizing the Euclidean distance between corresponding point clouds. Initial approximations (three points) were manually identified by the user, trying to guarantee a good distribution around the area of interest and along the three main directions ( $X$ ,  $Y$ ,  $Z$ ). A solid-rigid transformation based on the three points identified was executed. Afterwards, an automatic iterative process to align the different scans was performed taking the Euclidean distance as a minimization criterion.
3. Generating cross-sections and technical drawings of the electrical towers, focusing on the steel profiles that make up each section of the tower and the arrangement of the connections used to define the linkage of these profiles. Different profiles were automatically generated along each main direction ( $X$ ,  $Y$ ,  $Z$ ) in order to obtain vector information of the main sections of the towers and, thus, initial approximations to support the technical drawings and CAD model generation.
4. Obtaining a computer aided design (CAD) model. Since the structural analysis based on a FEM model does not cope with dense laser models, an important step which allows us to pass from the 3D point clouds to a solid geometric model was performed. This step consists in extruding the sections obtained in the step before along its normal direction. Manual interaction is required in this step in order to solve the different intersections between profiles and their connections. In addition, specific existing libraries based on standard steel profiles (*i.e.* L-shaped and U channel profiles) were used for modeling the towers. Geometric modeling was done using Geomagic Spark, 2013 version.

### 3.3. Structural Analysis

The three towers are formed by angular steel profiles of different dimensions, and given the age of the towers and only for the purpose of the methodology developed in this article, we assume the lower specification for a steel material enabled by [26], type S-235.

This brings the following mechanical properties: Young's modulus of  $2.1 \times 10^8$  kN/m<sup>2</sup>, specific weight of 76.9729 kN/m<sup>3</sup>, Poisson's coefficient of 0.3, and yield stress of 235 MPa.

Furthermore, the data of the power line, support type of the tower, and the mechanical characteristics of the electrical drivers are detailed below:

- High voltage power line with rated voltage of 132 kV and 50 Hz AC
- Two duplex-circuit line with alignment support.
- Span: 300 m between supports.

- Electrical driver of aluminum galvanized steel, type LA-280.

The boundary conditions of the three towers are assumed to be articulated supports in each of the legs that make up the outer frame of the towers, so that they have only limited movements according to the global axes (*X, Y, Z*). The constraints upon the members are explained in each of the structural models discussed above.

The different load conditions are obtained according to [18]. The following descriptions summarize the loads, always bearing in mind that the towers are located in the province of Guadalajara (Spain) and that they are power lines with alignment support and with suspension insulator strings [18].

- Permanent loads: The self-weight of the steel profiles that comprise the towers, electrical conductors, fittings, insulators, and the grounding wire.
- Wind load: It acts upon steel members of the towers, the insulators, and the suspension insulator strings.
- Imbalance of tensile forces: A longitudinal force equivalent to 25% of all unilateral tractions of electrical drivers and grounding wire. This tensile force will be applied at the point where the electrical conductors and the grounding wire are attached to the support, thus taking into account the torsion that these forces could create.
- Electrical conductor failure: A unilateral tensile force related to a single electrical conductor or a grounding cable's failure. The minimum admissible value for the failure is 50% of the broken cable's tension in the power lines that have two conductors per phase.

Taking into account aforementioned load patterns, the current standards [18] refer to certain calculation hypotheses that establish the load cases, shown in Table 1.

**Table 1.** Load cases considered in structural analysis of towers.

Tower Type	Force Direction	Hypothesis 1	Hypothesis 2	Hypothesis 3
Alignment support and suspension insulator strings	Vertical	Permanent loads, considering the electrical conductors and the grounding cables to withstand wind load according to a 120 km/h wind speed		
	Transversal	Wind load (120 km/h) on electrical conductors, cables, grounding cables and supports of tower	Not applicable	Not applicable
	Longitudinal	Not applicable	Imbalance of tensile stress	Electrical conductor and grounding cable failure

In order to clarify such load cases considered, in Figure 3 is detailed upon finite element model of one of the case studies herein analyzed (Tower 1), the arrangement of the loads in each of the three scenarios previously commented. Similarly, loads are arranged in Towers 2 and 3.

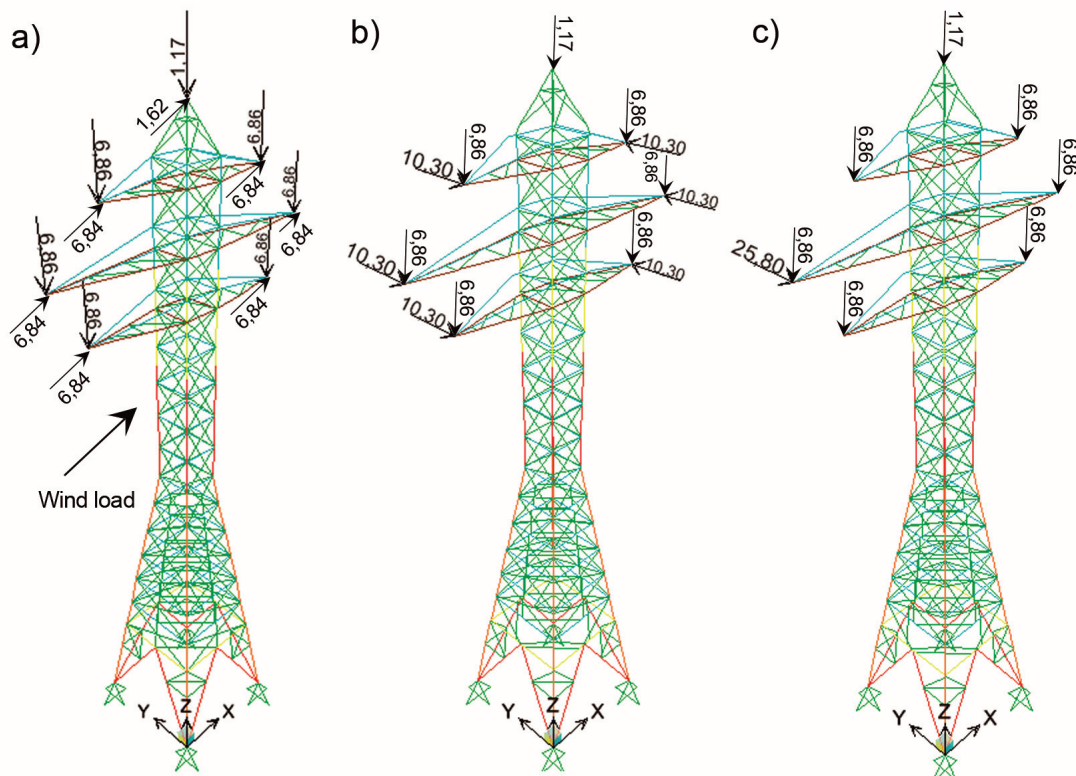


**Figure 3.** Loads cases considered in structural analysis. (a) Hypothesis 1: wind; (b) Hypothesis 2: Imbalance tractions; (c) Hypothesis 3: electrical conductor failure.

## 4. Experimental Results and Discussion

### 4.1. Case Studies

Since this study arises as a consequence of the need to analyze the structural viability of a series of electricity transmission towers that serve as support to an old power electricity line located between the cities of Guadalajara and Torija (Spain), three different cases studies were chosen for the development of the aforementioned methodology.

The electricity transmission towers chosen correspond to a type of tower known as “support alignment” which are disposed over different sections of electricity line. Additionally, in order to extend the study over different structural typologies, each tower corresponds to a different morphology.

The first tower is formed by both a main body support and another principal body (comprising horizontal bracings and diagonal bracings according to a St Andrew’s disposition) and three horizontal symmetrical bodies for the support of the cables. The second tower only has a support body (formed by horizontal bracings and secondary diagonal bracings according to a St Andrew’s disposition) and three asymmetric horizontal bodies. The third tower is similar to the second one, with exception in the diagonals forming the support body which are not arranged according to a St Andrew’s disposition.

Figure 4 shows a photograph of the three towers that composes cases studies described above.



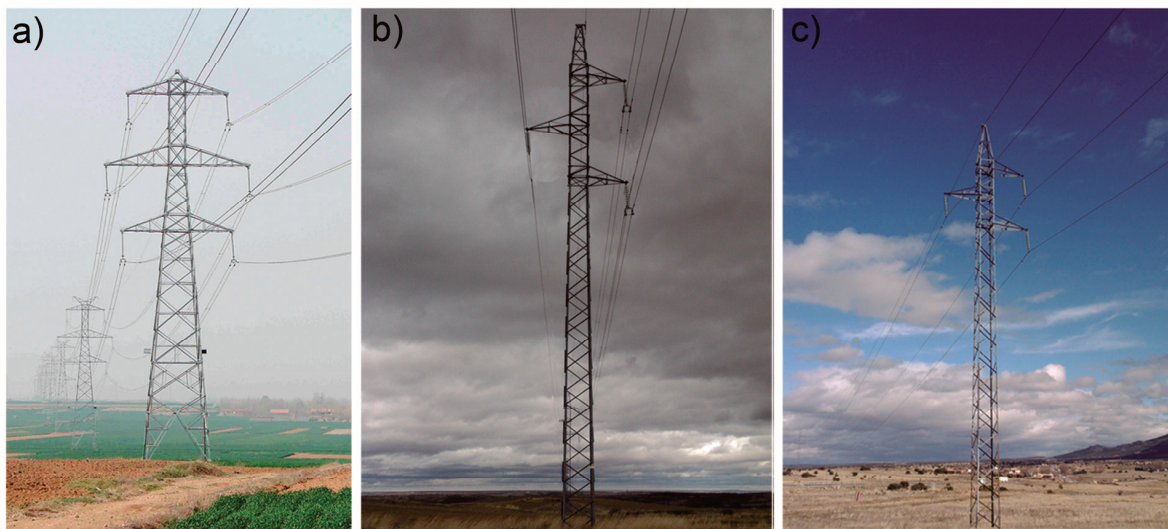


**Figure 4.** Transmission towers considered in this study: (a) tower 1; (b) tower 2; (c) tower 3.

#### 4.2. Geometric Modeling

Following all steps described in Section 3.2, the point cloud data obtained as a result of a laser scanning survey was subsequently transformed into a CAD model valid for its implementation in the finite element software package SAP2000.

This is a key step required in this kind of reverse engineering process, since data obtained from laser scanning technology do not represent any valid information by itself for the purpose of finite element analysis without suitable data processing [27].

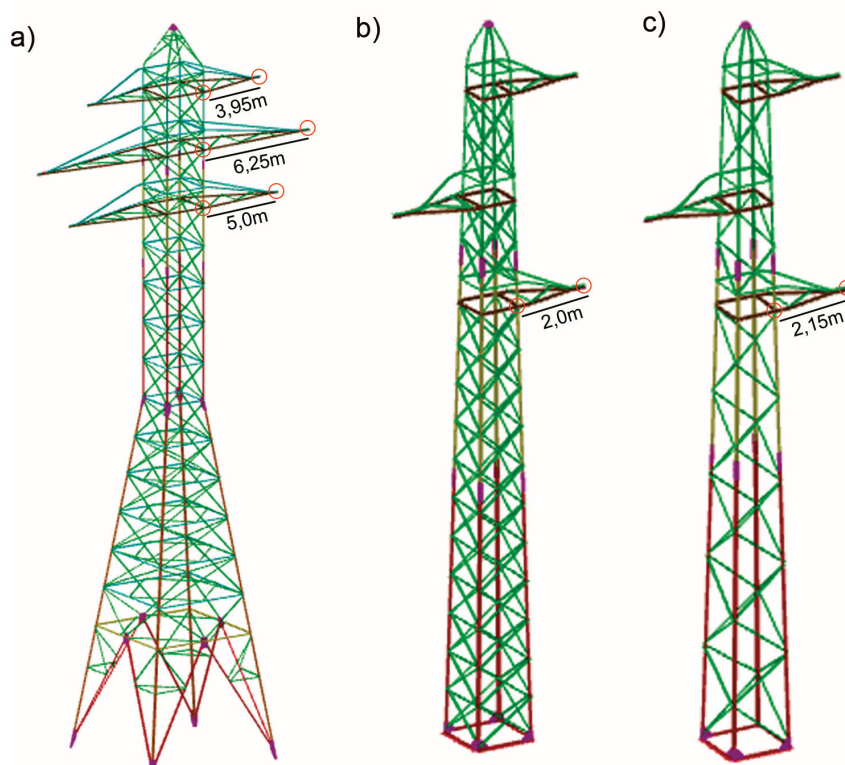
Therefore, taking this into account, CAD models for each one of towers analyzed together with drawings about its current disposition and assembly information were obtained.

Figure 5 shows CAD wire models obtained for each one of towers analyzed. Once such geometrical models were obtained, they were directly imported as a DXF file to SAP2000 software for the finite element analysis stage.

Main geometric data concerns to dimensions of the base, height of the tower, and length of horizontal bodies are displayed in Table 2. The length of the horizontal bodies of the towers is measured from the main body of the tower up to the farthest node. Tower 1 has three horizontal bodies with different dimensions, while in towers 2 and 3, all the horizontal bodies have similar dimensions.

**Table 2.** Main geometric data for transmission towers analyzed.

Tower	Base Dimensions (m)	Height (m)	Length of Horizontal Body (m)
1	7.25 × 7.25	37.25	3.95
			6.25
			5.0
2	1.5 × 1.5	18.50	2.0
3	1.5 × 1.5	18.50	2.15



**Figure 5.** Geometrical CAD wireframe models of transmission towers analyzed: (a) tower 1; (b) tower 2; and (c) tower 3.

### 4.3. Structural Analysis

As was previously indicated, finite element models of transmission towers were analyzed in SAP2000 software. Within this package, frame elements were chosen so that stiffness against rotations could be considered in all of those nodes assumed to behave as rigid joints. For all other cases where moments will not be considered (as, for example, in diagonal members pin jointed to truss chords), releases end options in nodal degrees of freedom could be imposed for transforming frame elements to truss elements and, thus, only axial forces be considered. For all structural models herein developed, analysis was carried out considering linear elastic behavior.

Table 3 shows the number of frame elements and the number of degrees of freedom for each of the finite element model developed, taking into account the type of transmission tower structure and structural model approach.

**Table 3.** Number of frames elements and degrees of freedom for each one of the three different structural models considered upon cases studies analyzed.

Tower	Model 1		Model 2		Model 3	
	Frame Elements	Degrees of Freedom	Frame Elements	Degrees of Freedom	Frame Elements	Degrees of Freedom
1	419	3320	419	3896	683	6772
2	241	1909	241	2348	321	3308
3	181	1448	181	2100	226	2408

## 4.3.1. Displacements

In this section, displacements [12,14,28] experimented by each tower under different load cases and structural models are analyzed and discussed.

To carry out the analysis and comparison, representative points of the three towers associated with the nodes of the horizontal bodies and the upper node of the dome were selected. Figure 6 shows an example of these nodes together with the displacements experimented for each tower under Loading Case 1 (wind load) and structural model considering real geometry for upper node of the dome (Node 1).

Table 4 reports both the values of maximum displacements obtained for Model 3 (real geometry) and the node where they take place (one of the aforementioned) for the different loading scenarios considered in each one of the transmission towers analyzed. Table 5 represents a comparison (in absolute value) between maximum displacements for Models 1 and 2 with respect to Model 3 (considered as the most accurate).

In both tables, the structural model considered is represented by “M” followed by a number indicating the corresponding model described in Section 2. Load cases considered are indicated by “H” denoting each one of the hypothesis described in Section 3.3 and Table 1 is applicable.

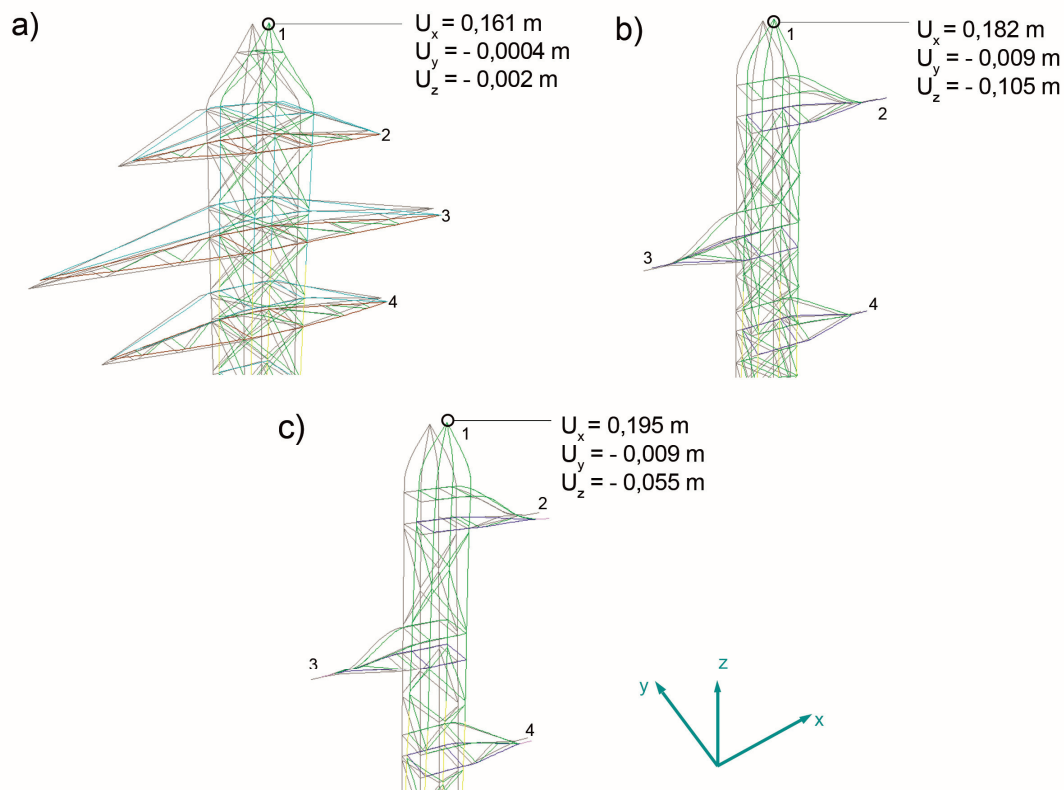


**Figure 6.** Nodes considered for analysis of displacements according to the global axis directions in each tower and structural model analyzed. (a) tower 1; (b) tower 2; (c) tower 3.



**Table 4.** Values of the maximum displacements experimented for Model 3 in all transmission towers and load cases considered with the indication of the node where they take place.

Tower	Model	Displacement U <sub>x</sub> (mm)/Node			Displacement U <sub>y</sub> (mm)/Node			Displacement U <sub>z</sub> (mm)/Node		
		H1	H2	H3	H1	H2	H3	H1	H2	H3
1	M3	161/1	14/3	12/4	8/3	162/3	140/3	132/3	8/2	8/2
2	M3	182/1	44/2	11/2	9/1	88/1	125/3	123/2	11/2	15/2
3	M3	195/1	52/2	15/2	9/1	97/1	146/3	85/2	21/3	18/2

**Table 5.** Comparison between displacements experimented by Models 1 and 2 with respect to Model 3 in all transmission towers and load cases considered.

Tower	Models Compared	Maximum Deviation U <sub>x</sub> (mm)/Node			Maximum Deviation U <sub>y</sub> (mm)/Node			Maximum Deviation U <sub>z</sub> (mm)/Node		
		H1	H2	H3	H1	H2	H3	H1	H2	H3
1	M3 front M1	93/1	6.3/3	4/4	5/3	52/3	62/3	27/3	4/2	4.6/2
	M3 front M2	95/1	6.3/3	4/4	5/3	65/3	78/3	29/3	4/2	5/2
2	M3 front M1	66/1	8.3/2	7/2	4/1	44/1	39/3	35/2	4/2	9/2
	M3 front M2	80/1	9/1	8/2	6/1	43/2	48/3	38/2	5/2	10/2
3	M3 front M1	75/1	9/2	6/2	7/1	38/1	37/3	38/2	3/3	5/2
	M3 front M2	65/3	7/1	7/2	4/2	32/2	42/3	43/3	5/3	6/3

The results displayed in Table 5 show that principal differences always take place in all towers under Hypothesis 1 (wind load case). The differences found between Model 3 and Model 1, reaching 95 mm in the global *X* direction is remarkable.

There are also significant differences for all towers, although less than aforementioned for displacements of nodes in the global *Y* direction under Hypotheses 2 and 3 (Imbalance tractions and cable break). The reasons that can explain these differences may be due to the following factors:

1. Consideration of the initial small vertical deviations of the towers' main bodies along with the application of wind forces in Hypothesis 1, precisely in that direction, may have accentuated the displacements in global *X* direction obtained in Model 3.
2. The fact of considering the true connections of the profiles onto the nodes (misalignment) has a drastic consequence upon the behavior of the structure since it directly affects to its stiffness.

In Models 1 and 2 "ideal nodes" connecting various elements mobilize stiffness of all concurrent elements (truss chords, diagonal, and horizontal members): axial stiffness in Model 1, and axial and bending stiffness in Model 2; in Model 3, however, it does not occur equally.

When considering real geometry, the existence of "intermediate" nodes inserted into the truss chords cause local bending moments and, thereby, additional rotations that accentuate local deformations of the structures. Therefore, we can state that the improper execution of the connections leads to a less stiff structure and may be the main cause of the differences found between the

displacements obtained in the three towers for global  $X$  direction under Hypothesis 1 and for global  $Y$  direction under Hypotheses 2 and 3.

A representative example of this behavior can be seen in Figure 7, which shows the deformed shape of tower 1 for Models 2 and 3 under Load Case 3 (electrical conductor break), which subjects the body of the tower to a torque.

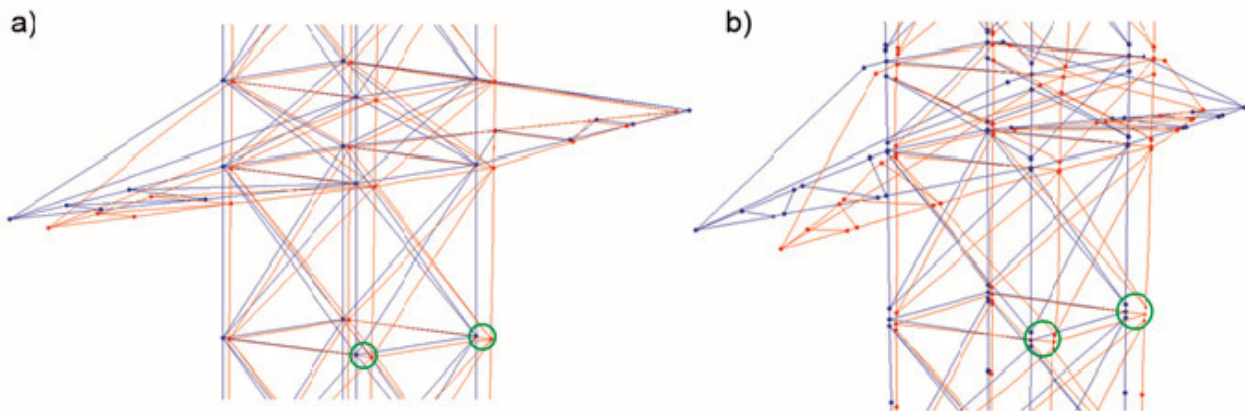


**Figure 7.** Detail of the different structural behavior of the Tower 1 under Load Case 3 in Model 2 (a) and Model 3 (b). Undeformed shape is shown in blue and deformed shape in red.

#### 4.3.2. Stresses in Structural Elements

Finally, a comparison regarding the stresses in structural elements [12,14,15,16,29] is also established. Table 6 shows, based on the finite element results obtained, the maximum normal stresses for each transmission tower and its respective structural model. Particularly, it details for each tower, and for each model, the maximum normal stress in which member it occurs, and under which loading case is developed.

**Table 6.** Structural elements with maximum normal stresses for all transmission towers analyzed and structural models considered.

Tower	Model	Maximum Stress (Mpa)/Frame Element		
		Hypothesis 1	Hypothesis 2	Hypothesis 3
1	1	215.15/90	165.26/401	195.56/468
	2	225.36/90	170.23/401	205.21/468
	3	252.30/696	185.96/433	230.20/696
2	1	218.96/380	155.50/442	221.32/405
	2	222.56/380	163.89/442	232.45/405
	3	234.21/178	181.78/439	245.63/189
3	1	222.25/272	167.25/353	221.45/107
	2	232.63/272	175.63/353	226.12/107
	3	252.58/272	195.56/353	233.16/104

Based on Table 6, it can be observed that the differences in maximum normal stresses between Model 1 and Model 2 for all towers are quite small and the maximum of these values are always

produced in the same members for both models. On the contrary, significant differences appear when compared to Model 3. Consider the case of Tower 1 and under Load Case 1 where the differences is approximately 37 MPa.

Moreover, it could be observed that the maximum stresses in Model 3 no longer occur at the same members that for Models 1 and 2. This is due to the singular arrangement of nodes in Model 3 (members do not intersect at a single point) which leads to a different discretization of frame elements compared to Models 1 and 2.

Rising stresses in Model 3 are mainly due to secondary stresses caused by the additional bending moments derived from small geometric eccentricities at diagonal and horizontal member's connections upon truss chords which are neglected in Model 1 and Model 2.

The higher the eccentricity is at the connections, the greater the induced bending moments will be. Likewise, the level of induced secondary stresses will be influenced by the stiffness of the truss chords; the greater is their stiffness the greater bending moments will be induced.

This is perhaps the cause of the observed differences for Tower 1 under Load Case 1, where the stiffness of the truss chords relative to the overall stiffness of the whole structure is greater than in the other two towers, thus providing greater increased stresses (37 MPa) with respect to the theoretical Model 1.

It should be also noted that for Model 3, under certain load cases in all towers, some elements exceed the yield point of the material. This circumstance is highlighted in Figure 8, where for tower 1 and under Load Case 1, the element with maximum normal stress reaches 252 MPa, exceeding the elastic limit of the material in 17 MPa. Figure 8 also shows a representative image of the above discussed; the effects of improper execution of nodes upon truss chords and, consequently, the different discretization of frame elements in the model with ideal geometry and those based on real geometry.

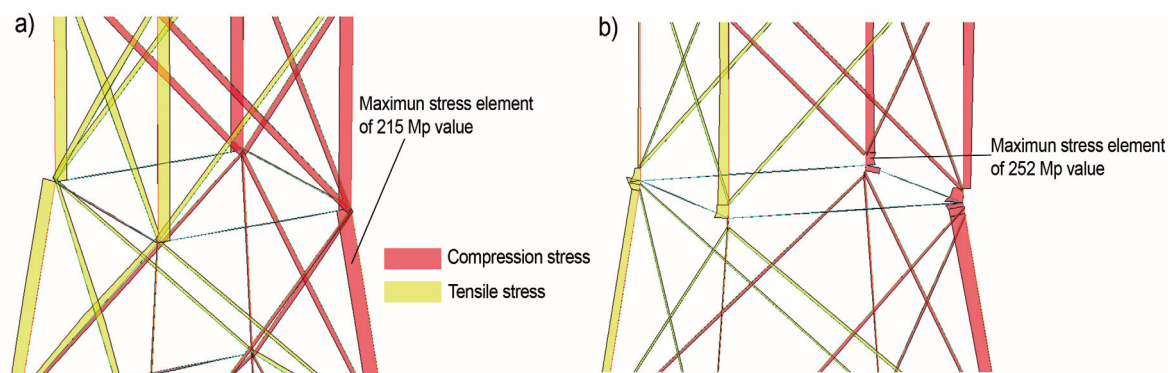


**Figure 8.** Normal stresses distribution onto Tower 1 for different structural models. (a) Model 1, with ideal representation of the nodes and maximum stress below the yield limit of steel; (b) Model 3, including the improper executions of the nodes and maximum stress exceeding the yield limit of steel.

As for results involving values of maximum normal stresses, they should be analyzed carefully. Due to the age of the structures, assumed material properties have been chosen according to the minimum value specified by the current regulatory codes; however, these values do not have to match the actual properties of the structure. Accordingly, appropriate experimental tests should be carried out in order to improve their characterization and, thus, derive proper conclusions about the real current safety state

of the structure. Note, also, that the structural analysis of transmission towers was carried out assuming a linear elastic behavior.

Nonetheless, the results herein obtained could be considered as acceptable, bearing in mind that the present work is focused in defining an overall methodology able to detect the geometric imperfections present in electricity transmission tower structures by means of precise laser scanning systems and the procedures to incorporate them in structural models based on finite element methods.

## 5. Conclusions

Terrestrial laser scanning enabled performing a non-invasive remote survey of different transmission tower structures; it should be noted that these are objects of great complexity, not only for their size, but also by their geometry and their high heights. This technology allowed detecting significant imperfections in terms of connections between the members at the nodes, loss of verticality of the towers and the lack of horizontality in the horizontal bracings. The aforementioned imperfections motivated the consideration of different structural models for the towers, in order to analyze how this affects their structural behavior. To that purpose, three different models have been carried out: first, a model with an ideal geometry and considering perfectly pin jointed nodes (supposed model in original calculations of the structures); second, a model with ideal geometry, but taking into account real existing continuity in some profiles by means of rigid connections and pin jointed connections of all others elements upon them; and finally, a third model similar to that previous, but with a real geometry incorporating all imperfections obtained from laser scanning data.

When analyzing the results obtained in terms of displacements and stresses yielded by the different structural models considered, significant differences were observed. At those nodes considered for the comparison of displacements, differences between models with ideal geometry, and models with real geometry reached several centimeters, becoming the highest value (for Node 1 in Tower 1 under wind loading) 9.5 cm respect to the  $X$  global direction.

The study of stresses brings some other conclusions. Considering models with ideal geometry and considering pinned joints (Model 1) or rigid joints (Model 2) no significant differences were found. Indeed, maximum normal stresses in elements always take place in the same elements for both models. On the contrary, the model which accounts for real geometry (Model 3) presented notable differences when compared with their respective idealized models. Notorious increases in stresses were detected under certain loading conditions, even reaching the elastic limit of the steel in some occasions.

Differences observed in displacements, stresses in elements and, thereby, whole structural behavior of towers suggest that a detailed survey and conscientious structural analysis has to be carried out when these type of structures will be required for future uses as, for example, new communication services that increase their service loads.

Further studies could contemplate performing nonlinear analysis to extend and improve the results herein obtained, either by considering geometric nonlinearity effects such as P-Delta effects and plastic behavior of steel material. Moreover, due to the nature of the structures (quite slender, and with very slender members) the issue of structural stability should also be addressed. Therefore, it is expected that the combination in the use of the information already available, with the procedure herein

developed, together with the consideration of more advanced topics related to strength and structural stability evaluation, will bring a deep insight in the behavior of the towers.

### Acknowledgments

This study was funded in part by the Universities of Salamanca and Vigo. Authors would like to thank Remote Sensing and the anonymous reviewers which provided numerous comments and suggestions that contributed to improve significantly an earlier version of the manuscript.

### Author Contributions

All authors contributed extensively to the work presented in this paper.

### Conflicts of Interest

The authors declare no conflict of interest.

### References

1. Ghilani, C.D.; Wolf, P.R. *Adjustment Computations: Spatial Data Analysis*, 4th ed.; John Wiley & Sons: Hoboken, NJ, USA, 2006.
2. Villarino, A.; Riveiro, B.; Gonzalez-Aguilera, D.; Sanchez-Aparicio, L. The integration of geotechnologies in the evaluation of a wine cellar structure through the Finite Element Method. *Remote Sens.* **2014**, *6*, 11107–11126.
3. Costanzo, A.; Minasi, M.; Casula, G.; Musacchio, M.; Buongiorno, M.F. Combined use of terrestrial laser scanning and IR thermography applied to a historical building. *Sensors* **2014**, *15*, 194–213.
4. Fregonese, L.; Barbieri, G.; Biolzi, L.; Bocciarelli, M.; Frigeri, A.; Taffurelli, L. Surveying and monitoring for vulnerability assessment of an ancient building. *Sensors* **2013**, *13*, 9747–9773.
5. Choi, S.W.; Kim, B.R.; Lee, H.M.; Kim, Y.; Park, H.S. A deformed shape monitoring model for building structures based on a 2D laser scanner. *Sensors* **2013**, *13*, 6746–6758.
6. Ioannidis, C.; Valani, A.; Georgopoulos, A.; Tsiligiris, E. 3D model generation for deformation analysis using laser scanning data of a Cooling Tower. In Proceedings of the 3rd IAG/12th FIG Symposium, Baden, Switzerland, 22–24 May 2006.
7. González-Aguilera, D.; del Pozo, S.; Lopez, G.; Rodriguez-Gonzálvez, P. From point cloud to CAD models: Laser and optics geotechnology for the design of electrical substations. *Opt. Laser Technol.* **2012**, *44*, 1384–1392.
8. Shu, Q.; Yuan, G.; Zhang, Y.; Guo, G. Research on anti-foundation-displacement performance and reliability assessment of 500 KV transmission tower in mining subsidence area. *Open Civ. Eng. J.* **2011**, *5*, 87–92.
9. Yang, F.; Yang, J.; Han, J.; Zhang, Z. Study on the limited values of foundation deformation for a typical UHV transmission tower. *IEEE Trans. Power Deliv.* **2010**, *2*, 2752–2758.



10. Yuan, G.L.; Li, S.M.; Xu, G.A.; Si, W.; Zhang, Y.F.; Shu, Q.J. The anti-deformation performance of composite foundation of transmission tower in mining subsidence area. *Proc. Earth Plan. Sci.* **2009**, *1*, 571–576.
11. Shu, Q.J.; Yuan, G.L.; Guo, G.L.; Zhang, Y.F. Limits to foundation displacement of an extra high voltage transmission tower in a mining subsidence area. *Int. J. Min. Sci. Technol.* **2012**, *22*, 13–18.
12. Yang, F.; Li, Q.; Yang, J.; Zhu, B. Assessment on the stress state and the maintenance schemes of the transmission tower above goaf of coal mine. *Eng. Fail. Anal.* **2013**, *31*, 236–247.
13. Prasad Rao, N.; Kalyanaraman, V. Non-linear behaviour of lattice panel of angle towers. *J. Constr. Steel Res.* **2001**, *57*, 1337–1357.
14. Da Silva, J.G.S.; da S. Vellasco, P.C.G.; de Andrade, S.A.L.; de Oliveira, M.I.R. Structural assessment of current steel design models for transmission and telecommunication towers. *J. Constr. Steel Res.* **2005**, *61*, 1108–1134.
15. Prasad Rao, N.; Samuel Knight, G.M.; Mohan, S.J.; Lakshmanan, N. Studies on failure of transmission line towers in testing. *Eng. Struct.* **2012**, *35*, 55–70.
16. Klinger, C.; Mehdiانpour, M.; Klingbeil, D.; Bettge, D.; Häcker, R.; Baer, W. Failure analysis on collapsed towers of overhead electrical lines in the region Münsterland (Germany) 2005. *Eng. Fail. Anal.* **2011**, *18*, 1873–1883.
17. Zhuge, Y.; Mills, J.E.; Ma, X. Modelling of steel lattice tower angle legs reinforced for increased load capacity. *Eng. Struct.* **2012**, *43*, 160–168.
18. Órgano MINISTERIO DE INDUSTRIA, TURISMO Y COMERCIO. *Real Decreto 223/2008 Reglamento sobre Condiciones Técnicas y Garantías de Seguridad en Líneas Eléctricas de Alta Tensión y sus Instrucciones Técnicas Complementarias ITC-LAT 01 A 09*, 1st ed.; Boletín Oficial del Estado: Madrid, Spain, 2008.
19. Wilson, E. *Integrated Finite Element Analysis and Design of Structures*, 7th ed.; Computers and Structures, Inc: Berkeley, CA, USA, 1998.
20. Eurocode 3: Design of steel structures—Part 1-1: General Rules and Rules for Buildings EN 1993-1-1: 2005. Available online: <https://law.resource.org/pub/eur/ibr/en.1993.1.1.2005.pdf> (accessed on 4 July 2015).
21. Beer, F.; Johnston, E.R., Jr.; Mazurek, D. *Vector Mechanics for Engineers: Statics*, 10th ed.; McGraw-Hill Science: London, UK, 2012.
22. Hibbeler, R.C. *Mecánica Vectorial Para Ingenieros: Estática*, 10th ed.; Pearson Educación: Mexico D.F., México, 2004.
23. Eurocode 1: Actions on structures Part 1-1: General Actions—Densities, Self-Weight, Imposed loads for buildings. UNE-EN 1991-1-1: 2003. Available online: <http://infostore.saiglobal.com/emea/details.aspx?ProductID=400059> (accessed on 4 July 2015).
24. Argüelles, R.; Arriaga, F.; Atienza, J.R.; Martínez, J.J. *Estructuras de Acero II: Uniones y Sistemas Estructurales*, 1st ed.; Bellisco: Madrid, Spain, 2001.
25. Besl, P.; McKay, N. A method for registration of 3D shapes. *IEEE Pattern Anal. Machine Intell.* **1992**, *14*, 239–256.
26. Eurocode 0—Basis of Structural Design UNE-EN 1990: 2003. Available online: <http://infostore.saiglobal.com/store/details.aspx?ProductID=400051> (accessed on 4 July 2015).

27. Laefer, D.F.; Truong-Hong, L.; Fitzgerald, M. Processing of terrestrial laser scanning point cloud data for computational modelling of building facades. *Recent Pat. Comput. Sci.* **2011**, *44*, 16–29.
28. Liu, Y.C.; Liu, Z.D. Study on stabilization and rectification technology for inclined transmission tower. *Rock Soil Mech.* **2008**, *29*, 173–176.
29. Villarino, A.; Riveiro B.; Martínez-Sánchez, J.; Gonzalez-Aguilera, D. Successful applications of geotechnologies for the evaluation of road infrastructures. *Remote Sens.* **2014**, *6*, 7800–7818.

© 2015 by the authors; licensee MDPI, Basel, Switzerland. This article is an open access article distributed under the terms and conditions of the Creative Commons Attribution license (<http://creativecommons.org/licenses/by/4.0/>).





## 4. CONCLUSIONES

En la Tesis Doctoral se ha propuesto, desarrollado y probado una metodología para la modelización geométrica tridimensional de infraestructuras, a través de la hibridación de técnicas geomáticas y su análisis estructural por el método de los elementos finitos. Presentándose su aplicación a las infraestructuras asociadas a las carreteras, las edificaciones subterráneas pertenecientes al Patrimonio Histórico y las estructuras metálicas en celosía, como las torres de soporte de líneas de alta tensión.

A continuación se destacan las **conclusiones** más relevantes de los artículos científicos desarrollados en la Tesis Doctoral:

- La fotogrametría digital terrestre y el TLS, se muestran como técnicas geomáticas óptimas en la reconstrucción geométrica en 2D y 3D de las infraestructuras asociadas al trazado de una carretera. En concreto, su aplicación en estructuras históricas, como los puentes de fábrica, permite generar modelos que describan el sistema de construcción y la configuración de sus elementos constituyentes. Destacan por ser herramientas de carácter no invasivo y no destructivo, fáciles y rápidas, tanto en la adquisición de datos en campo como en el procesamiento de la información en laboratorio, y accesibles para la mayoría de técnicos intervinientes. Resultan idóneas en la obtención de información métrica, en los casos, en que no hay constancia de planos de construcción de estas infraestructuras, reflejando tanto las características dimensionales como su textura.

- Se ha avanzado en estrategias de transformación de las nubes de puntos, obtenidas de los sensores geomáticos, en representaciones gráficas de formatos de dibujo universal del tipo CAD, aptos para su aplicación en campos de la ingeniería y la arquitectura. De esta manera, la geomática se posiciona como el primer paso de posteriores análisis estructurales, permitiendo optimizar el tiempo de generación de un modelo geométrico preciso que pueda ser exportado para una simulación numérica. Esto proporciona datos valiosos con los que diagnosticar la salud estructural de las construcciones.
  
- La combinación de diversos sensores geomáticos en unidades móviles terrestres, permite la toma masiva de datos que generen mapas cartográficos de las carreteras y sus infraestructuras asociadas. Esto automatiza los trabajos de inventario geométrico e inspección, consiguiendo una alta productividad en la realización de estas labores, además de evitar la subjetividad en el diagnóstico del estado actual de las infraestructuras. Toda la información reunida puede ser visualizada y editada en aplicaciones de *software* que constituyan un sistema de gestión de las infraestructuras viarias.
  
- La hibridación de técnicas geomáticas como el TLS y el GPR en una edificación subterránea de carácter patrimonial, permite aprovechar las sinergias obtenidas con la georreferenciación de ambas tecnologías, disponiendo de un modelo geométrico completo con el que relacionar la geometría exterior con las características físicas internas de las partes integrantes de la construcción. Esto optimiza el tiempo de generación de un modelo estructural preciso, que puede ser implementado en simulaciones numéricas por elementos finitos. Esta disciplina de análisis estructural se considera adecuada en este tipo de construcciones, ya que permite la simulación bajo diferentes solicitaciones y condiciones, además de aportar resultados precisos, confiables y detallados. Los resultados de la evaluación estructural proporcionan información relevante para el estudio de la estabilidad, capacidad portante y vida útil de estas estructuras subterráneas, contribuyendo a complementar y mejorar las labores de conservación y preservación.

- El TLS es un sensor geomático cuya aplicación en estructuras metálicas en celosía garantiza eficacia y calidad en los resultados. Debido a la complejidad geométrica de estas, el grado de detalle del TLS aporta una representación métrica de alta precisión, que complementado con su carácter remoto reduce riesgos durante el proceso de medición en este tipo de estructuras. El TLS se establece como herramienta perfecta para crear modelos fidedignos de la realidad geométrica, que puedan ser implementados de manera semiautomática en simulaciones numéricas por elementos finitos. La posibilidad de obtener modelos geométricos precisos y detallados de este tipo de estructuras, permite analizar y cuantificar la incidencia que las singularidades constructivas detectadas tienen en el comportamiento de la estructura.

Finalmente como **conclusión general** de la presente Tesis Doctoral, se muestra una metodología de trabajo global, que combina los sensores geomáticos con el análisis estructural por elementos finitos, lo que redundará en un incremento de la precisión de los modelos numéricos necesarios para entender el comportamiento estructural de las construcciones. Este método de trabajo es una herramienta de carácter no invasivo, rápida, precisa, accesible para la mayoría de técnicos intervinientes y de múltiples aplicaciones que sirven de importante complemento en los trabajos de mantenimiento, conservación, preservación, inspección e inventario de infraestructuras.



## **5. LÍNEAS DE INVESTIGACIÓN FUTURAS**

A raíz del desarrollo de la Tesis Doctoral se proponen las siguientes **líneas de investigación futuras**:

- La hibridación con otras herramientas, como la tomografía infrarroja o métodos ultrasónicos, que permitan obtener nuevas sinergias que complementen la caracterización de las estructuras.
- Avanzar en un método de trabajo conjunto que combine los sensores láser escáner y fotogramétricos con la evaluación dinámica de estructuras, principalmente a través del análisis modal. Con el objetivo de aumentar la precisión de los modelos numéricos, necesarios para entender el comportamiento de las infraestructuras.
- Aplicación de métodos de clasificación multiespectral de imágenes, a partir de diferentes sensores geomáticos, que permitan identificar y cuantificar patologías que presenten una relación con la estabilidad y vida útil de las construcciones.
- Desarrollar metodologías de calibración robusta de modelos numéricos, capaces de localizar e interpretar los daños principales presentes en las construcciones a partir de modelos geométricos precisos.





## 6. REFERENCIAS BIBLIOGRÁFICAS

Albermani, F.G.A.; Kitipornchai, S. Numerical simulation of structural behaviour of transmission towers. *Thin-walled structures* **2003**, *41*(2), 167–177.

Annan A.P. *Ground Penetrating Radar Principles, Procedures & Applications*, 1st ed.; Sensors & Software Inc: Mississauga, Canada, 2003.

Arayici, Y. An approach for real world data modelling with the 3D terrestrial laser scanner for built environment. *Automation in Construction* **2007**, *16*, 816–829

Arias, P.; Armesto, J.; Di-Capua, D.; González-Drigo, R.; Lorenzo, H.; Pérez-Gracia, V. Digital photogrammetry, GPR and computational analysis of structural damages in a mediaeval bridge. *Engineering Failure Analysis* **2007**, *14*(8), 1444–1457.

Asociación de Empresas de Conservación y Explotación de Infraestructuras. *Libro Verde de la Conservación de las Infraestructuras en España*, 1st ed.; Acex: Madrid, España, 2010.

Capra, A.; Costantino, D.; Rossi, G.; Angelini, M.G., Leserri, M. Survey and 3d modelling of Castel del Monte. In Proceedings of XX Symposium of International Cooperation to Save the World's Cultural Heritage, Torino, Italy, September 2005; pp. 183–189.

Conde-Carnero, B.; Riveiro, B.; Arias, P.; Caamaño, J. C. Exploitation of geometric data provided by laser scanning to create fem structural models of bridges. *Journal of Performance of Constructed Facilities* **2015**, doi: 10.1061/(ASCE)CF.1943-5509.0000807.

Endo, Y.; Pelà, L.; Roca, P.; da Porto, F.; Modena, C. Comparison of seismic analysis methods applied to a historical church struck by 2009 L'Aquila earthquake. *Bulletin of Earthquake Engineering* **2015**, 1–30.

Farjas, M.; García, F.J. *Modelización Tridimensional y Sistemas Láser Escáner 3D Aplicados al Patrimonio Histórico*, 1st ed.; La Ergástula: Madrid, Spain, 2008.

Gonen, H.; Dogan, M.; Karacasu, M.; Ozbasaran, H.; Gokdemir, H. Structural failures in retrofit historical masonry arch bridge. *Engineering Failure Analysis* **2013**, 35, 334–342.

González-Drigo, R.; Pérez-Gracia, V.; Di Capua, D.; Pujades, L. G. GPR survey applied to modernista buildings in Barcelona: The cultural heritage of the College of Industrial Engineering. *Journal of Cultural Heritage* **2008**, 9(2), 196–202.

Guang-lin, Y.; Shi-ming, L.; Guo-an, X.; Wei, S.; Yun-fei, Z.; Qian-jin, S. The anti-deformation performance of composite foundation of transmission tower in mining subsidence area. *Procedia Earth and Planetary Science* **2009**; 1, 571–576.

Hernández, S.; Romera, L.E. Computer Modelling of the Basilica of Pilar in Zaragoza (Spain). *Structural Studies, Repairs and Maintenance of Heritage Architecture VIII*, Halkidiki, Grece, 2003; Brebbia C.A.; pp. 597– 606.

Herranz, A. *La Dotación de Infraestructuras en España, 1844-1935*, 1st ed.; Banco de España. Servicio de Estudios de Historia Económica: Madrid, Spain, 2004.

Heyman, J. *The Stone Skeleton: Structural Engineering of Masonry Architecture*, 1st ed.; Cambridge University Press: Cambridge, UK, 1997.

Huerta, S. The analysis of masonry architecture: a historical approach: to the memory of professor Henry J. Cowan. *Architectural Science Review* **2008**, 51(4), 297–328.

Kanli, A.I.; Taller, G.; Nagy, P.; Tildy, P.; Pronay, Z.; Toros, E. GPR survey for reinforcement of historical heritage construction at fire tower of Sopron. *Journal of Applied Geophysics* **2015**, 112, 79–90.

Klinger, C.; Mehdiانpour, M.; Klingbeil, D.; Bettge, D.; Häcker, R.; Baer, W. Failure analysis on collapsed towers of overhead electrical lines in the region Münsterland (Germany) 2005. *Engineering Failure Analysis* **2011**, *18*, 1873–1883.

Komorski, A.; Skejić, D.; Dujmović, D. Reliability assessment of overhead transmission line towers in the Republic of Croatia. *Tehnicki Vjesnik-Technical Gazette*. **2013**, *20*(3), 381–390

Kuang, M.M. Analysis of foundation rectification method of 220kv Tower 012 on Sihui Duanzhou line. *Guangdong Electric Power* **2002**, *15*(1), 67–69.

Laefer, D.; Truong-Hong, L.; Fitzgerald, M. Processing of terrestrial laser scanning point cloud data for computational modelling of building facades. *Recent Patents on Computer Science* **2011**, *4*(1), 16–29.

Lorenzo, H.; Arias, P.; Armesto, J.; Riveiro, B.; Solla, M.; González Jorge, H.; Varela, M. Ten years of applying geomatics to construction engineering in Spain: a review. *Dyna* **2012**, *79*, 129–146.

López, J.; Oller, S.; Oñate, E. *Cálculo del Comportamiento de la Mampostería Mediante Elementos Finitos*, 1st ed; CIMNE: Barcelona, España, 1998.

Lubowiecka, I.; Arias, P.; Riveiro, B.; Solla, M. Multidisciplinary approach to the assessment of historic structures based on the case of a masonry bridge in Galicia (Spain). *Computers & Structures* **2011**, *89*(17), 1615–1627.

Lubowiecka, I.; Armesto, J.; Arias, P.; Lorenzo, H. Historic bridge modelling using laser scanning, ground penetrating radar and finite element methods in the context of structural dynamics. *Engineering Structures* **2009**, *31*(11), 2667–2676.

Mañana-Borrazás, P.; Rodríguez, A.; Blanco-Rotea, R. Una experiencia en la aplicación del láser escáner 3D a los procesos de documentación y análisis del patrimonio construido: su aplicación a Santa Eulalia de Bóveda (Lugo) y San Fiz de Solovio (Santiago de Compostela). *Arqueología de la Arquitectura* **2008**, *5*, 15–32.

Mark, R. *Experiments in Gothic Structures*, 1st ed.; The Massachusetts Institute of Technology Press: Massachusetts, USA, 1982.

Martínez, G.; Roca, P.; Caselles, O.; Clapés, J.; Barbat, A. H. Determinación experimental y analítica de las propiedades dinámicas para la Catedral de Mallorca. *Structural Engineering (Intersections/Intersecții)* **2007**, 4(2).

Molina, D.F.G.; Tubío, F.D.P. El láser escáner 3D aplicado al patrimonio arquitectónico de Priego de Córdoba: la Torre del Homenaje. *Antiquitas* **2012**, 24, 277–302.

Orbán, Z.; Gutermann, M. Assessment of masonry arch railway bridges using non-destructive in-situ testing methods. *Engineering Structures* **2009**, 31(10), 2287–2298.

Pereira, J.R.A. *Introducción a la Historia de la Arquitectura*, 1st ed.; Reverté: Barcelona, Spain, 2005.

Rao, N.P.; Knight, G.M.S.; Mohan, S.J.; Lakshmanan, N. Studies on failure of transmission line towers in testing. *Engineering Structures* **2012**, 35, 55–70.

Riveiro, B.; Caamaño, J.C.; Arias, P.; Sanz, E. Photogrammetric 3D modelling and mechanical analysis of masonry arches: an approach based on a discontinuous model of voussoirs. *Automation in Construction* **2011**, 20(4), 380–388.

Riveiro, B., Morer, P., Arias, P.; de Arteaga, I. Terrestrial laser scanning and limit analysis of masonry arch bridges. *Construction and Building Materials* **2011**, 25(4), 1726–1735.

Roca, P.; Cervera, M.; Gariup, G. Structural analysis of masonry historical constructions. Classical and advanced approaches. *Archives of Computational Methods in Engineering* **2010**, 17(3), 299–325.

Roca, P.; Cervera, M.; Pelà, L.; Clemente, R.; Chiumenti, M. Continuum FE models for the analysis of Mallorca Cathedral. *Engineering Structures* **2013**, 46, 653–670.

Rui-Wamba, J. *Arquitectura e Infraestructura*, 1st ed.; Fundación Esteyco: Madrid, España, 2011.

Saloustros, S.; Pelà, L.; Roca, P.; Portal, J. Numerical analysis of structural damage in the church of the Poblet Monastery. *Engineering Failure Analysis* **2015**, 48, 41–61.

Santos-Assunção, S.; Perez-Gracia, V.; Caselles, O.; Clapes, J.; Salinas, V. Assessment of complex masonry structures with GPR compared to other non-destructive testing studies. *Remote Sensing* **2014**, *6*(9), 8220–8237.

Shu, Q.; Yuan, G.; Zhang, Y.; Guo, G. Research on anti-foundation-displacement performance and reliability assessment of 500 kv transmission tower in mining subsidence area. *Open Civil Engineering Journal* **2011**, *5*, 87–92.

Silva, T. *Como Estimar a Vida Útil de Estruturas Projetadas com Critérios que Visam a Durabilidade*. In II Workshop sobre Durabilidade das Construções, Sao José dos Campos, Brasil, 2001; pp. 133–143.

Solla, M.; Lorenzo, H.; Rial, F. I.; Novo, A. GPR evaluation of the roman masonry arch bridge of Lugo (Spain). *NDT & E International* **2011**, *44*(1), 8–12.

Solla, M.; Lorenzo, H.; Riveiro, B.; Rial, F.I. Non-destructive methodologies in the assessment of the masonry arch bridge of Traba, Spain. *Engineering Failure Analysis* **2011**, *18*(3), 828–835.

Tang, P.; Huber, D.; Akinci, B.; Lipman, R.; Lytle, A. Automatic reconstruction of as-built building information models from laser scanned point clouds: a review of related techniques. *Automation in Construction* **2010**, *19*(7), 829–843.

Van de Ven, M.M.; Fabregat, P.R.; Ruiz, M.C. *Análisis Estructural de la Mezquita Pequeña Santa Sofía de Estambul*. CIMNE: Barcelona, España, 2004

Vosselman, G.; Dijkman, S. 3D building model reconstruction from point clouds and ground plans. *International Archives of Photogrammetry Remote Sensing and Spatial Information Sciences* **2001**, *34* (3/W4), 37–44.

Walsh, S.B.; Borello, D.J.; Guldur, B., Hajjar, J.F. Data processing of point clouds for object detection for structural engineering applications. *Computer-Aided Civil and Infrastructure Engineering* **2013**, *28*(7), 495–508.

Wright, P. *Introducción a la Ingeniería*, 1st ed.; Limusa: México, 2004.

Yang, F.; Li, Q.; Yang, J.; Zhu, B. Assessment on the stress state and the maintenance schemes of the transmission tower above goaf of coal mine. *Engineering Failure Analysis*. **2013**, *31*, 236–247.

Zhang, J.Q.; Yang, K.; Wang, Y.D.; Tang, Y.C. Research on foundation treatment of high voltage transmission towers erected above goaf of coal mine. *Power System Technology* **2006**, *2*, 006.

Zienkiewicz, O.C.; Cheung, Y.K. *The Finite Element Method in Structural and Continuum Mechanics*, 1st ed.; Mc Graw-Hill: London, UK, 1967.

## **7. ANEXO. FACTOR DE IMPACTO DE LAS PUBLICACIONES**

La revista de impacto en la que se han publicado los diferentes artículos originales que componen la presente Tesis Doctoral, está indexada en el *Journal Citation Reports®*, adjuntándose a continuación la información detallada referente a los parámetros estadísticos y bibliométricos de la revista.

Nombre de la revista:	<b>REMOTE SENSING</b>
URL:	<b><a href="http://www.mdpi.com/journal/remotesensing">www.mdpi.com/journal/remotesensing</a></b>
Editorial:	<b>MDPI</b>
ISSN:	<b>2072-4292</b>
Factor de impacto (2014):	<b>3.180</b>
Ranking de la revista:	<b>5/28</b>
Cuartil:	<b>Q1</b>





Journal: Remote Sensing

Mark	Journal Title	ISSN	Total Cites	Impact Factor	5-Year Impact Factor	Immediacy Index	Citable Items	Cited Half-life	Citing Half-life
	<a href="#">REMOTE SENS-BASEL</a>	2072-4292	3061	<a href="#">3.180</a>	<a href="#">3.257</a>	<a href="#">0.505</a>	572	<a href="#">2.5</a>	<a href="#">7.9</a>
<a href="#">Cited Journal</a> <a href="#">Citing Journal</a> <a href="#">Source Data</a> <a href="#">Journal Self Cites</a>									

CITED JOURNAL DATA CITING JOURNAL DATA IMPACT FACTOR TREND RELATED JOURNALS

Journal Information

**Full Journal Title:** Remote Sensing  
**ISO Abbrev. Title:** Remote Sens.  
**JCR Abbrev. Title:** REMOTE SENS-BASEL  
**ISSN:** 2072-4292  
**Issues/Year:** 12  
**Language:** ENGLISH  
**Journal Country/Territory:** SWITZERLAND  
**Publisher:** MDPI AG  
**Publisher Address:** POSTFACH, CH-4005 BASEL, SWITZERLAND  
**Subject Categories:** REMOTE SENSING

**Eigenfactor<sup>®</sup> Metrics**  
**Eigenfactor<sup>®</sup> Score**  
 0.01044  
**Article Influence<sup>®</sup> Score**  
 0.772

SCOPE NOTE  
 VIEW JOURNAL SUMMARY LIST VIEW CATEGORY DATA

Journal Rank in Categories: JOURNAL RANKING

Journal Impact Factor

Cites in 2014 to items published in: 2013 = 893    Number of items published in: 2013 = 316  
 2012 = 697    2012 = 184  
 Sum: 1590    Sum: 500  
 Calculation:  $\frac{\text{Cites to recent items}}{\text{Number of recent items}} = \frac{1590}{500} = 3.180$

5-Year Journal Impact Factor

Cites in {2014} to items published in: 2013 = 893    Number of items published in: 2013 = 316  
 2012 = 697    2012 = 184  
 2011 = 513    2011 = 137  
 2010 = 428    2010 = 141  
 2009 = 241    2009 = 73  
 Sum: 2772    Sum: 851  
 Calculation:  $\frac{\text{Cites to recent items}}{\text{Number of recent items}} = \frac{2772}{851} = 3.257$

## Journal Self Cites ▲

The tables show the contribution of the journal's self cites to its impact factor. This information is also represented in the [cited journal graph](#).

<b>Total Cites</b>	3061	<b>Self Cites</b>	920 (30% of 3061)
<b>Cites to Years Used in Impact Factor Calculation</b>	1590	<b>Self Cites to Years Used in Impact Factor Calculation</b>	528 (33% of 1590)
<b>Impact Factor</b>	3.180	<b>Impact Factor without Self Cites</b>	2.124

## Journal Immediacy Index ▲

Cites in 2014 to items published in 2014 = 289  
 Number of items published in 2014 = 572  
 Calculation:  $\frac{\text{Cites to current items}}{\text{Number of current items}} = \frac{289}{572} = 0.505$

## Journal Cited Half-Life ▲

The cited half-life for the journal is the median age of its items cited in the current JCR year. Half of the citations to the journal are to items published within the cited half-life.

**Cited Half-Life: 2.5 years**

Breakdown of the citations *to the journal* by the cumulative percent of 2014 cites to items published in the following years:

Cited Year	2014	2013	2012	2011	2010	2009	2008	2007	2006	2005	2004-all
# Cites from 2014	289	893	697	513	428	241	0	0	0	0	0
Cumulative %	9.44	38.61	61.39	78.14	92.13	100.00	100.00	100.00	100.00	100.00	100

### Cited Half-Life Calculations:

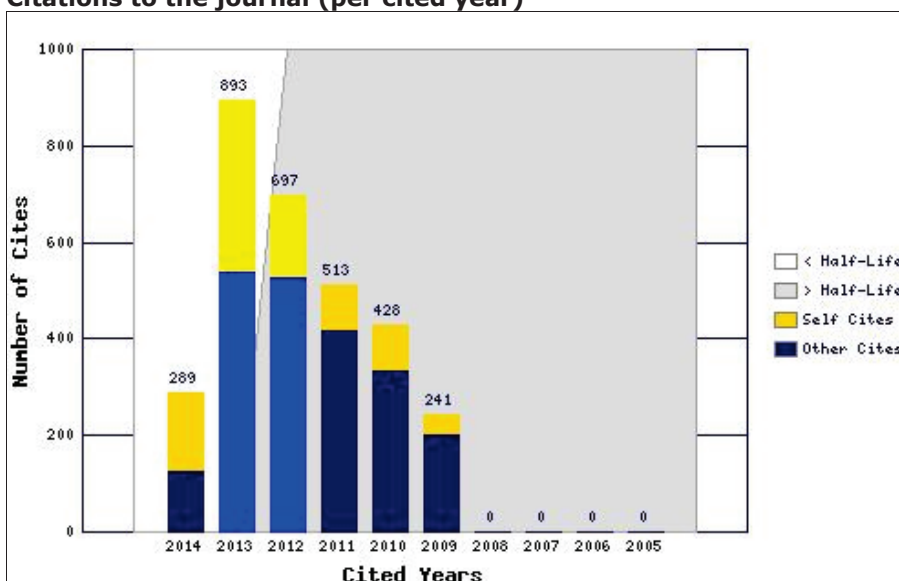
The cited half-life calculation finds the number of publication years from the current JCR year that account for 50% of citations received by the journal. Read help for more information on the calculation.

## Cited Journal Graph ▲

[Click here for Cited Journal data table](#)

This graph shows the distribution by cited year of citations to items published in the journal REMOTE SENS-BASEL.

### Citations to the journal (per cited year)



- The white/grey division indicates the cited half-life (if < 10.0). Half of the journal's cited items were published more recently than the cited half-life.
- The top (gold) portion of each column indicates Journal Self Citations: citations to items in the journal from items in the same journal.
- The bottom (blue) portion of each column indicates Non-Self Citations: citations to the journal from items in other journals.
- The two lighter columns indicate citations used to calculate the Impact Factor (always the 2nd and 3rd columns).

## Journal Citing Half-Life ▲

The citing half-life for the journal is the median age of the items the journal cited in the current JCR year. Half of

the citations in the journal are to items published within the citing half-life.

**Citing Half-Life: 7.9 years**

Breakdown of the citations **from the journal** by the cumulative percent of 2014 cites to items published in the following years:

Cited Year	2014	2013	2012	2011	2010	2009	2008	2007	2006	2005	2004-all
# Cites from 2014	1047	2371	2435	2217	1993	1865	1804	1466	1356	1354	12068
Cumulative %	3.49	11.40	19.53	26.92	33.57	39.79	45.81	50.70	55.22	59.74	100

**Citing Half-Life Calculations:**

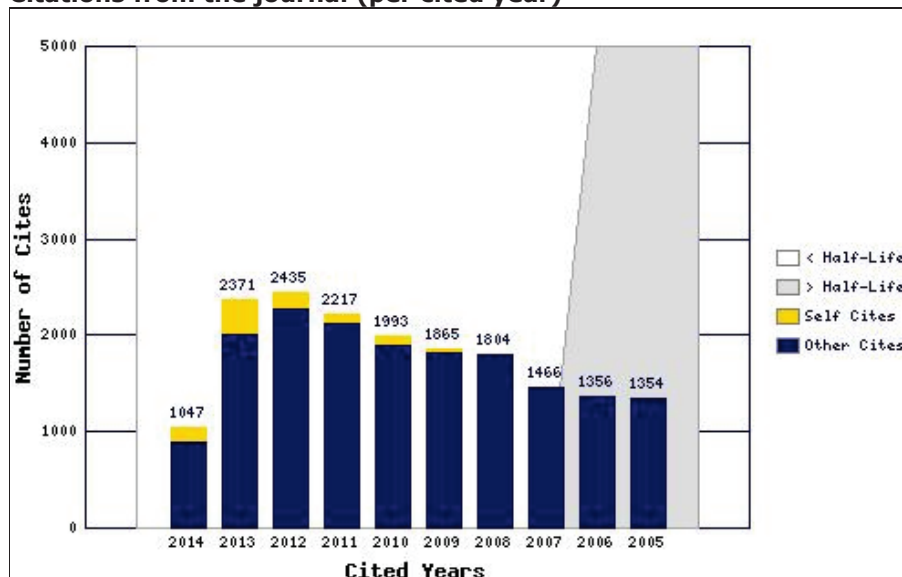
The citing half-life calculation finds the number of publication years from the current JCR year that account for 50% of citations in the journal. Read help for more information on the calculation.

**Citing Journal Graph** 

[Click here for Citing Journal data table](#)

This graph shows the distribution by cited year of citations from current-year items in the journal REMOTE SENS-BASEL.

**Citations from the journal (per cited year)**



- The white/grey division indicates the citing half-life (if < 10.0). Half of the citations from the journal's current items are to items published more recently than the citing half-life.
- The top (gold) portion of each column indicates Journal Self-Citations: citations from items in the journal to items in the same journal.
- The bottom (blue) portion of each column indicates Non-Self Citations: citations from the journal to items in other journals.

**Journal Source Data** 

	Citable items			Other items
	Articles	Reviews	Combined	
Number in JCR year 2014 (A)	555	17	572	10
Number of references (B)	27646	2188	29834	142.00
Ratio (B/A)	49.8	128.7	52.2	14.2

[Acceptable Use Policy](#)  
Copyright © 2015 Thomson Reuters.

Rank in Category: Remote Sensing

Journal Ranking *i*

For 2014, the journal **Remote Sensing** has an Impact Factor of **3.180**.

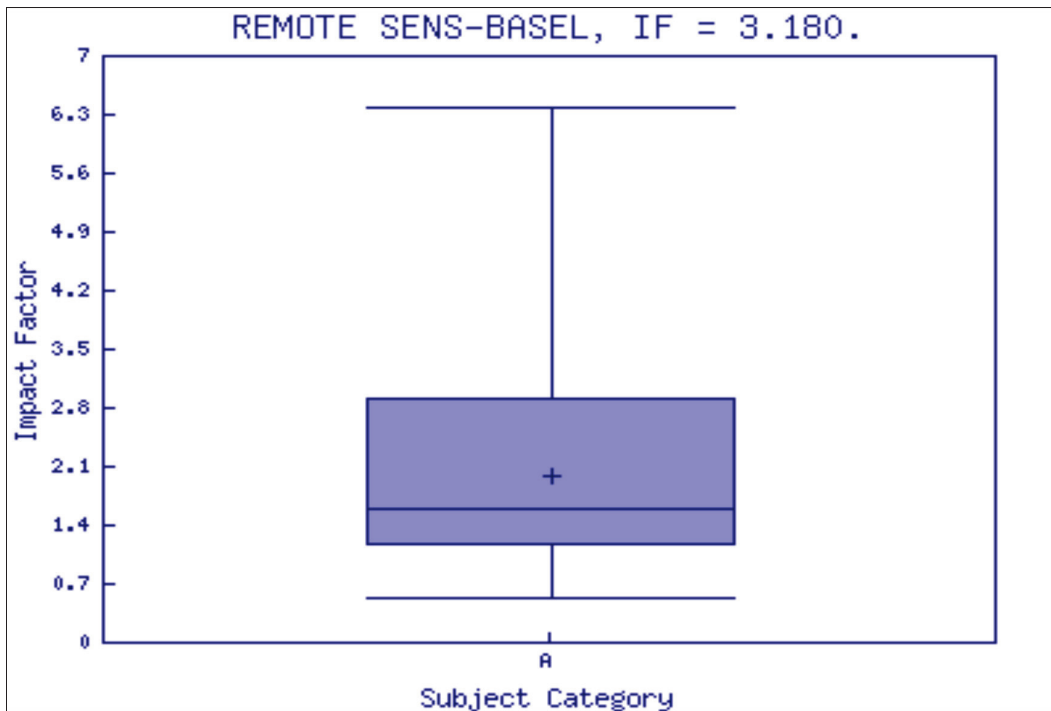
This table shows the ranking of this journal in its subject categories based on Impact Factor.

Category Name	Total Journals in Category	Journal Rank in Category	Quartile in Category
REMOTE SENSING	28	5	Q1

Category Box Plot *i*

For 2014, the journal **Remote Sensing** has an Impact Factor of **3.180**.

This is a box plot of the subject category or categories to which the journal has been assigned. It provides information about the distribution of journals based on Impact Factor values. It shows median, 25th and 75th percentiles, and the extreme values of the distribution.



Key  
A - REMOTE SENSING